uOttawa

L'Université canadienne
Canada's university

FACULTÉ DES ÉTUDES SUPÉRIEURES ET POSTOCTORALES

uOttawa

L'Université canadienne
Canada's university

FACULTY OF GRADUATE AND POSDOCTORAL STUDIES

Susan J. Marthaler
AUTEUR DE LA THÈSE / AUTHOR OF THESIS

M.Sc. (Microbiology and Immunology)
GRADE / DEGREE

Department of Biochemistry, Microbiology and Immunology
FACULTÉ, ÉCOLE, DÉPARTEMENT / FACULTY, SCHOOL, DEPARTMENT

Uncoiling the Mysteries of $DivIVA_{EF}$:
The Biological Functioning of the *Enterococcus faecalis* Cell Development Protein

TITRE DE LA THÈSE / TITLE OF THESIS

Jo-Anne Dillon
DIRECTEUR (DIRECTRICE) DE LA THÈSE / THESIS SUPERVISOR

CO-DIRECTEUR (CO-DIRECTRICE) DE LA THÈSE / THESIS CO-SUPERVISOR

EXAMINATEURS (EXAMINATRICES) DE LA THÈSE / THESIS EXAMINERS

Min Lin

Kathryn Wright

Gary W. Slater
LE DOYEN DE LA FACULTÉ DES ÉTUDES SUPÉRIEURES ET POSTDOCTORALES /
DEAN OF THE FACULTY OF GRADUATE AND POSTDOCORAL STUDIES

Uncoiling the Mysteries of $DivIVA_{Ef}$: The Biological Functioning of the *Enterococcus faecalis* Cell Development Protein.

Susan J Marthaler
(M. Sc. candidate)

March 7th, 2005.

A thesis submitted to the
School of Graduate Studies and Research
University of Ottawa
In partial fulfillment of the requirements for the
Degree: M. Sc.
Department of Biochemistry, Microbiology and Immunology
Faculty of Medicine

Your file Votre référence
ISBN: 0-494-11343-X
Our file Notre référence
ISBN: 0-494-11343-X

STUDENT REPORT

Current Program: M. Sc. – Molecular Microbiology
Program Start: September 2002
Supervisor: Dr. JR Dillon
Committee Members: Dr. D Franks and Dr. C Lee

Academics:

1) MIC 5124 – Introduction to Immunology:
   - Completed: Dec. 2002 (A).
2) MIC 8228 – Adv. topics in Gene Expression and & Protein Synthesis:
   - Completed: April 2003 (A-).
3) All mandatory seminar courses for scholastic years: 2002-2004.
4) Departmental seminar presentation: "The Great Bacterial Divide in a split decision: Elucidating the biological functions of *Enterococcus faecalis* $DivIVA_{Ef}$". Presented: Feb. 24, 2004.
5) BMI Poster Competition of 2003: Awarded 2nd prize (Master's program).

Scholarships:

1) Nominated: Strategic Area of Development (SAD) award (2002).
2) Ontario Government Scholarship (OGS): 2002-2004.
3) University of Ottawa Excellence Scholarship: 2002-2004.

Professional Development:

1) Research Grants:
   a. Assisted in writing a Canadian Institute of Health Research (CIHR) grant for a fluorescence microscope (Awarded: 2003).
   b. Assisted in writing Grant (XG-02075R) progress report (2002-2003). For the continued studies of oligomerization & overexpression of $DivIVA_{Ef}$ funded by The Hospital for Sick Kids Foundation (Awarded: 2003).
   c. New CIHR grant: Operating grant for expanded studies on $DivIVA_{Ef}$ and a potential binding partner.
   d. Provided data and assisted in writing Grant (XG-02075R). Annual progress report (2003-2004).
2) 15th International Society of Sexual Transmitted Diseases (ISSTDR) Congress: July 2003. Volunteer Staff.

Manuscripts in preparation:

1) Ramirez S, Liao M, **Marthaler S**, Rigden M and Dillon JR. 2004. *Enterococcus faecalis divIVA*: An essential gene involved in cell division, cell growth and chromosomal segregation. (Submission 27718. accepted Feb. 2005: *Microbiology*).

2) **Marthaler S**, Knapp JS, Borthagaray G, Fiorito S, Bölmström A, Sealy J, Li H, Prabhakar H and Dillon JR. 2004. Multi-Centre Evaluation and Comparison of the Etest and the Agar Dilution Method for the Testing of Antimicrobial Susceptibility of Neisseria gonorrhoeae. (To be submitted to Journal of Antimicrobial Chemotherapy, pending).

ABSTRACT

Cell division mechanisms involving native proteins MinCDE or MinCD and DivIVA have been explored using *Esherichia coli* (Ec) and *Bacillus subtilis* (Bs), respectively. My research examines the Gram-positive coccal-shaped *Enterococcus faecalis* (Ef) protein DivIVA, which functions without any Min proteins.

To determine whether *E. coli* could be used as a suitable indicator system, DivIVA$_{Ef}$ overexpression and morphological studies were undertaken. Constructs with unique mutations created along the 699-nucleotide length of the *divIVA$_{Ef}$* gene to abrogate specific coiled-coil domains at the N-terminal, C-terminal and two central regions were investigated in this model. The original mutations were previously used in different systems and therefore required PCR amplification, double digest with new restriction enzymes prior to subcloning in pUC18 for transformation in *E. coli* (Ramirez-Arcos *et al.*, 2005; Rigden *et al.*, 2005).

DivIVA$_{Ef}$ overexpression was detected by Western blot using a monoclonal anti-His antibody. *E. coli* transformants carrying constructs with abrogated central coiled-coil domains prevented DivIVA$_{Ef}$ overexpression, suggesting that DivIVA$_{Ef}$ was unable to oligomerize rendering the protein nonfunctional. This is the first report demonstrating that DivIVA$_{Ef}$ overexpression occurs in the presence or absence of Min proteins, and thereby indicating a unique DivIVA$_{Ef}$ biological function relative to DivIVA$_{Bs}$. Moreover, mutations abrogating the central coiled-coil domains did not overexpress DivIVA$_{Ef}$ in *E. coli* PB103 or PB114 transformants and did not affect the cell phenotype suggesting alterations in this region of the protein may deleteriously affect the biological function of DivIVA$_{Ef}$.

Morphological studies using phase contrast microscopy demonstrated that wild type *divIVA$_{Ef}$* transformants exhibited an engorged spherical cell phenotype using *E. coli* KJB24 (*minB, rodA*$^-$) or *E. coli* WM1250 (Δ*minB*, *rodA*$^-$); as well as, exhibiting a filamentous phenotype using bacillary *E. coli* PB103 (*minB*) or *E. coli* PB114 (Δ*minB*). This is the first report demonstrating that the presence of wild type *divIVA$_{Ef}$* may arrest cell division in *E. coli.* As with the rod-shaped *E. coli* strains, mutations abrogating the central coiled-coil domains did not overexpress DivIVA$_{Ef}$ in *E. coli* WM1250 cells and did not affect the cell phenotype suggesting alterations in this region of the protein may deleteriously affect the biological function of DivIVA$_{Ef}$.

The Nisin-Controlled Expression (NICE) system demonstrated DivIVA$_{Ef}$ overexpression using *E. faecalis* JH2-2 carrying a *P$_{nisA}$::divIVA$_{Ef}$* fusion construct cloned into the *E. faecalis* - *E. coli* shuttle vector pMSP3545. This is the first report indicating DivIVA$_{Ef}$ overexpression can be induced with 1.5 μg/ml nisin without altering the natural cell phenotype as demonstrated by electron transmission microscopy.

DivIVA$_{Ef}$ overexpression, in a non-inducible manner, was demonstrated using *E. faecalis* JH2-2 transformants carrying *divIVA$_{Ef}$*, under the control of its own promoter (*P$_{nisA}$::P$_{divIVAEf}$::divIVA$_{Ef}$*). This overexpression system is simple and efficient compared to the NICE system. This is the first report indicating DivIVA$_{Ef}$ overexpression can be achieved in a non-inducible manner without altering the inherent cell phenotype as demonstrated by electron transmission microscopy.

This research is grounding breaking with regards to the biological functioning of the cell division protein DivIVA$_{Ef}$ and could assist other investigators to examine species-specific roles of DivIVA.

ACKNOWLEGEMENTS

"I have never let my schooling interfere with my education."
- Mark Twain (1835-1910).

"A fact is a simple statement that everyone believes. It is innocent, unless found guilty. A hypothesis is a novel suggestion that no one wants to believe. It is guilty, until found effective."

- Edward Teller (1908 - 2003).

Both quotes are simple truths for me. Mark Twain eloquently describes how I have lived my life so far and Edward Teller reminds me of what must still be achieved. The two diverging concepts of schooling and education serendipitously intersected at the Dillon laboratory and an explosion of learning ensued. Wherever one learns, there are mentors and teachers.

Each member of the Dillon laboratory taught me something different. Sometimes it related to my education, but more often than not, someone reminded me that my schooling still continues. The easy and very hard lessons will be a benchmark for my future schooling. With that said, to those who taught me easier lessons, I thank you; to those who taught me hard lessons, I thank you the most. I will always remember you fondly, Dr. Dillon – thank you for facilitating all exploration with knowledge and forbearance.

In particular, I wish to thank Dr. Mingmin Liao, who is not only that rare breed of gentleman, but in his wisdom, always effectively encouraged me with his enormous scientific talent. It was an honour to have you as my laboratory supervisor.

Funding for this project was provided by a grant awarded to Dr. JA Dillon by: The Sick Kids Hospital (Toronto). Susan Marthaler, who was granted OGS Scholarships from the Ontario Government during 2002-2004, further contributed to funding. Dr. G Dunny (U of Minnesota) graciously provided *Enterococcus faecalis* strains: OG1RF and JH2-2; as well as, furnishing plasmid DNA for: pMSP3535X, pMSP3535 and pMSP3535VA. Dr. S Patterson (Carleton University) kindly provided *Bacillus subtilis* 1756.

TABLE OF CONTENTS

ITEM **PAGE**

10. Tables

11. Figures

11. Figures

11. Figures

LIST OF ABBREVIATIONS

aa	amino acid
Amp	ampicillin
ATP	adenosine 5'-triphosphate
BHI	brain heart infusion
bp	base pairs
Bs	*Bacillus subtilis*
BYGT	BHI + yeast extract, glucose and Tris (BYGT)
ddH_2O	double distilled water
DNA	deoxyribonucleic acid
DNTP	deoxynucleotide triphosphate
DTT	dithiothreitol
Ec	*Escherichia coli*
EDTA	ethylene diamine tetra-acetic acid
Ef	*Enterococcus faecalis*
Ery	erythromycin
g	gram
GTP	guanosine triphosphate
GTPase	guanosine triphosphate dephosphorylase
Hr	hour
Hrs	hours
IPCR	inverse polymerase chain reaction
kb	kilobase pairs
LB	Luria-Bertani
IPTG	isopropropyl-β-D-thiogalactopyranoside
µg	microgram
µl	microlitre
µM	micromolar
µm	micron
mg	milligram
ml	militre
mM	milimolar
Met	methionine
min	minutes
MinCD	MinC and MinD complex
MinCDE	MinC, MinD, MinE
MW	molecular weight
NaOH	sodium hydroxide
NEB	New England Biolabs
ng	nanogram
O/N	over-night
PBS	phosphate-buffered saline
PCR	polymerase chain reaction
pDNA	plasmid DNA
RT	room temperature
s	seconds
SDM	site-directed mutagenesis
SDS	sodium dodecyl (lauryl) sulfate
TAE	tris-acetate-EDTA buffer
TEM	transmission electron microscope
Tet	tetracycline
3D	three-dimension
V	volts

1. INTRODUCTION

Overview

Cell division is not only central but also vital to the survival of all eukaryotic and prokaryotic species. While the conditions, processes and mechanisms differ substantially between and within kingdoms, the objective of cell division remains the complete equipartitioning of the progenitor cell, genetically and cellularly, between two viable daughters. Cell growth and cell viability rely completely on accurate and well-organized cell division (Lutkenhaus and Adinall, 1997). The preponderance of studies with bacterial cell division use rod-shaped species, such as the Gram-negative *Escherichia coli* (*Ec*) and the Gram-positive *Bacillus subtilis* (*Bs*) as model organisms. Several proteins act in concert to ensure the correct cytokinetic septum location found at the mid-cell region. Two genetic loci of particular importance the division cell wall cluster (*dcw*) and the *minB* operon have encoded products implicated in the site selection for septation and cell division (Ayala *et al.*, 1994; Katis *et al.*, 2000; Koch, 2003; Lutkenhaus and Addinall, 1997; Massidda *et al.*, 1998; Pucci *et al.*, 1997; Tamames *et al.*, 2001; Vicente *et al.*, 1998; Yura *et al.*, 1994). Because the preponderance of research surrounding protein homologues related to cell division has been achieved using rod-shaped bacteria, elucidation of cell division in coccal-shaped bacteria remains elusive at best. Moreover, no obviously distinct mid-cell is evident in spherical cells suggesting that these bacteria may have the potential for multiple division sites unlike their rod-shaped counterparts and this renders the question of cell division control mechanisms profoundly more interesting (Begg and Donachie, 1998; Corbin *et al.*, 2002; Daniel and Errington, 2003; Donachie *et al.*, 1995). My research focuses on the coccal-shaped *Enterococcus faecalis* (*Ef*) as a

model organism concentrating on cell division protein DivIVA ($DivIVA_{Ef}$) to investigate cell division mechanisms of Gram-positive cocci.

1.1 Cell division:

The fundamental prerequisite for the proliferation of certain bacterial cells occurs by the asexual form of cell division in a process known as binary fission (Westling-Häggström *et al*, 1977). Binary fission occurs when and only if conditions are favorable. An individually expanding cell divides into two daughter cells comprising the normal complement of chromosomes. New cells then increase their size permitting further rounds of binary fission, as long as the surrounding environment remains permissive (Donachie and Begg, 1970). Such division can occur at different points along the cell including longitudinal, transverse, symmetrical or asymmetrical, dependent on the bacterial cell state (i.e.: vegetative vs. sporulative) and bacterial species.

One of the defining characteristics of bacterial cell division is the synchronized assembly of different proteins to orchestrate cytoplasmic division known as cytokinesis (Errington *et al.,* 2003). Other essential processes involved in cell division processes include chromosome replication and nucleoid separation that ensure complete equipartitioning of the progenitor cell genetically (Errington *et al.,* 2003). Proper DNA replication, packaging and chromosomal segregation occur concurrently and are prerequisites for cell division (Lemon and Grossman, 2001; Margolin, 2000; Mitchell and Moyle, 1956; Møller-Jensen *et al.*, 2000).

In rod-shaped bacteria, three potential division sites exist and include: the mid-cell region separating already replicated daughter chromosomes and the polar regions of the cell (Errington *et al.*, 2003). Typically, rod-shaped cells, such as *E. coli*, divide in one

plane perpendicular to the long axis at the mid-point of the cell with demonstrable fidelity (Westling-Häggström *et al*, 1977). Each cell can sub-divide repeatedly with division always at the same point of origin (Edwards *et al.*, 2000; Errington *et al.*, 2003). Prior to cell division in *E. coli*, an indented ring called the septum forms in the cell wall and cell membrane. To induce septation, the polymerization of FtsZ brings about invagination of the cytoplasmic membrane in concert with the synthesis of septal peptidoglycan (Edwards *et al.*, 2000; Lutkenhaus and Addinall, 1997). As the time of cell division grows near, some bacteria, like *E. coli*, exhibit a gradual septal contraction that eventually pinches off and separates the two daughter cells by synthesizing a new cross wall at the septum that will divide the two halves. Conversely, *B. subtilis* forms a new cross-wall without any concomitant constriction of the elongated cell and a pair of sister cells joined at a double membrane sharing a single cell wall results (Errington *et al.*, 2003). During this process, the cytoplasm divides with the newly replicated chromosomes partitioned into separate daughter cells. However, some cell division processes like the annular invagination of the cell wall and membrane layers at the mid-cell point along the long axis of the cell are similar in both *B. subtilis* and *E. coli* (Szeto, 2004; Weart and Levin, 2003).

Cocci have the capability to divide at any of several planes and interestingly, at a number of planes resulting in different geometries to produce clusters of progeny cells. For example, spherical cells with a capability to divide on one plane only will form chains, such as *Streptococcus pneumoniae*; and three-plane division produces irregular clusters, as is the case with *Staphylococcus aureus* (Coykendall, 1989; Kahl *et al.*, 2003; Westling-Häggström *et al.*, 1977). Conversely, the Gram-negative coccal-shaped *N.*

gonorrhoeae achieve two-plane cell division by asymmetrical membranal invagination with cells growing perpendicular to the invagination (Fitz-James, 1964; Szeto, 2004). Another round of division transpires in the perpendicular plane to the nascent septum completing the cytokinetic process (Szeto, 2004; Westling-Häggström *et al.*, 1977). Such bi-directional growth produces tetrads of gonococcal cells rather than two daughter cells.

Interestingly, mutant *E. coli* KJB24 (*minB, rodA*$^-$) cells that are round in shape owing to the lack of the cell shape determinant *rodA*-, divide similar to gonococcal cells (Begg and Donachie, 1998; Corbin *et* al., 2002). Growth and division occur normally in spherical mutants but division is delayed permitting fast-growing cells to become 6-fold larger (volume) than wild-type cells (Begg *et al.*, 1995).

The Gram-positive coccal-shaped *E. faecalis* is the model organism for my research and has a novel process of cytokinesis relative to *E. coli*, *B. subtilis* or *N. gonorrhoeae*. *E. faecalis* divides sequentially along parallel planes; does not possess an obvious midcell and thus, has the potential for multiple division sites. How is the mid-cell of this coccal-shaped organism orchestrated?

Higgins *et al.* (1971) proposed a cell division model wherein peripheral surface enlargement is favored over cell wall thickening during chromosome replication, while chromosome termination is characterized by cell wall thickening, septation and by the last stages of cell separation. Once the mid-cell point has been defined by unknown mechanisms, a wall band develops circumferentially. The center of this wall band grows bi-directionally, to create the required cell elongation necessary for the cell division machinery, forming two "wall notches". Over time, new wall growth occurring between the notches increases the cell size. At some undefined point, as the wall notches continue

to grow apart, the septal wall commences its inward growth towards a mirror replica at the transverse side of the cell. The two wall halves meet at some internal cell mid-point. As the septal wall-halves approach each other, the outer cell wall appears to thicken over its entirety. It is postulated to maintain a surface area to volume ratio enabling the cell to support and continue its growth. The restriction of the septal wall observed in *E. coli* and other organisms does not appear to hold true (Edelstein, 1980; Higgins and Shockman, 1976; Higgins and Shockman, 1971; Shockman *et al.*, 1974).

Not only are the mechanisms of cell division in *E. faecalis* unknown, but also which constituent proteins are involved and how they interact is not yet known. The nucleoid occlusion model, which suggests that cell division is predominantly inhibited specifically in the surrounding environment of the nucleoid, should apply to coccal-shaped organisms and adds another layer of complexity to resolve.

Some cocci carry only the site for septum formation, while others exhibit two sites for peptidoglycan assembly to include lateral wall formation. The preference for the site of septum formation permits a continued coccal shape, which prevents lateral wall formation (Begg and Donachie, 1998; Begg and Donachie, 1995; Corbin *et al.*, 2002; Daniel and Errington, 2003). However, septum formation can be inhibited either by mutations, antibiotics or when the cell surface extension is blocked (LLeo *et al.*, 1990). Thus, cocci need a centrally formed septum, no change in maximum diameter and the dimensions of a mature pole to split in the formation of two new daughter cells (Koch, 2003).

The cell wall must break in discrete locations during cell division, without permitting the cell membrane to burst. Autolysin activity must be carefully controlled throughout

this period of growth. Indiscriminate autolysis of the cell wall would eventually cause a weakening in the cell walls leading to cell rupture (Errington *et al.*, 2003). Once division has occurred, cell wall synthesis must concentrate on accommodating the expanding cell and not dividing it in half. Septation is completed by annular invagination of cell walls and membrane layers (Edwards *et al*; 2000).

The mechanisms responsible for cytokinesis are not fully elucidated, although many genes required for division have been characterized. New cytological techniques are creating advanced investigation opportunities for the examination of the cytoplasm. Once viewed as an unstructured environment, it is now deemed highly organized; with a spatially arranged nucleoid possessing genes at determinant positions; and with non-uniform protein localization (Errington, 2003; Frenkiel-Krispin *et al.*, 2004).

1.2 Regulation of cell division site placement

What ensures correct cytokinetic septum location at mid-cell? The encoded products from both the division cell wall cluster (*dcw*) and the *minB* operon function uniquely, but collectively to ensure accurate cell division processes.

As the *dcw* cluster name suggests, cell wall synthesis is key during cell division processes. The invagination of the cell wall and membrane layers as well as the synthesis of peptidoglycan must be coordinated with high fidelity involving spatial and temporal regulation of a process known as septation. Not only is the cell wall an active participant in the process of cell division, this rigid structure safeguards against osmotic and mechanical lysis, and functions in the contours defining morphology (Daniel and Errington, 2003; Koch, 1985; Mirelman, 1978; Touhami *et al.*, 2004).

The *dcw* cluster contains the filament temperature sensitive (*fts*) family of genes, which are involved in the cell wall biosynthesis and cell division (Ayala *et al.*, 1994; Koch, 2003; Tamames *et al.*, 2001; Tamames, 2001b). The genes are unidirectional, closely located and in some bacterial species, such as *E. coli*, they can actually overlap (Lutkenhaus and Addinall, 1997; Yura *et al.*, 1994). FtsZ is one of the most important members of the *fts* family and is not only the driving force of the cytokinetic event; it represents the earliest defined stage of cell division (Bi and Lutkenhaus, 1991; Feucht *et al.*, 2001; Hu *et al*; 1999; Huang *et al,* 1996; Lutkenhaus and Addinall, 1997; Ramirez-Arcos *et al.,* 2001). This protein lacks a clear membrane-spanning sequences suggesting it might well be peripheral membrane protein (Errington *et al.*, 2003; Rothfield *et al.*, 1999; Wang *et al.*, 1992). FtsZ self-assembles by GTPase activity into polymerized protofilaments that grow bi-directionally from the nucleation sites, which eventually develop into a contractile ring-like structure referred to as the Z-ring (Bi and Bouché and Pichoff, 1998; Bramhill and Thompson, 1994; Lutkenhaus and Addinall, 1997; Lutkenhaus, 1991). It is thought that the nucleation sites may be a significant point of control for the timing and positioning of septation (Marston *et al;* 1998).

FtsZ is not only the most conserved of all septation proteins; it is known to be present in bacterial cells with a high concentration up to a reported 15,000 molecules/cell in *E. coli* (Lu *et al*; 1998). Interestingly, increased FtsZ levels in *E. coli* produce a minicell phenotype, as the excess division potential is forced to the cell poles, while decreased FtsZ levels delay or inhibit cell division corresponding to the amount reduced (Katis *et al.,* 2000). Finally, the placement of the Z ring is determined by two factors including nucleoid occlusion (DNA-free regions of the cell) and the Min system (Errington, 2003;

Harry and Lewis, 2003; Marston *et al.*, 1998; Migocki *et al.*, 2002; Ramirez-Arcos *et al.*, 2004; Ramirez-Arcos *et al.*, 2002; Ramirez-Arcos *et al.*, 2001; Shih and Rothfield, 2003; Szeto *et al.*, 2001).

Pucci *et al.* (1997) discovered that the *dcw* cluster of two Gram-positive cocci, *Staphylococcus aureus* and *E. faecalis*, contained fewer genes and showed no widespread gene overlaps with intergenic spacing of >100 base pairs relative to *E. coli*. But, Vicente *et al.* (1998) demonstrated that the gene orders of *dcw* clusters amongst Gram-positive and Gram-negative organisms are conserved. The occurrence of similarity in gene order and gene conservation might assist in the prediction of function, protein interaction and genetic evolutionary relationship between species (Tamames *et al.*, 2001b). Individual bacterial species may possess unique arrays of genes within the *dcw* cluster, but over 24 species have a recognized *dcw* cluster homologue thought to be the result of evolutionary events ultimately affecting shape and growth according to phylogenetic analysis (Vicente *et al.*, 1998; Tamames *et al.*, 2001; Tamames *et al.*, 2001b).

Researchers have shown that the analyzed *dcw* clusters of Gram-positive bacteria lack the gene *ftsW* whose encoded product is the essential shape, elongation, division and sporulation protein thought to participate in the translocation of lipid-linked precursors needed in the synthesis of peptidoglycan involved in early and later cytokinesis (Ishino *et al.*, 1989; Khattar *et al.*, 1997; Khattar *et al.*, 1994; Noirclerc-Savoye *et al.*, 2003).

1.2.1 Nucleoid Occlusion

The event characterizing nucleoid occlusion encompasses an exquisitely orchestrated series of division processes, which predominantly inhibit division notably in the surrounding nucleoid environment. In-depth elucidation of the mechanisms of nucleoid occlusion is problematic owing to the complexities of defining the perimeter of a diffuse nucleoid; in determining the exact point in time of chromosome replication termination since individual cells differ to some extent; and finally, in discerning the individual forces driving segregation of newly replicated chromosomes dependent on bacterial species (Errington *et al.*, 2003; Gueiros-Filho and Losick, 2002). For these reasons, nucleoid occlusion, in mechanistic terms, is still insufficiently understood. In nucleoid free regions of the cell however, the MinCD complex of both *B. subtilis* and *E. coli* inhibits the Z-ring assembly at the polar regions of the cell (Cha and Stewart; 1997; Donachie, 2001; Edwards *et* al; 2000; Wu and Errington, 2004). Moreover, nucleoid occlusion in the presence of the Min proteins is thought to account for the small number of mini-cells (anucleated or lacking DNA) resulting from improper cell division in wild-type populations attributable to cell division arrest (Norris *et al.*, 2004; Ryan and Shapiro, 2003; Woldringh *et al.*, 1991).

1.2.2 The Min system

The *minB* operon, aptly named because mutations in any of the three genes *minC, minD* or *minE* involves an increase in the occurrences of minicells (Ryan and Shapiro, 2003). The presence or absence of Min proteins required for site selection in bacterial cell division occurs in one of three ways: the presence of all Min proteins that oscillate; the presence of some Min proteins and DivIVA; and lastly, the absence of all Min

homologues but possessing DivIVA with uncharacterized mechanisms (i.e.: *E. faecalis*) (Stahlberg *et al.*, 2004).

The combined effort of MinC, MinD and MinE (MinCDE) represents a clearly defined system for the location of Z ring development (Ryan and Shapiro, 2003; Errington *et al.*, 2003). The presence of all or some the Min proteins are not limited to Gram-negative bacteria (i.e.: *E. coli*) since certain Gram-positive bacteria (i.e.: *B. subtilis*) possess MinC and MinD (MinCD) proteins (Figure 1).

The Gram-negative rod-shaped *E. coli* is a model organism for the illustration of cell division with all three Min proteins. MinC interacts with FtsZ to preclude it polymerization and ultimately prevent septation. MinD, an ATPase, first dimerizes and then interacts with both MinC and membrane phospholipids resulting in MinCD association with the inner membrane (Szeto, 2004; Ryan and Shapiro, 2003; Errington *et al.*, 2003). The combined efforts of MinCD are coordinated to inhibit cell division and achieve this by rapid oscillation from pole to pole (Szeto *et al.*, 2005; Szeto *et al.*, 2004; Szeto, 2004; Thanedar and Margolin, 2004). The MinCD complex arrives first and stays the longest at the inner membrane.

MinE interacts directly with MinD specifically by its N-terminal region and determines the cellular location or topological specificity of MinCD complex to the membrane through its C-terminus (Pichoff *et al.*, 1997; Szeto, 2004). The ability of MinE to antagonize MinCD prevents the inhibition of polymerization of the Z ring at mid-cell since the Min proteins oscillate from pole to pole in a spiral structure and in effect, drop their concentration at the mid-cell region (Margolin, 2001; Margolin, 2001b; Rothfield *et al.*, 2001; Ryan and Shapiro, 2003; Gitai and Shapiro, 2003). Interestingly, the

Figure 1: Schematic diagrams of midcell site selection with Min proteins. **A-** *E. coli* cell division model with MinCDE. MinD dimerization and association with MinC, newly formed MinCD complex localizes to the membrane at the cell poles. MinE ring forms near the midcell activating the ATPase activity of MinD, which triggers MinCD dissociation for return to cytoplasm. MinC and MinD diffuse along a concentration gradient towards the opposite cell pole. At opposite cell pole, low MinE concentration permits reformation of MinCD complex and renewed cell membrane association. Cell pole and MinE association triggers ring dissociation permitting reformation at midcell. The cell division cycle recommences (Ramirez-Arcos *et al.,* 2002). **B-** *B. subtilis* cell division model with MinCD and DivIVA. DivIVA associates with the cell poles sequestering the MinCD division inhibitor complex away from the middle of the cell. DivIVA associates with the new cell pole during septal contraction and marks it as a used site of cell division. Following septation, the MinCD complex is drawn to the newly formed cell poles and sequestered there by DivIVA. (Edwards and Errington, 1997; Marston and Errington, 1999; Thomaides *et al*, 2001).

Figure 1

A.

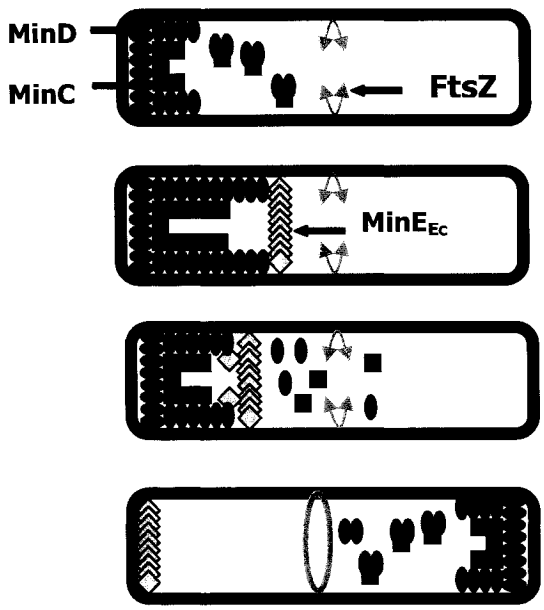

B.

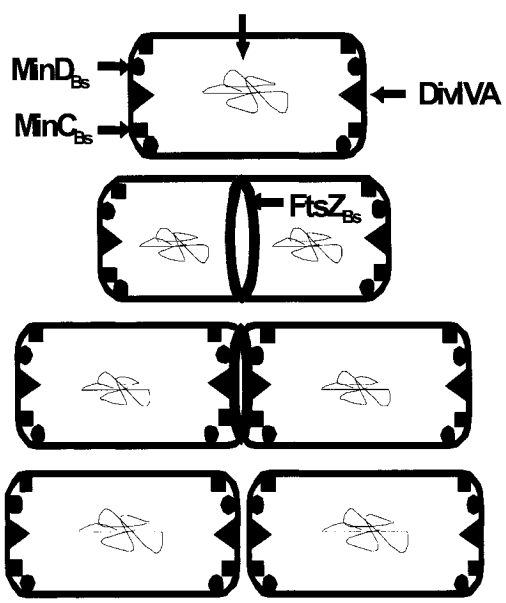

inactivation of MinE results in the formation of long filamentous cells (Jacobs and Shapiro, 1999).

The Gram-positive rod-shaped *B. subtilis* is a model organism exemplifying cell division with MinC and MinD (Figure 1) (Anderson *et al.*, 2004; Cha and Stewart, 1997; Edwards *et al.*, 2000; Howard, 2004; Muchová *et al.*, 2002). Inactivation of either *minC* or *minD* results in a minicell phenotype in *B. subtilis* (Cha and Stewart, 1997). It is interesting to note however, that most Gram-positive bacterial species lack some or all Min proteins and use different mechanisms to place the division site (Ryan and Shapiro, 2003).

1.3 Identification and characterization of *divIVA*

DivIVA homologues are mainly present in Gram-positive bacteria (Edwards *et al.*, 2000). Reeves et al. (1973) originally discovered this protein due to a mutation in *B. subtilis* that led to a major reduction in septation frequency and to the development of aberrant polar divisions yielding the minicell phenotype (Edwards *et. al.*, 2000).

The identification of *divIVA* came about much later, when researchers hypothesized that the encoded 19.5 kDa cytokinetic protein $DivIVA_{Bs}$ replaced $MinE_{Bs}$ since it appeared to specify the cellular location of MinCD to both cell poles where $DivIVA_{Bs}$ also localizes early in cytokinesis (Cha and Stewart, 1997; Edwards and Errington, 1997; Stahlberg *et al.*, 2004). An excellent model for cell division processes involving DivIVA has been developed since the initial identification (Anderson *et al.*, 2004; Ben-Yehuda and Losick, 2002; Errington *et al.*, 2003; Harry and Lewis, 2003; Scheffers and Errington, 2004; Stahlberg *et al.*, 2004; Wu and Errington, 2004).

1.4 DivIVA is found on the *dcw* cluster

Bioinformatic analysis has indicated that the *dcw* cluster of *E. faecalis* includes *fts*Z, *fts*A, *fts*Q, *fts*H, *fts*E, as well as, *fts*K, *fts*X *fts*W and *divIVA* gene homologues (Massidda *et al.,* 1998; Pucci *et al.,* 1997; Ramirez-Arcos *et al.*, 2005). The 3'-end of the open reading frame (ORF) of *ftsZ* ends with isoleucyl-tRNA synthetase (*ileS*) gene which is found directly downstream of *divIVA* in such organisms as *S. pneumoniae, B. subtilis* and *E. faecalis* (Edwards *et al.*, 2000; Hill, 1996; Massidda *et al.,* 1998; Pucci *et al.,* 1997).

Ramirez-Arcos *et al.* (2004) identified $DivIVA_{Ef}$ homologues by aligning the $divIVA_{Ef}$ sequence using *E. faecalis* V583 and found 24 organisms possessing similar DivIVA proteins. Bioinformatic analysis has shown that the *divIVA* gene possesses a G + C content of 35.19%, encoding 234 amino acids (aa) with a putative molecular weight of 26.65 kDa. A high degree of homology is exhibited between $DivIVA_{Ef}$ and $DivIVA_{Bs}$ at 34% identity and 63% similarity, which is intriguing due to some major differences between the two bacterial species. $DivIVA_{Bs}$ acts in concert with Min proteins in vegetative cells and is deemed to be involved in sporulation while *E. faecalis* does not possess any Min proteins and does not have a sporulative cell state. Figure 2 depicts this multi-sequence alignment demonstrating the conservation of the N-terminal region and the variability of the C-terminal length and sequence. Since DivIVA varies in length and sequence, protein structure and function may differ in accordance to bacterial species and the species-related mechanisms of action.

While little is known about cell division in *E. faecalis*, its clinical importance is highlighted since it is the leading cause of 90% of enterococcal pathogens in pediatric wards (Gilmore *et al.*, 2002; Swartz, 1994). This organism forms part of the intestinal

Figure 2: Alignment and structural analysis of $DivIVA_{Ef}$ to determine probable regions involved in self-association. **A-** Bioinformatic analysis depicting a multi-sequence alignment of DivIVA to determine regions of homology by % identity. **Black box** = conservation across N-terminal area; **green boxes** = conservation across two individual central regions and **yellow box** = diversity at C-terminal area; **B-** the structural analysis predicts the probable regions involved in self-association.
Figure 2A and 2B taken from: Marc Rigden. 2005. Determining the role of coiled-coil domain interactions in the oligomerization of DivIVA from *Enterococcus faecalis*. M. Sc. Thesis. Department of Biochemistry, Microbiology, and Immunology, Faculty of Medicine, University of Ottawa.

Figure 2

A.

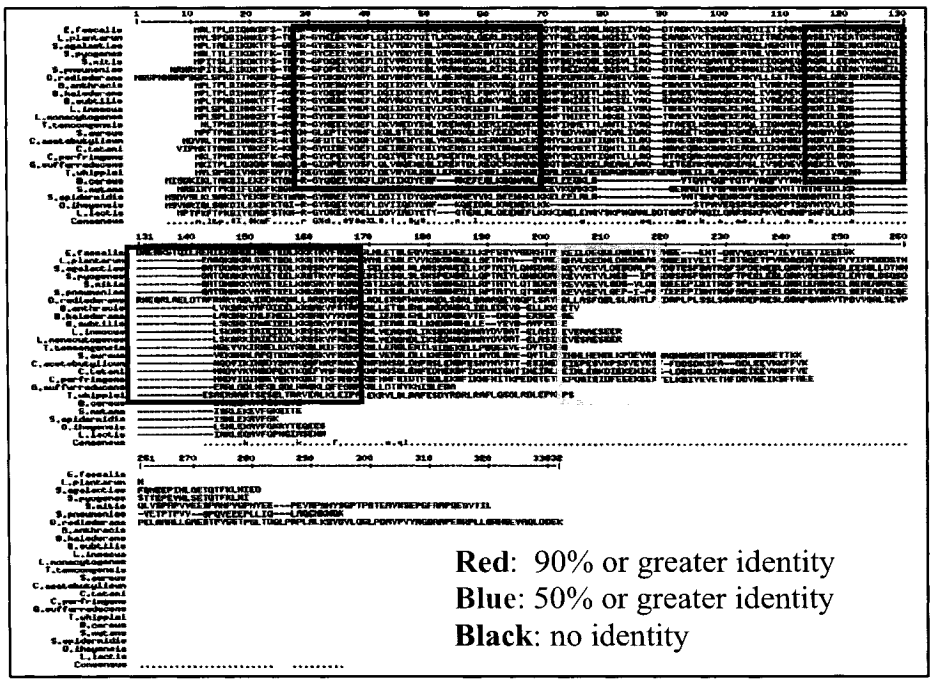

Conservation of DivIVA (various bacteria)

B.

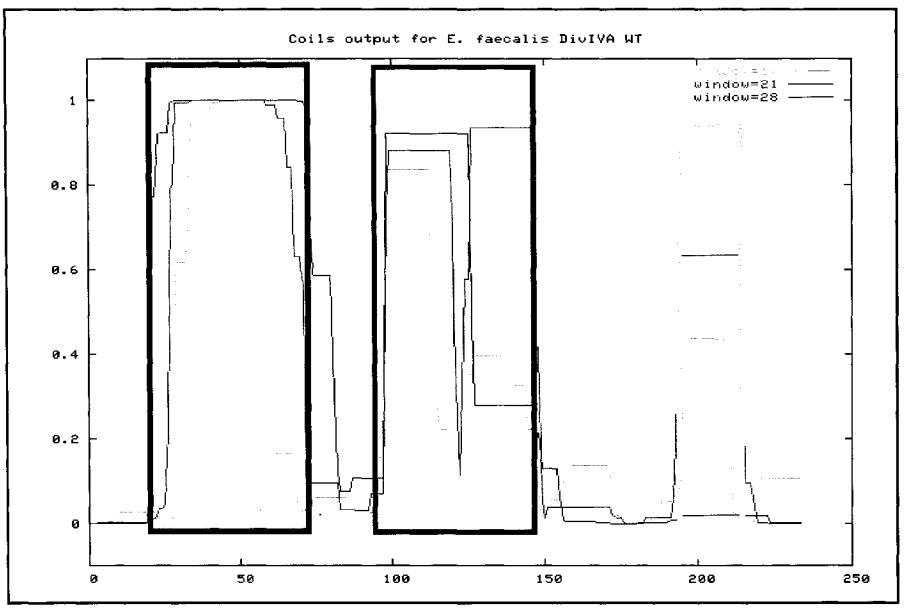

Predicted coiled-coil domains of *E. faecalis* DivIVA

microflora and possesses a broad array of antimicrobial resistances including: aminoglycosides (i.e.: kanamycin); β-lactams (i.e.: penicillin); chloramphenicol; and tetracycline (Kek and Chow, 2002; Moellering, 1992; Williamson *et al.*, 1985). Moreover, enterococci have an extraordinary ability to acquire resistance from vancomycin-resistant enterococci (VRE) further undermining effective treatments (CDC, 1993; Chenowth and Schaberg, 1990). Should VRE gain a foothold in hospitals, they will become reservoirs for transmitting resistance to other nosocomial pathogens like methicillin-resistant *S. aureus* (MRSA) (Swartz, 1994). Vancomycin is a last resort in the antibiotic treatment approach for both enterococci and MRSA strains (Karkowsky *et al.* 1999; Still *et al.* 2001; Tenover *et al.* 2001). Clearly, there is an urgent need for the development of novel antimicrobial targets to treat enterococcal infection. Although bacterial growth and cell wall synthesis have been the focus of antimicrobial research for many years, resulting in the development of such antimicrobials as the penicillins and cephalosporins; recent genome projects and improved molecular tools have stimulated new research alternatives for potential antimicrobial targets. I have focused on developing a cell division model for *E. faecalis* in the hopes of discovering a novel antimicrobial target through the cell division protein $DivIVA_{Ef}$.

1.5 Localization of DivIVA

Research has shown that while the mechanism of action for $DivIVA_{Bs}$ is unique from the topological specifier MinE found in *E. coli*, both proteins operate with the same division inhibitor complex MinCD in unique bacterial systems (Marston *et al.*, 1998). Moreover, $MinCD_{Bs}$ and $DivIVA_{Bs}$ are not thought to oscillate like the Min counterparts found in *E. coli* (Edwards and Errington, 1997; Marston *et al.*, 1998).

In *B. subtilis,* FtsZ presumably signals the on-set of septation since nucleoid occlusion is diminished due to chromosome segregation, while $DivIVA_{Bs}$ is recruited to the septum late in the cell cycle (Edwards and Errington, 1997; Hu *et al*; 1999; Huang *et al,* 1996; Marston and Errington, 1999; Thomaides *et al*; 2001). The resulting daughter cells have both polar regions protected from Z-ring formation (Levin *et al.*, 1998; Muchová *et al*, 2002).

Conversely with *E. coli*, the $DivIVA_{Bs}/MinCD_{Bs}$ complex does not initiate FtsZ polymerization at the mid-cell, but rather the complex functions to inhibit alternative sites of selection for cell division (Barák *et al.*, 2004).

The localization of DivIVA is so specific that it has been proposed as a model system to demonstrate cytology-based protein-protein interactions (Ding *et al.,* 2002). Further, $DivIVA_{Bs}$ is able to localize to old cell divisional sites without assistance from other proteins (Hamoen and Errington, 2003; Harry and Lewis, 2003; Marston and Errington, 1999; Marston *et al.*, 1998).

In contrast, sporulating *B. subtilis* exhibit asymmetrical cell division that occurs close to one of the cell poles. $DivIVA_{Bs}$ localizes to a small, well-defined spot at one pole adjacent to the broader localization of MinCD (Marston and Errington, 1999; Thomaides *et al*; 2001). This asymmetrical division site led to the postulation that $DivIVA_{Bs}$ may also play a role in the chromosomal segregation machinery by positioning the *oriC* region of the chromosome, which functions in the initiation of DNA replication, at cell poles (Thomaides *et al.*, 2001; Wu and Errington, 1997). The vastly different cell states exemplified by vegetative and sporulating cells may use different protein complexes, yet

both seem to require DivIVA involvement with its ordered oligomeric structures (Stahlberg *et al.*, 2004).

1.6 The role of DivIVA in cell development

Clearly, a substantial amount of investigation has been conducted using $DivIVA_{Bs}$ and only recently, have researchers focused on DivIVA homologues in other species. The Gram-negative soil bacterial species *Myxococcus xanthus* possesses a DivIVA homologue, known as the FruD protein, involved in cell growth (Akiyama *et al.*, 2003). Another DivIVA homologue, found in the Gram-positive actinomycetes *Streptomyces coelicolour* and *Brevibacterium lactofermentum*, is involved in apical growth (Flärdh *et al.*, 2003; Ramos *et al.*, 2003). Finally, Fadda *et al.* (2003) recently demonstrated that the inactivation of *divIVA* in *S. pneumoniae* resulted in severe growth inhibition producing aberrant cell morphology, chromosomal segregation and cell division. This is suggestive of the necessity for *divIVA* in proper septation yet it has been shown to be non-essential in this bacterial species (Fadda *et al.*, 2003). Interestingly, the divIVA homologues of *B. subtilis, S. coelicolour, B. lactofermentum* and *E. faecalis* have been shown to be essential (Edwards and Errington, 1997; Flärdh 2003; Marston and Errington, 2001; Ramos *et al.*, 2003; Ramirez-Arcos *et al.*, 2004b)

The disruption of *divIVA* results in severe defects in cell morphology, including inhibition of septation, cell engorging, and filamentation depending on the host species while the complete deletion of $DivIVA_{Bs}$ results in a minicell phenotype, characterized by anucleated and filamentous cells, due to complete cell division arrest (Cha and Stewart, 1997; Edwards *et. al.,* 2000; Edwards and Errington, 1997; Muchová *et al;* 2002; (Ramirez-Arcos *et al.*, 2004b; Ramos *et al.,* 2003). It is now well established that

$DivIVA_{Bs}$ overexpression produces a filamentous (grossly elongated cells) phenotype attributed to the inhibition of cell division (Edwards *et. al.,* 2000; Edwards and Errington, 1997; Muchová *et al;* 2002).

Ramirez-Arcos *et al.* (2004b) from our group demonstrated that $divIVA_{Ef}$ is not able to complement two Gram-positive organisms possessing *divIVA* and they include a *B. subtilis divIVA* mutant and an *S. pneumoniae* mutant strain. This provides additional support to the notion of a species-specific function for DivIVA. We were also able to show that $DivIVA_{Ef}$ is involved in chromosomal segregation in the native *E. faecalis* JH2-2 using DAPI stain.

Our laboratory has identified a binding partner of $DivIVA_{Ef}$ using genomic DNA library and yeast 2 hybrid (Y2H) technologies. Bioinformatic analysis established that the genetic insert encoded aa 79 – 209 from a putative ORF in *E. faecalis*. The tentatively named MLJD1 is exclusive to Gram-positive species, is highly conserved and has three domains (Liao *et al.*, unpublished data, 2004).

1.7 The oligomerization of DivIVA

Coiled-coil domains are the main structural element oligomerizing fibrous proteins including myosin, fibrinogen and keratin (Lupas *et al.,* 1996; Lupas, 1991). These domains are composed of repeating heptads that possess specific hydrophobic interaction interfaces with an ability to mediate protein-protein interactions in eukaryotic, prokaryotic and viral environments are the key characteristic (Gugolya *et al.,* 2003; Hebrard *et al.*, 2001; Lupas, 1996; Park *et al.,* 1999).

Our laboratory analyzed predicted coiled-coil domains of $DivIVA_{Ef}$ using the Coils MTIDK matrix (Figure 2b) (Lupas, 1996; Rigden, 2005). The four coiled-coil regions

include an N-terminal, first central, second central and a C-terminal region along the length of *divIVA*$_{Ef}$. More typically, only the N-terminal and central coiled-coil domains are common to all divIVA homologues. Rigden *et al.* (2005) has recently demonstrated that disruption of either the N- or C-terminal coiled coil domain of $DivIVA_{Ef}$ does not lead to an altered complex formation as measured by size exclusion chromatography and native gel electrophoresis.

Intriguingly, protein-protein interaction analyses by yeast two-hybrid assays revealed that $DivIVA_{Ef}$ weakly interact with $DivIVA_{Bs}$ relative to self-interaction of each protein by $P<0.05$ (Ramirez-Arcos *et al.*, 2004). Perhaps this is not so surprising given the high homologous in sequence and that both encoded proteins form 10-12mer complexes (Muchová *et al.*, 2002; Rigden, 2005).

1.8 The structure of DivIVA

Little information is available on the structure of DivIVA other than its propensity to oligomerize in *B. subtilis* (Muchová *et al.*, 2002). Recently, Stahlberg *et al.*, (2004) published groundbreaking information as to the quaternary structure of $DivIVA_{Bs}$ using cryonegative stain transmission electron microscopy (TEM). They propose a model for the quaternary structure of a biologically active variant of $DivIVA_{Bs}$ known as DivIVA9. TEM imaging revealed $DivIVA9_{Bs}$ oligomerization produced a bone-shaped building block aggregated into dimers end-to-end and was capable of assembling into staggered two-dimensional networks. The researchers postulate that DivIVA may be able to recognize cell poles by forming a lattice-like network spanning the cell poles or that DivIVA oligomers may be directed to the cell poles by hyperstructures permitting certain proteins to be sequestered there to carry out specific processes involved with cell

division. The same researchers felt that different oligomeric structures of $DivIVA_{Bs}$ may be required for vegetative and sporulating cells (Stahlberg *et al.*, 2004).

The confirmation of a potential binding partner; $DivIVA_{Ef}$ self-interaction at coiled-coil domains; the *divIVA* gene locus on the *dcw* cluster; high conservation of DivIVA in Gram-positive organisms; the known functions of $DivIVA_{Bs}$; and the results of complementation experiments have all contributed to the elucidation of a possibly species specific and multi-functional $DivIVA_{Ef}$.

1.9 Rationale, Hypothesis and Objectives

1.9.1 Rationale:

The Dillon laboratory has contributed significantly to the area of site selection in bacterial cell division of Gram-negative cocci using *N.* gonorrhoeae as a model system. In a number of studies using this model system, rod-shaped *E. coli* strains were employed for overexpression studies since the Min proteins are involved in cell division of *N.* gonorrhoeae. Mutant *E. coli* KJB24 (Begg and Donachie, 1998) lacking the rod shape determinant *rodA*$^-$, producing coccal-shaped cells, were successfully employed to assess the morphological effects of gonococcal Min overexpression since the aberrant *E. coli* phenotype more closely follows the natural cell phenotype of *N. gonorrhoeae.*

E. faecalis was selected as a Gram-positive model system to study the site selection for cell division in cocci by assessing the biological role of DivIVA since the gene is highly conserved and distributed across 24 Gram-positive organisms (Figure 1).

The effects of overexpression or disruption of DivIVA have been the mainstay of virtually all studies examining this protein. The importance of DivIVA oligomerization and the coiled-coil domain crucial to complex formation has never been examined.

Moreover, abrogation of individual coiled-coil domains resulting in the inhibition of $DivIVA_{Ef}$ to oligomerize, the biological functioning of this protein might be elucidated.

To assess coiled-coil domains, mutations have been introduced along the length of $divIVA_{Ef}$ to disrupt specific coiled-coil domains (Rigden, 2005). In the present research, the various $divIVA_{Ef}$ constructs containing the wild type or mutated $divIVA_{Ef}$ amplicons were introduced into rod-shaped *E. coli* PB103 (*minB*) (de Boer *et al.*, 1988) *E. coli* PB114 (Δ*minB*) (de Boer *et al.*, 1989), mutant coccal-shaped *E. coli* KJB24 (*minB, rodA*$^-$) and *E. coli* WM1250 (Δ*minB, rodA*$^-$) (Margolin, Case Western Reserve University) to investigate the effects $DivIVA_{Ef}$ overexpression on cell morphology. The introduction of $divIVA_{Ef}$ constructs in *E. coli* was predicted to change the inherent cell phenotype based on the results obtain in the gonococcal experiments (Szeto *et al.*, 2004; Szeto, 2004; Szeto, 2005). According to Thomaides *et al.* (2001) even low-levels of *divIVA* expression should be inhibitory to *E. coli* cell development.

There are several reasons for testing the suitability of rod-shaped *E. coli* strains as an indicator system for $DivIVA_{Ef}$ overexpression. First, this system has been used to investigate gonococcal Min proteins demonstrating that they are functional in heterologous *E. coli* systems (Ramirez-Arcos *et al.*, 2004b; Ramirez-Arcos *et al.*, 2002; Ramirez-Arcos *et al.*, 2001; Szeto *et al.*, 2001). Second, $DivIVA_{Bs}$ is functional with MinCD in Gram-positive bacilli (Anderson *et al.*, 2004; Ben-Yehuda and Losick, 2002; Cha and Stewart, 1997; Errington *et al.*, 2003; Edwards and Errington, 1997; Harry and Lewis, 2003; Scheffers and Errington, 2004; Stahlberg *et al.*, 2004; Wu and Errington, 2004). Thus, it was feasible to investigate $DivIVA_{Ef}$ overexpression in bacilli, given the

high homology between the $DivIVA_{Ef}$ and $DivIVA_{Bs}$. Finally, *E. coli* possesses a cell wall readily disrupted; facilitates transformation and cell preparations for SDS-Page.

Constructs with wt or mutated $divIVA_{Ef}$ were transformed in round mutant *E. coli* KJB24 for $DivIVA_{Ef}$ overexpression and morphological studies. *E. coli* KJB24 was employed for several reasons. The round mutant *E. coli* KJB24 offer a spherical environment that more closely resembles the native *E. faecalis* JH2-2 compared with *E. coli* bacilli including strains PB103 and PB114; and *E. coli* KJB24 has an isogenic derivative known as *E. coli* WM1250 that lacks Min proteins, which raises three intriguing questions: First, would coccal-shaped *E. coli* transformants carrying $divIVA_{Ef}$ overexpress $DivIVA_{Ef}$ in a manner different from rod-shaped *E. coli* transformants? Second, what are effects on $DivIVA_{Ef}$ when Min proteins are present or absent? Finally, does this change whether bacilli or cocci are employed?

Investigation of $DivIVA_{Ef}$ in the presence or absence of Min proteins in *E. coli* bacilli and cocci is groundbreaking research. Western blot and phase contrast microscopy would be used to assess $DivIVA_{Ef}$ overexpression and morphological studies, respectively. This should shed some light on how $DivIVA_{Ef}$ might function differently from $DivIVA_{Bs}$ knowing that only *B. subtilis* possess Min proteins.

The development of the NICE system for use in *E. faecalis* is a novel approach. Nisin would be used to induce $DivIVA_{Ef}$ overexpression in a controlled manner. Alternatively, a second homologous $DivIVA_{Ef}$ overexpression system would be supported in a non-inducible manner using the native $DivIVA_{Ef}$ promoter ($P_{divIVAEf}$) to contrast with the NICE system. Two systems would provide novel approaches to enhance $DivIVA_{Ef}$ overexpression.

1.9.2 Hypothesis:

DivIVA$_{Ef}$ is implicated as a cell developmental protein in the Gram-positive coccus Enterococcus faecalis. DivIVA$_{Ef}$ possesses an N-terminal, two central and a C-terminal coiled-coil domain inherent to the oligomerization of DivIVA$_{Ef}$ Thus, mutations affecting specific coiled-coil regions will abrogate the normal biological function of DivIVA$_{Ef}$ in the heterologous E. coli system as determined by overexpression and morphological studies.

1.7.3 Objectives:

1) ***To determine whether E. coli can be used as a suitable indicator system for DivIVA$_{Ef}$ function:***
   a. *Construction of wild type divIVA$_{Ef}$ and mutated divIVA$_{Ef}$ amplicons in pUC18.*
   b. *The overexpression of wild type and mutated* DivIVA$_{Ef}$ *detectable by antibodies for Western blot analysis.*
   c. *Observation of cell morphology of transformants carrying wild type or mutated divIVA$_{Ef}$ in the heterologous E. coli system using:*
      i. ***Round** mutant E. coli KJB24 (minB, rodA$^-$) and its isogenic E. coli WM1250 (ΔminB, rodA$^-$)*
      ii. ***Rod-shaped** E. coli PB103 (minB) and its isogenic E. coli PB114 (ΔminB)*

2) ***To optimize and implement the Nisin-Controlled Expression (NICE) system for DivIVA$_{Ef}$ overexpression in the native E. faecalis JH2-2.***

3) ***To overexpress DivIVA$_{Ef}$ when divIVA$_{Ef}$ is under the control of its own promoter (P_{divIVA}) in the native E. faecalis JH2-2.***

METHODS & MATERIALS

2.1 Bacterial strains, plasmids and growth conditions:

All bacterial strains used in this research are presented in Table 1. Unless otherwise stated, *E. coli* DH5-α was used for the propagation of all plasmids.

E. coli DH5-α (Clontech; Mississauga, ON) is an easy strain to transform and permits efficient plasmid DNA extraction. Therefore, initially all constructs were transformed in *E. coli* DH5-α grown at 37°C, for 16 - 24 hours, and shaken at 100 rpm in Luria-Bertani (LB) (Difco, Detroit, Michigan) broth supplemented with 100 μg ampicillin (Amp)/mL (Sigma-Aldrich; St. Louis, MO) or at 37°C overnight (O/N) on LB_{amp100} agar plates. All *E. coli* DH5-α transformants were preserved at -70°C in Brain and Heart Infusion (BHI) broth (Difco) containing 20% glycerol.

E. coli PB103, *E. coli* PB114, *E. coli* KJB24 and *E. coli* WM1250 were transformed with *divIVA*$_{Ef}$ constructs grown at 37°C for 16 - 24 hours and shaken at 100 rpm in LB_{amp100} broth or at 37°C O/N on LB_{amp100} agar plates. These strains were employed in $DivIVA_{Ef}$ overexpression and morphological studies. *E. coli* DR105 – see appendix I.

E. faecalis JH2-2 was transformed with wt *divIVA*$_{Ef}$ grown at 37°C for 16 - 24 hours without agitation in BHI or BHI (1.9%) with 0.5% yeast extract, 0.2% glucose and 1% 1M tris (pH 8)(BYGT) broth supplemented with 10 μg erythromycin (Ery)/mL (Difco) or at 37°C O/N on BHI $_{Ery125}$ plates for overexpression and morphological studies or immunogold localization.

Table 1: List of Strains

Name	Description	Source/Reference
E. coli DH5-α	*[sup*E44Δ*lacU169* (80 *lacZ* Δ*M*15) *hsd*R17*rec*A1 *end*A1 *gyr*A96 *thi*-1 *rel*A1]	Gibco-BRL
E. coli PB103	*dadR1 trpE61 trpA62 tna-5 purB*$^+$ [W3110 K12F$^-$ IN(*rrnD-rrnE)*]	deBoer *et al.*, 1988.
E. coli PB114	*dadR1 trpE61 trpA62 tna-5 purB*$^+$ λ^- *ΔminCDE aph (Kan*^{r}*)* [W3110 K12F$^-$ IN (*rrnD-rrnE)*]	deBoer *et al.*, 1989.
E. coli KJB24	*RodA* (am), kan^r, *thyA* in W3110 (Sup^0)	Begg and Donachie, 1998.
E. coli WM1250	*fadR*::Tn*10*, ΔminCDE::*aph* in KJB24	Corbin *et al.*, 2002.
E. faecalis JH2-2	Derived from the clinical isolate *E. faecalis* JH2. Rif^R Fus^R	Jacobs and Hobbs, 1974.
E. faecalis OG1RF carrying pMSP3535X	Spontaneous resistant mutant. Rif^R and Fus^R (P_{nisA}::*prgX*$_{Ef}$)	Bryant ***et al.***, 2000; Christie and Dunny, 1986.
E. coli DR105	*Zcf-117::Tn10/dadR1 trpE61 trp62 tna-5 minC3*	deBoer, Case Western Reserve U.

2.2 Polymerase chain reaction (PCR) amplification:

All primers employed in this research are presented in Tables 2. Oligonucleotide primers used for PCR amplification were designed using Primer Designer software (Scientific and Education Software; Durham, NC) and were synthesized by the University of Ottawa Core Facility for DNA Synthesis and Sequencing.

Wild type *divIVA*$_{Ef}$ and all mutant *divIVA*$_{Ef}$ amplicons were PCR amplified from constructs pMR1 – pMR12 (Table 3. Rigden, 2005) using the 5' primer IVA-1 and the 3' primer IVA-5 incorporating *Eco*RI and *Bam*HI restriction sites respectively, to create the construct series known as "**pSM**". Alternatively, wt and mutant *divIVA*$_{Ef}$ amplicons from pMR1 – pMR12 were PCR amplified using the 5' primer IVA-1 and the 3' primer IVA-His incorporating *Eco*RI and *Bam*HI restriction sites respectively produced *divIVA*$_{Ef}$*::6XHis* – tag fusion for the generation of constructs known by "**pSM_.His**".

The *prgX*$_{Ef}$ amplicon was amplified from pMSP3535X (Dr. G Dunny) template DNA to create pSR-X using the 5' primer prgX-1 and the 3'primer prgX-2 incorporating *Eco*RI and *Bam*HI, respectively (Combined effort: Dr. S. Ramirez and S. Marthaler). Alternatively, to create the *prgX*$_{Ef}$*::(6X)His* – tag fusion for the construct pX-18, the 5' primer prgX-1 was used with a 3'primer known as prgX-His6 to incorporated *Bam*HI (Table 2).

The above-mentioned PCR protocol was carried out in the Perkin Elmer GenAmp PCR system 9600 thermocycler (Perkin Elmer; Wellesly, MA) as follows: 3- minutes (min) at 94°C (plasmid DNA) or 5-min at 94°C (*E. faecalis* JH2-2 whole cells); 30 cycles of denaturation for 15-seconds (s) at 94°C, annealing for 15-s at temperatures varying between 42 - 50°C (depending on primers used); extension at 72°C

Table 2: List of Primers

Name	Sequence	Products
IVA-1	5'-GCGCGAATTCATGGCATTAACTCC ATTAGA-3'	*divIVA$_{Ef}$* and *divIVA$_{Ef}$::6XHis*
IVA-2	5'-GCGCGGATCCCTATTTTGATT CTTCTTCAA-3'	*divIVA$_{Ef}$* and RBS-*divIVA$_{Ef}$ ::6XHis*
IVA-3	5'-GCGCCCATGGCATTAACTCCATTA GATATT-3'	*divIVA$_{Ef}$* (pSMSPSRDiv-1)
IVA-4	5'-GCGCTCTAGACTATTTTGATTCTT CTTCAA-3'	P$_{divIVAEf}$::*divIVA$_{Ef}$*
IVA-5	5'-GCGCGGATCCATGGCATTAACTCC ATTAGA-3'	*divIVA$_{Ef}$* (pSM series)
IVA-His	5'-GCAGCCGGATCTCAGGATCCTTAG TGGTGGTGGTGGTGGTGCTCGAG-3'	*divIVA$_{Ef}$* and *divIVA$_{Ef}$::6XHis* (pSM.His series)
PRGX-1	5'-GCGCGAATTCATGACTGC TCTTTTATTTC-3'	*prgX$_{Ef}$* (pSR-X). (pSM series, pSM.His series)
PRGX-2	5'-CGCCGGATCCAATGTTTAAG ATAGC-3'	*prgX$_{Ef}$* (pSR-X). (pSM series)
PRGX-His6	'5 –CGCGGATCCAATGTGGTGGTG GTG GTGGTGGTTTAAGATAG GTTC-3'	*prgX$_{Ef}$* (pSR-X). (pSM.His series)
PRGX-*NcoI*	'5-GCGCCCATGGATGAC TGCTCTTTTATTTC -3'	*prgX$_{Ef}$* (pSR-X) homologous system
PRGX-45	'5-GCGCTCTAGAAATGTGGTGGTGGT GGTGGTGGTTTAAGATAGGTTC -3'	*prgX$_{Ef}$* (pSR-X) homologous system
IVA-PRO	5'-GCGCCTGCAGTCTCGAAC TTTTGTTTA AGAAAACC -3'	*P$_{divIVAEf}$-divIVA$_{Ef}$* (pMSPSRDIV-2)
IVA-6-Xba	5'-GCGCTCTAGATTCCTTAACTG CTGTATG-3'	*P$_{divIVAEf}$-divIVA$_{Ef}$* (pMSPSRDIV-2)
IVA-7-Ssp	5'-GCGCAATATTGAAGT ATTGTAATTTTTCTTC-3'	*divIVA$_{Ef}$*(pSM8Ef) *divIVA$_{Ef}$*(pSM9Ef)
IVA-8-Ssp	5'-GCGCAATATTGAAATTCTTGATG AACAAG-3'	*divIVA$_{Ef}$*(pSM7Ef)
IVA-9-Ssp	5'-GCGCAATATTAATTGCTTCTGCTA AGATTTG-3'	*divIVA$_{Ef}$*(pSM7Ef)
IVA-10-Ssp	5'-GCGCAATATTATTGAACGTGCCCG TCAATTAG-3'	*divIVA$_{Ef}$*(pSM9Ef)

NB:

Restriction sites for the following enzymes are underlined: *Bam*HI (IVA-2, IVA-5, IVA-His, PRGX-2); *Eco*RI (IVA-1, PRGX-1, PRGX-His6,); *Pst*1 (IVA-PRO); *Xba*1 (IVA-4, PRGX-45, IVA-6-Xba); *Nco*1 (IVA-3, PRGX-Nco1); and *Ssp*1 (IVA-7-Ssp; IVA-8-Ssp, IVA-9-Ssp, IVA-10-Ssp)

for 0.5- to1.0- min (depending on the expected product size, where 1 minute/kb); a final 5-min extension at 72°C; and an infinite hold at 4°C. Reactions were carried out in a final volume of 100 µl containing: 75.5 µl ddH_2O, 10 µl 1x PCR buffer containing 1.5 mM $MgCl_2$ (Boehringer Mannheim Corp; Laval, QUE), 2 µl deoxylnucleotide triphosphate (dNTP) (100mM) (Boehringer Mannheim), 1 µl of each primer (0.2 µg/µl), 0.5 µl *Taq* DNA Polymerase for PCR amplifications (Boehringer Mannheim) and 10 µl of desired plasmid DNA (10 :g/mL) or 0.5 McFarland Standard (Remel, Lenexa, KA) bacterial cultures suspended in ddH_2O.

The wt *divIVA*$_{Ef}$ amplicon was cloned in fusion with *nisA* under the control of the nisin promoter (*PnisA*) (*P*$_{nisA}$*::divIVA*$_{Ef}$), in the *E. faecalis-E. coli* shuttle vector pMSP3545 (Dr. G Dunny, U of Minnesota), to create pMSPSRDiv-1 using the 5' primer IVA-3 and the 3'primer IVA-4 containing *Nco*I (Fermentas) and *Xba*I (Fermentas), respectively (Ramirez-Arcos *et al.*, 2004).

Alternatively, the wt *divIVA*$_{Ef}$ amplicon was cloned under the control of its natural promoter (P$_{divIVA}$) in the *E. faecalis-E. coli* shuttle vector pMSP3545 (Table 3. Dr. G Dunny, U of Minnesota) to produce the construct pMSPSRDiv-2 (*P*$_{nisA}$*::*P$_{divIVA}$*::divIVA*$_{Ef}$) using the 5' primer IVA-Pro and the 3' primer IVA-4 incorporating *Pst*I and *Xba*I, respectively (Ramirez-Arcos *et al.*, 2004).

2.3 Plasmid construction:

All plasmids employed in this research are presented in Table 3. All *divIVA*$_{Ef}$ amplicons were PCR cleaned using the QIAquick PCR purification kit, in accordance with manufacturer specifications (QIAgen; Mississauga, ON) and the Sorvall® MC 12V centrifuge (Sorvall; Guelph, ON). The amplicons were then screened using 1% agarose

Table 3: List of Plasmids

Name	Description	Source/Reference
pET30a	Kan^r P_{T7}::6XHis.	Novagen
pMR1	Kan^R P_{T7}::*divIVA*$_{Ef}$(L29D)*::6XHis*	Marc Rigden[a]
pMR2	Kan^R P_{T7}::*divIVA*$_{Ef}$ (E37P)*::6XHis*	MR
pMR3	Kan^R P_{T7}::*divIVA*$_{Ef}$ (E37P, N43P, L46D)*::6XHis*	MR
pMR4	Kan^R P_{T7}::*divIVA*$_{Ef}$(E37P, N43P, L46D, L50D, L57F)*::6XHis*	MR
pMR5	Kan^R *P_{T7}::divIVA*$_{Ef}$(E37P, N43P, L46D, L50E, L57F)*::6XHis*	MR
pMR6	Kan^R *P_{T7}::divIVA*$_{Ef}$(1-190)*::6XHis*	MR
pMR7	Kan^R P_{T7}::*divIVA*$_{Ef}$()130-190)*::6XHis*	MR
pMR8	Kan^R *P_{T7}::divIVA*$_{Ef}$()60-190)*::6XHis*	MR
pMR9	Kan^R *P_{T7}::divIVA*$_{Ef}$()60-130)*::6XHis*	MR
pMR10	Kan^R P_{T7}::*divIVA*$_{Ef}$(L143P)*::6XHis*	MR
pMR11	Kan^R *P_{T7}::divIVA*$_{Ef}$ (L104P)*::6XHis*	MR
pMR12	Kan^R *P_{T7}::divIVA*$_{Ef}$(L104, L143P)*::6XHis*	MR
pMR13	Kan^R *P_{T7}::divIVA*$_{Ef}$(L104P, I115P)*::6XHis*	MR
pMR14	Kan^R *P_{T7}::divIVA*$_{Ef}$(L104P, I115P, L143P)*::6XHis*	MR
pMR15	Kan^R *P_{T7}::divIVA*$_{Ef}$(L104P, I115P, I125P)*::6XHis*	MR
pMR16	Kan^R *P_{T7}::divIVA*$_{Ef}$(L104P, I115P, I125P, L143P)*::6XHis*	MR
pUC18	Amp^r *P_{lac}::lacZ*	Amersham Pharmacia
pSM1	Amp^r *P_{lac}::divIVA*$_{Ef}$ (L29D)	This study
pSM2	Amp^r *P_{lac}::divIVA*$_{Ef}$ (E37P, N43P, L46D, L50D, L57F)	This study
pSM3	Amp^r *P_{lac}::divIVA*$_{Ef}$ (E37P, N43P, L46D, L50E, L57F)	This study
pSM4	Amp^r *P_{lac}::divIVA*$_{Ef}$ (E37P)	This study
pSM5	Amp^r *P_{lac}::divIVA*$_{Ef}$ (E37P, N43P, L46D)	This study
pSM6	Amp^r *P_{lac}::divIVA*$_{Ef}$	This study
pSM7	Amp^r *P_{lac}::divIVA*$_{Ef}$ (E37P, N43P, L46D, L50Y, L57F)	This study
pSM8	Amp^r *P_{lac}::divIVA*$_{Ef}$ (E37P, N43P, L46E, L50D, L57F)	This study
pSM9	Amp^r *P_{lac}::divIVA*$_{Ef}$ (1-190)	This study
pSM10	Amp^r *P_{lac}::divIVA*$_{Ef}$ (Δ60 - 190 aa)	This study
pSM11	Amp^r *P_{lac}::divIVA*$_{Ef}$ (Δ131 - 189 aa)	This study
pSM12	Amp^r *P_{lac}::divIVA*$_{Ef}$ (Δ60 - 130 aa)	This study
pSM13	Amp^r *P_{lac}::divIVA*$_{Ef}$ (L143P)	This study

pSR-X	Amp^r P_{lac}::*prgX*	Ramirez *et al.*, 2004.
pDiv.His	Amp^r P_{lac}::*divIVA$_{Ef}$*::*6XHis*	This study
pSM1.His	Amp^r P_{lac}::*divIVA$_{Ef}$* (L29D)::*6XHis*	This study
pSM2.His	Amp^r P_{lac}::*divIVA$_{Ef}$* (E37P)::*6XHis*	This study
pSM3.His	Amp^r P_{lac}::*divIVA$_{Ef}$* (E37P, N43P, L46D)::*6XHis*	This study
pSM4,His	Amp^r P_{lac}::*divIVA$_{Ef}$* (E37P, N43P, L46D, L50D & L57F)::*6XHis*	This study
pSM5.His	Amp^r P_{lac}::*divIVA$_{Ef}$* (E37P, N43P, L46D, L50E, L57F)::*6XHis*	This study
pSM6.His	Amp^r P_{lac}::*divIVA$_{Ef}$* (1-190)::*6XHis*	This study
pSM7.His	Amp^r P_{lac}::*divIVA$_{Ef}$* (Δ130 – 190)::*6XHis*	This study
pSM8.His	Amp^r P_{lac}::*divIVA$_{Ef}$* (Δ60 - 190)::*6XHis*	This study
pSM9.His	Amp^r P_{lac}::*divIVA$_{Ef}$* (Δ60 - 130)::*6XHis*	This study
pSM10.His	Amp^r P_{lac}::*divIVA$_{Ef}$* (L104P)::*6XHis*	This study
pSM12.His	Amp^r P_{lac}::*divIVA$_{Ef}$* (L104P, L143P)::*6XHis*	
pX-18	Amp^r P_{lac}::*prgX$_{Ef}$*::*6XHis*	This study
pMSP3545[a]	Erm^R P$_{nisA}$::*nisA*	Dr. G. Dunny[b]
pMSPSRDiv-1	Erm^R P_{nisA}::*divIVA$_{Ef}$*	Ramirez *et al.*, 2004.
pMSPSRDiv-2	Erm^R P_{nisA}::$P_{divIVAEf}$-::*divIVA$_{Ef}$*	Ramirez *et al.*, 2004.
pMSP3535X	Erm^R, replicons: pAMβ1,ColE1; *nisRK*, P_{nisA}:: *prgX$_{Ef}$*	Dr. G. Dunny[b]

NB:

a) From Rigden M. 2005. Determining the role of coiled-coil domain interactions in the oligomerization of DivIVA from *Enterococcus faecalis.* M. Sc. Thesis University of Ottawa.

b) Dr. G. Dunny at University of Minnesota.

gel DNA electrophoresis with TAE for 1-Hr at 100V using the Bio-Rad Power Pac 300 (Bio-Rad Laboratories; Mississauga, ON) (Sambrooke and Russell, 2001). The 1Kb+ DNA or Supercoiled DNA Ladders (Invitrogen; Burlington, ON) were used depending on anticipated amplicon size. Gel photography was achieved using the Multi-Image Light Cabinet using the Alpha Imager 1220 software file version 5.04 (Alpha Innotech Corporation; San Leandro, CA).

All *divIVA*$_{Ef}$ amplicons were subcloned in pUC18 for use in the heterologous overexpression system such that *divIVA*$_{Ef}$ would be under the control of the lactose promoter (P_{lac}). Isopropropyl-β-thiogalactopyranoside (IPTG) can be used to bind to the lac repressor releasing P_{lac} to promote transcription and translation of *lac*Z triggering overexpression of DivIVA$_{Ef}$ (Sambrooke and Russell, 2001). Using this rationale, each *divIVA*$_{Ef}$ amplicon of the construct series "**pSM**" or the construct series "**pSM_.His**" (Table 2) was double digested with *Eco*RI (Invitrogen; Burlington, ON) and *Bam*HI (Fermentas; Burlington, ON) to facilitate ligation of the amplicons and pUC18. The *Eco*RI and *Bam*HI restriction sites are found on the multi-cloning site (MCS) of pUC18. Double digests were achieved using *Eco*RI (Invitrogen) and *Bam*HI (Fermentas). The reaction volume (100 µl) contained: 75 µl ddH_2O, 10 µl of purified insert DNA or 0.01µg/ml plasmid DNA (pDNA), 10 µl 10X *Eco*RI buffer (Invitrogen) and 2.5 µl of each primer (0.2 :g/:L). Reactions were incubated O/N at 37°C.

The *prgX*$_{Ef}$ amplicons were PCR cleaned and double digested with *Eco*RI (Invitrogen) and *Bam*HI (Fermentas) prior to ligation together with double digested and PCR purified pUC18 to produce the constructs pSR-X (*prgX*$_{Ef}$) and pX-18 (*prgX*$_{Ef}$*::His*). The construct pSR-X (*prgX*$_{Ef}$) was transformed in *E. coli* KJB24 while pX-18 was

transformed in *E. coli* KJB24, WM1250, PB103 and PB114 for overexpression and morphological studies.

The double digested vector and amplicons were then PCR purified (Qiagen) and ligation reactions containing 16 µl insert DNA, 1 µl pDNA, 2 µl 10X buffer (NEB) and 2 µl T4 DNA Ligase (NEB) were conducted. The 21 µl ligation reaction was incubated at 37^0C for 1.0- to 1.5-Hrs and then transformed in 50 µl $CaCl_2$ competent *E. coli* DH5-α (Clontech) cells using the heat shock method (Sambrooke and Russell, 2001). Following an incubation of ~16 hrs at 37°C, positive isolates were screened by agarose gel electroporation and DNA was obtaining using the "cracking method" with: 25 µl of a 1:9 cracking buffer (0.2 ml 0.5 M EDTA (pH8), 0.1 g SDS, 0.005 g bromophenol blue, 1.0 ml glycerol and 7.8 ml ddH_2O) and 1 M NaOH in 25 µl ddH_2O and an individual isolate.

For use with the homologous overexpression system, double digestions of the shuttle vector pMSP3545 and all $divIVA_{Ef}$ amplicons were achieved with *Nco*I (Fermentas) and *Xba*I (Fermentas). The double digested vector and amplicons were then PCR purified (Qiagen). The 100 µl ligation reaction and the Cracking method were identical to those mentioned above.

E. faecalis JH2-2 was as the indicator $DivIVA_{Ef}$ overexpression homologous system. *E. faecalis* JH2-2 was transformed using electroporation with either pMSPSRDiv-1 (P_{nisA}::$divIVA_{Ef}$) or pSMSPSRDiv-2 (P_{nisA}::$P_{divIVAEf}$::$divIVA_{Ef}$).

All $divIVA_{Ef}$ constructs to be transformed into *E. faecalis* JH2-2 required the following electroporation protocol: 10 µl of 10mM chilled $CaCl_2$, 10 µl of 10mM chilled $MgCl_2$, and 2 µl of full-length $divIVA_{Ef}$ construct subcloned into the plasmid pMSP3545. The selected settings included: 2.5V, 200 Ω, and 25 µFD (1 pulse for 3

seconds). The eletroporated cells were septically transferred into an Eppendorf tube containing 1 ml of chilled BYGT where the cells rested for 5 minutes. The cell were then incubated for 2-hr at 37°C without agitation and plated on BHI_{Ery10} agar plates followed by a final incubation for 16- to 20-Hrs at 37°C.

All constructs created for the heterologous or homologous overexpression systems were initially identified by agarose gel electrophoresis (1%) following the cracking method and confirmed using DNA sequencing performed by the University of Ottawa Core Facility for DNA Synthesis and Sequencing.

2.4 *divIVA$_{Ef}$* construct series:

Across the multi-sequence alignment of DivIVA (Figure 2A), three areas of high consensus are found and include: a large N-terminal, two smaller central regions and a small C-terminal. Based on bioinformatic analysis (Figure 2B), these regions contain predicted coiled-coil domains in $DivIVA_{Ef}$ thought to be involved with the protein's ability to self-interact and the conservation of coiled-coil domains across species. By abrogating the coiled-coil domains individually to prevent $DivIVA_{Ef}$ oligomerization, it might be possible to arrest cell division (Rigden, 2005).

To render the N-terminal coiled-coil domain non-functional, point mutations were introduced: L29D, E37P, E37P-N43P-L46D, E37P-N43P-L46D-L50D-L57F and E37P-N43P-L46D-L50D-L57F. The C-terminal mutation involved a deletion from aa 190 – 233. The two central domains collectively comprise aa 60 – 190. The first central coiled-coil domain ranges from aa 60 – 130 while the second central coiled-coil domain involves aa 130 – 190 (Rigden, 2005).

In the present research, wt *divIVA*$_{Ef}$ and all mutant *divIVA*$_{Ef}$ amplicons were PCR amplified from constructs pMR1 – pMR12 (Rigden, 2005) using the 5' primer IVA-1 and the 3' primer IVA-5 incorporating *Eco*RI and *Bam*HI respectively, to create the construct series pSM1 to pSM10 known as the "**pSM_**" series that required the cloning vector pUC18 for transformation in *E. coli* (Figure 3). This series included: pUC18 (negative control), pSM6 (wt *divIVA*$_{Ef}$ - positive control) pSM1 (L29D from pMR1), pSM2 (E37P, N43P, L46D, L50D, L57F from pMR4), pSM3 (E37P, N43P, L46D, L50E, L57F from pMR5), pSM4 (E37P from pMR2), pSM5 (E37P, N43P, L46D from pMR3), pSM9 (1 – 190 from pMR6), pSM10 (Δ60 – 190 from pMR8), pSM11 (Δ130 – 190 from pMR7), pSM12 (Δ60 – 130 from pMR9) and pSM13 (L104P, L143P from pMR12). The constructs pSM1 to pSM8 afftect the N-terminal coiled-coil domain, pSM11 to pSM13 abrogate the central coiled-coil domains and pSM9 affects the C-terminal coiled-coil domain of *divIVA*$_{Ef}$ (Figure 3).

Alternatively, wild type and mutant *divIVA*$_{Ef}$ amplicons from pMR1 – pMR12 were PCR amplified using the 5' primer IVA-1 and the 3' primer IVA-His incorporating *Eco*RI and *Bam*HI respectively, to produce the *divIVA*$_{Ef}$*::6XHis* fusion amplicon for the generation of constructs pSM1.His to pSM12.His known as the **pSM_.His** series that required the subcloning in vector pUC18 for transformation using *E. coli* strains (Figure 3). This series included: pUC18 (negative Control), the positive control pDiv.His (*divIVA::6XHis*) pSM3.His (E37P, N43P, L46D from pMR3), pSM4.His (E37P, N43P, L46D, L50D, L57F from pMR4), pSM6.His (1 – 190 from pMR6), pSM7.His (Δ130 – 190 from pMR7), pSM8.His (Δ60 – 190 from pMR8), pSM9.His (Δ60 – 130 from pMR9), and pSM12.His (L104P, L143P from pMR12). The constructs pSM3.His and

Figure 3: Flow chart depicting *divIVA*$_{Ef}$ constructs for this research. The heterologous overexpression systems are divided into two construct series. The first construct series known as "**pSM_.His**" abrogates the N-terminal, first central, second central and C-terminal coiled coil domains individually. The **pSM_.His** series is transformed in *E. coli* PB103 (*minB*), *E. coli* PB114 (Δ*minB*), *E. coli* KJB24 (*rodA*-, *minB*), and *E. coli* WM1250 (*rodA*-, Δ*minB*). The second heterologous overexpression system known as " **pSM_**" abrogates the N-terminal coiled-coil domain in different ways and both central coiled-coil domains are abrogated by a single large deletion. The homologous overexpression systems are investigated using two *divIVA*$_{Ef}$ constructs. The first construct known as pMSPSRDiv-1 examines DivIVA$_{Ef}$ overexpression in a nisin inducible manner while pMSPSRDiv-2 examines DivIVA$_{Ef}$ overexpression in a non-inducible manner with *divIVA*$_{Ef}$ under the control of its own native promoter.

Figure 3

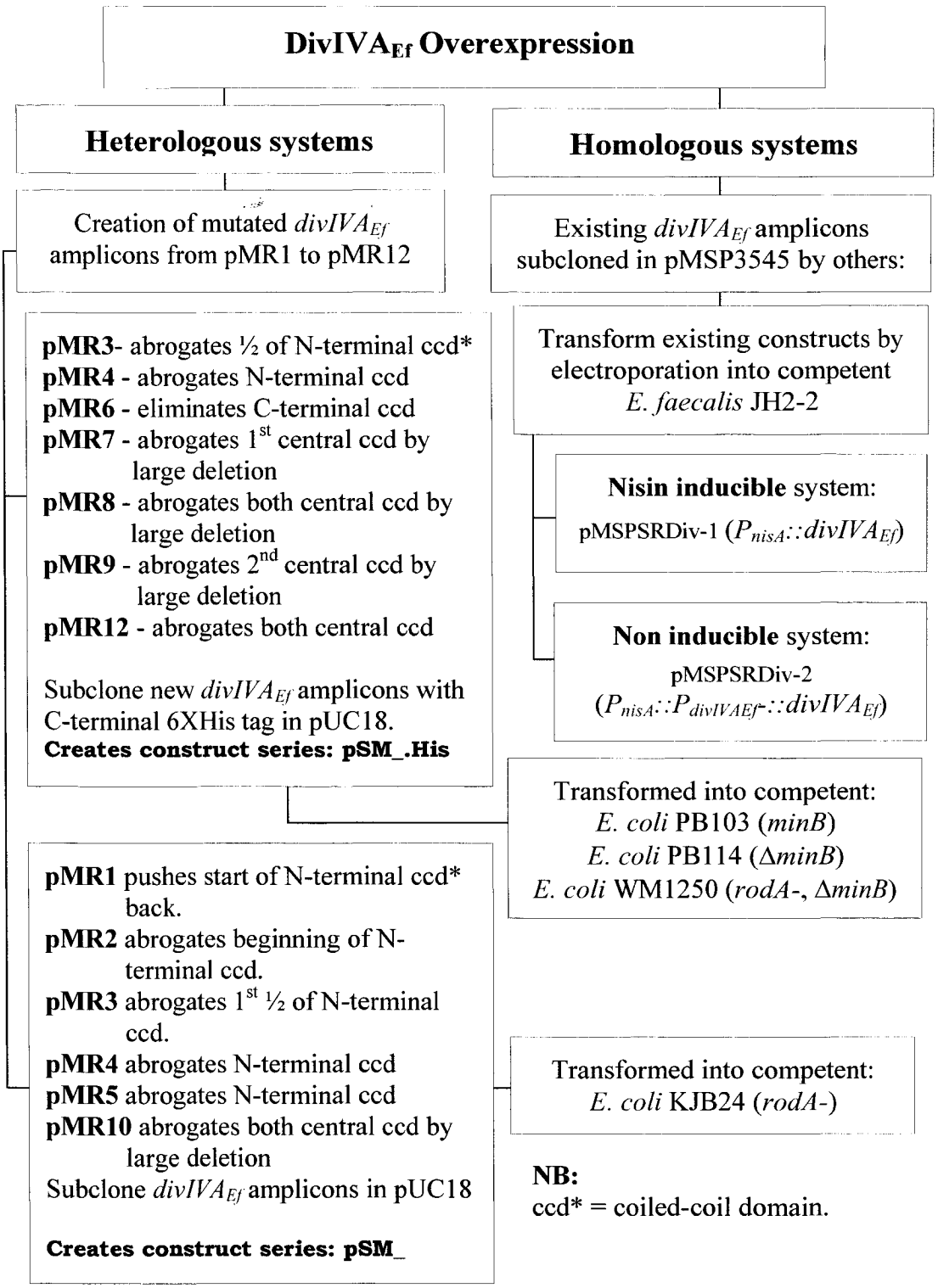
DivIVA$_{Ef}$ Overexpression
Heterologous systems
Homologous systems
Creation of mutated *divIVA$_{Ef}$* amplicons from pMR1 to pMR12
Existing *divIVA$_{Ef}$* amplicons subcloned in pMSP3545 by others:
pMR3- abrogates ½ of N-terminal ccd*
pMR4 - abrogates N-terminal ccd
pMR6 - eliminates C-terminal ccd
pMR7 - abrogates 1st central ccd by large deletion
pMR8 - abrogates both central ccd by large deletion
pMR9 - abrogates 2nd central ccd by large deletion
pMR12 - abrogates both central ccd
Subclone new *divIVA$_{Ef}$* amplicons with C-terminal 6XHis tag in pUC18.
Creates construct series: pSM_.His
Transform existing constructs by electroporation into competent *E. faecalis* JH2-2
Nisin inducible system:
pMSPSRDiv-1 (*P$_{nisA}$::divIVA$_{Ef}$*)
Non inducible system:
pMSPSRDiv-2
(*P$_{nisA}$::P$_{divIVAEf}$::divIVA$_{Ef}$*)
Transformed into competent:
E. coli PB103 (*minB*)
E. coli PB114 (Δ*minB*)
E. coli WM1250 (*rodA*-, Δ*minB*)
pMR1 pushes start of N-terminal ccd* back.
pMR2 abrogates beginning of N-terminal ccd.
pMR3 abrogates 1st ½ of N-terminal ccd.
pMR4 abrogates N-terminal ccd
pMR5 abrogates N-terminal ccd
pMR10 abrogates both central ccd by large deletion
Subclone *divIVA$_{Ef}$* amplicons in pUC18
Creates construct series: pSM_
Transformed into competent:
E. coli KJB24 (*rodA*-)
NB:
ccd* = coiled-coil domain.

pSM4.His abrogate the N-terminal coiled-coil domain, pSM7.His, pSM8.His, pSM9.His and pSM12.His abrogate the central coiled-coil domains and pSM6.His affects the C-terminal coiled-coil domain of *divIVA$_{Ef}$*.

Both the **pSM_** and the **pSM_.His** series were used in DivIVA$_{Ef}$ overexpression and morphological studies; employed SDS-Page, Western blot and phase contrast microscopy; and were transformed in *E. coli* strains PB103 (*minB*), *E. coli* PB114 (Δ*minB*), *E. coli* KJB24 (*minB, rodA*$^-$) or *E. coli* WM1250 (Δ*minB, rodA*$^-$).

The *E. faecalis* JH2-2 homologous overexpression system comprised two construct series. The first series is comprised by nisin inducible system and requires a single construct known as pMSPSRDiv-1 (*P$_{nisA}$::divIVA$_{Ef}$*). The second series is also comprised by a single construct known as pMSPSRDiv-2 (*P$_{nisA}$::divIVA$_{Ef}$*), which is a non inducible overexpression system (Figure 3).

2.5 Growth Curves:

Cell growth in *E. coli* KJB24 (*minB, rodA*$^-$) transformed with either pUC18 (negative control) or pSM6 (wt *divIVA$_{Ef}$* - positive control) was conducted to observe growth and the optimal mid-exponential phase for IPTG induction for DivIVA$_{Ef}$ overexpression and cell morphology studies. Samples were tested in triplicate. Cell growth in *E. coli* KJB24 and *E. faecalis* JH2-2 was examined using both liquid and solid media. The aim was to establish the optimal time for the addition of IPTG required for DivIVA$_{Ef}$ overexpression using either background. The *E. coli* transformants carried one of: pUC18 (negative control) or pSM6 (wt *divIVA$_{Ef}$* – positive control) while the *E. faecalis* JH2-2 transformants carried one of: pMSP3545 (negative control), pMSPSRDiv-1 (*P$_{nisA}$::divIVA$_{Ef}$*) or pSMSPSRDiv-2 (*P$_{nisA}$::P$_{divIVAEf}$::divIVA$_{Ef}$*).

To ensure that equivalent numbers of *E. coli* KJB24 and *E. faecalis* JH2-2 cells would be used in growth studies, the inocula were standardized as follows. Each species was diluted 10-fold from O/N liquid LB_{Amp100}, BHI_{Ery10} or BYGT $_{Ery10}$ cultures to obtain an optical density at 600 nm (OD_{600}) of ~0.05. The O/N cultures of *E. coli* KJB24 or *E. faecalis* JH2-2 were diluted tenfold to inoculate 60 ml of liquid LB_{Amp100}, BHI_{Ery10} or BYGT $_{Ery10}$ with ~1 x 10^6 cells and incubated at 37°C for 8- to 12-Hrs. *E. coli* KJB24 cells were grown with agitation while *E. faecalis* JH2-2 were grown without agitation.

One milliliter of culture was removed at times (t) = 0.5-, 1-, 1.5-, 2-, 2.5-, 3-, to 12-Hrs to measure the OD_{600}. The experiment was stopped after three time points measured similar absorbencies indicating the onset of stationary phase.

At every time point (t), 20 µl of sample was plated using the drop plate method of enumeration (section 2.6.1). The plates were incubated for 24-Hrs prior to counting. Growth studies were performed in triplicate for each bacterial species.

E. faecalis JH2-2 was grown in either 10 ml of BHI_{Ery10} or BYGT $_{Ery10}$ broth at 37°C without agitation. The next day (~16 – 20 hrs), a 1:10 dilution in 10 ml of either fresh BHI with Ery_{125} or BYGT with Ery_{125} was incubated at 37°C without agitation, to an absorbancy reading of OD_{600nm} ~0.9 – 1.0. A nisin concentration titration experiment was carried out to determine optimal induction concentration. Cultures were incubated post-nisin induction 4-Hrs at 37°C without agitation. The samples were then harvested, at 12,000 rpm for 30 seconds and all supernatant was removed. Pellets were preserved at – 20^0C for future SDS-Page and Western blot analysis. The identical cell fixation protocol, as found in section 2.8, was also used.

2.6 Cell enumeration by drop plate method:

To determine the number of viable colony forming units (CFU/ml), serial dilutions of bacterial cultures from cell growth experiments were prepared from 0 to 10^{-8} using LB_{Amp100}, BHI_{Ery10} or $BYGT_{Ery10}$ broth. Two 20 µl drops per sample were separately dispensed from each dilution onto a pre-warmed (37^0C) agar LB_{Amp100} or BHI_{Ery125} plate to absorb into the agar (~10-min). The plates were incubated at 37^0C for 16- to 20-Hrs.

Counts were averaged for each dilution at a specific time point and adjusted for the dilution factor. The data was organized into either a logarithmic (CFU/ml vs. time) or an absorbancy (OD_{600} vs. time) graph.

2.7 $DivIVA_{Ef}$ Overexpression:

The **pSM** or **pSM_.His** series constructs were transformed in one of: *E. coli* PB103, *E. coli* PB114, *E. coli* KJB24 or *E. coli* WM1250 (Table 1). To ensure that equivalent numbers of *E. coli* cells would be used in overexpression studies, the inocula were standardized as follows. Each strain was diluted 10-fold from O/N liquid LB_{Amp100} cultures to obtain an OD_{600} ~0.05. The O/N cultures were then diluted tenfold to inoculate 10 ml of liquid LB_{Amp100} broth (OD_{600} ~0.4 – 0.6). Cultures were then induced with IPTG (t = 0-Hrs) and further incubated at 37°C with agitation for 2-, 4- and 6-hr post-IPTG induction. All constructs were tested in duplicate.

E. faecalis JH2-2 cultures were diluted 10-fold from O/N liquid BHI_{Ery10} or $BYGT_{Ery10}$ cultures to obtain an OD_{600} of ~0.05. The O/N cultures were diluted tenfold to inoculate 10 ml of BHI_{Ery10} or $BYGT_{Ery10}$ broth and incubated at 37°C without agitation. Cultures were then induced with nisin (t = 0-Hrs) at OD_{600} ~0.4 to 0.6 and further

incubated at 37°C without agitation for 3- and 4-hr post-nisin induction (OD_{600}~ 0.9 to 1.0). All constructs were tested in duplicate.

All samples used in overexpression studies were vortexed (12,000 rpm for 30-s), supernatant discarded and the pellets were maintained at 4°C for cell fixation (section 2.8) and at -20°C for SDS-Page and Western blots.

2.8 Cell fixation and microscopy:

2.8.1 Cell fixation for phase contrast microscopy:

The pelleted samples (12,000 rpm for 30-s) from overexpression studies were fixed with 6% formaldehyde (Sigma® Chemical; St. Louis, MO) and 0.2%glutaraldehyde (Fisher Chemical; Nepean, ON) as described by Ramirez-Arcos *et al.* (2001). Ten microlitre aliquots of fixed cells were adhered to cover slips pre-treated with 0.01% polylysine. Coverslips were then placed onto slides containing a drop of 50% glycerol and were sealed to the slide with clear nail polish to prevent dehydration of the medium. Fixed cells were maintained at 4^0C.

All images were visualized using phase contrast microscopy under the 100X oil immersion objective. Either the Zeiss Axioskop microscope or the Zeiss Axio (Vision 3.0) microscope was used. Images were obtained using Northern Eclipse software (version 5.0) or Northern Exposure (release 2.9), respectively. Image analysis software by Image-Pro version 3.0 (Media Cybernetics) was used to count and measure cells (~500 cells per construct).

Analyses of the cell length (μm) or cell area (μm^2) were achieved by creating cell length or cell diameter classes. Statistical classes were determined by calculating the average size (length or diameter = X) of transformants carrying the negative control per

bacterial species and/or strain. The average size was added to itself to create the next class 2X and so on. This would determine the number or –fold increase of cells within a total population.

2.8.2 Cell fixation for transmission electron microscopy:

The pelleted samples (12,000 rpm for 30-s) from overexpression studies were fixed with 1.6% glutaraldehyde (Fisher Chemical) in PBS (pH 7.4) as described by Ramirez-Arcos *et al* (2001).

To localize $DivIVA_{Ef}$ in its wild-type *E. faecalis* JH2-2 or to localize $DivIVA_{Ef}$ from *E. faecalis* JH2-2 transformants carrying pMSPSRDiv-1 or pMSPSRDiv-2, immunoelectron microscopy was performed by Peter Rippstein (Laboratory Pathology facilities, Civic Campus, Ottawa Hospital, Ottawa, On, Canada). $DivIVA_{Ef}$ immuno-localization in *E. faecalis* JH2-2 was performed using rabbit polyclonal -$DivIVA_{Ef}$ with a final antiserum dilution of 1:250. Samples were visualized using a Jeol 1230 Electron Microscope equipped with a digital AMT camera.

2.8 SDS-PAGE:

Proteins were separated by sodium dodecyl sulphate (SDS) polyacrylamide gel electrophoresis (SDS-PAGE) using the protocol described by Sambrooke and Russell (2001). SDS-PAGE was used to determine relative levels of protein expression, the presence of purified proteins, and for Western blot analysis (to confirm $DivIVA_{Ef}$ overexpression).

Sample preparation using the *E. coli* heterologous overexpression systems involved the addition of loading buffer (62.5 mM Tris-HCl, pH 6.8, 2% SDS, 25% glycerol, 0.01%

bromophenol blue) to each sample in a 1:5 ratio followed by boiling the samples for 5 minutes to ensure complete denaturation.

Sample preparation from the *E. faecalis* JH2-2 homologous overexpression systems involved adding lysozyme buffer (10mM Tris-HCl (pH 8), 50 mM EDTA, 0.5mM sucrose, 20 μg/ml lysozyme and ~60% ddH_20) for incubation at 37°C for 15-min. The cells were rinsed with wash buffer (10mM Tris-HCl (pH 8), 50 mM EDTA, 0.5mM sucrose, and ~70% ddH_20) two times. The above mentioned denaturation protocol could be conducted.

All denatured samples were loaded into gels (a 5% stacking and 12% resolving layer) for protein separation. Electrophoresis was conducted using 5 mM Tris-HCl, 50 mM glycine and 0.1% SDS, pH 8.3 as the running buffer and run at 100V until the bromophenol blue dye exited the gel. Unless used for Western blotting, gels were stained with Coomassie brilliant blue (Sambrooke and Russell, 2001) and destained using a 45% methanol, 10% acetic acid solution.

Three repetitions of densitometric analysis using Alpha Imager 1220 software (version 5.04; Alpha Innotech Corporation) were performed to standardize protein for Western blot analysis.

2.10 Western blot

Following electrophoresis and prior to staining with Coomassie brilliant blue, samples were transferred to Immobilon-P membranes (Millipore Corporation; Maine, US) for 1-Hr at 100 V. The protein running buffer contained 25 mM Tris base, 250 mM glycine, and 0.5% SDS for a 5X solution.

Blot of samples containing *divIVA$_{Ef}$* constructs with a C-terminal His tag (series "**pSM_.HIS**") in the *E. coli* system were probed for 1-Hr at room temperature (RT) with commercial monoclonal anti-His antibody (QIAgen) diluted 1:1000 in TTBS (0.05% Tween-20 in Tris-buffered saline), followed by incubation with goat anti-mouse IgG conjugated to alkaline phosphatase (1:3,000; Bio-Rad).

Blocking of samples containing *divIVA$_{Ef}$* constructs (series "**pSM_**") in the *E. coli* system included: 3% skim milk and blots were probed for 1-Hr (RT) with rabbit polyclonal anti- DivIVA$_{Ef}$ (Ramirez-Arcos *et al.,* 2001) diluted to 1:1000 to 1:2000 in TTBS, followed by incubation with goat anti-rabbit IgG conjugated to alkaline phosphatase (1:3,000; Bio-Rad) using previously described methods (Ramirez-Arcos *et al.*, 2001; Szeto *et al.*, 2001).

Blocking of samples containing *prgX$_{Ef}$* constructs in the *E. coli* system included: 3% skim milk and blots were probed for 1-Hr (RT) with anti-PrgX$_{Ef}$ (Dr. G Dunny, U of Minnesota) diluted 1:1000 or anti-His antibody (QIAgen) diluted 1:1000, respectively in TTBS, and incubation with goat anti-rabbit IgG conjugated to alkaline phosphatase (1:3,000; Bio-Rad).

Blocking of samples with *divIVA$_{Ef}$* constructs in the *E. faecalis* system included: 3% skim milk and blots were probed for 1-Hr (RT) with rabbit polyclonal anti-DivIVA$_{Ef}$ (Ramirez-Arcos *et al.,* 2001) diluted to 1:1000 - 1:2000 in TTBS, and incubation with goat anti-rabbit IgG conjugated to alkaline phosphatase (1:3,000; Bio-Rad) as previously described (Ramirez-Arcos *et al.*, 2001; Szeto *et al.*, 2001).

All blots were developed using the Atto Phos Plus kit (JBL Scientific Inc. San Luis Obispo, CA).

RESULTS:

Overview

One of the major objectives of my research was to microscopically assess the effects of DivIVA$_{Ef}$ overexpression on cell morphology using *E. coli*, PB103 (*minB*), PB114 (Δ*minB*), KJB24 (*minB*, *rodA*$^-$), and WM1250 (Δ*minB*, *rodA*$^-$). In *E. faecalis* JH2-2 only wt DivIVA$_{Ef}$ overexpression was also assessed. Overexpression means higher than native levels of a protein are produced, potentially resulting in a novel cell phenotype exhibiting filamentation or minicell formation suggestive of cell division inhibition (Errington *et al.*, 2003). To achieve these ends, both wt and mutated *divIVA$_{Ef}$* amplicons were cloned in a suitable vector sustainable in the bacteria used.

The cloning vector pUC18 is small in size (2686 base pairs (bp)) and it is a high copy number plasmid due to the absence of *rop* thought to regulate plasmid DNA replication (Cesareni *et al.*, 1982; Gordon *et al.*, 1997). There are four advantages to employing pUC18 as the cloning vector in the heterologous *E. coli* system. First, the pMB1 replicon *rep* is present and is responsible for plasmid replication. Second, the *bla* gene, encoding beta-lactamase conferring resistance to ampicillin (Amp) is present. Third, the region of *E. coli lac* operon containing: the CAP protein binding site, the promoter P_{lac}, the *lac* repressor binding site and the 5'-terminal part of the *lacZ* gene encoding the N-terminal fragment of beta-galactosidase are all present. Finally, the presence of a multicloning site (polylinker) permits the subcloning of foreign DNA of interest using the appropriate restriction sites (Fermentas www.fermentas.com/techinfo/nucleicacids/mappuc1819.htm). For these reasons, pUC18 was employed as the negative control in all overexpression and morphological studies where the heterologous *E. coli* systems were employed.

E. faecalis JH2-2 was selected since it is plasmid-free facilitating straightforward transformation, eliminating potential problems of plasmid recombination. The cloning vector for the homologous system made use of the *E. coli* - *E. faecalis* shuttle-vector pMSP3545 (Dr. G. Dunny, U of Minnesota). The plasmid pSMSP3545 is recognized as a suitable vector to investigate protein overexpression from enterococcal backgrounds (Bryan *et al.*, 2000). The implementation of a homologous system permitted the propagation of cells in *E. coli* due to the ColE1 origin of replication on the shuttle vector. It also permitted the highest DNA yield using *E. coli* prior to construct transformation by electroporation in *E. faecalis* JH2-2 where propagation will occur due to the pAMβ1 origin of replication. The pMSP3545 plasmid contains a marker for selection using erythromycin (Ery) and provides the *nisRK* genes, critical to the nisin-control expression (NICE) system (Bryan *et al;* 2000). The efficiency of genes under the control of the nisin promoter is reported to be greater than genes induced under the control of Gram-positive promoters like *PSpac, PxylA* and *PlacA* (Edwards *et al;* 2000).

3.1 Growth Curves

Cell growth was examined to ascertain the effects of $DivIVA_{Ef}$ overexpression on population size and population mass using heterologous and homologous systems. The cell population and population mass typically increase with time during which individual cells actually progress through changes in cell mass (i.e., growth, division, growth, division, growth, etc...).

Competent *E. coli* KJB24 cells were transformed with pUC18 (negative control) and grown in liquid LB_{Amp100}. Samples were taken at specified time points and plated on LB_{Amp100} to be counted and CFU/ml measured (Figure 4A). A classically characteristic

Figure 4: Unique cell growth in *E. coli* KJB24 transformed with pUC18 or pSM6 (wt $divIVA_{Ef}$). **A-** *E. coli* KJB24 transformed with pUC18 as measured by Log CFU/ml following plating on LB_{Amp100}; **B-** *E. coli* KJB24 transformed with pSM6 as measured by turbidity at OD_{600}. Error bars represent ±1 standard deviation (SD) based on samples done in triplicate.

Figure 4

A.

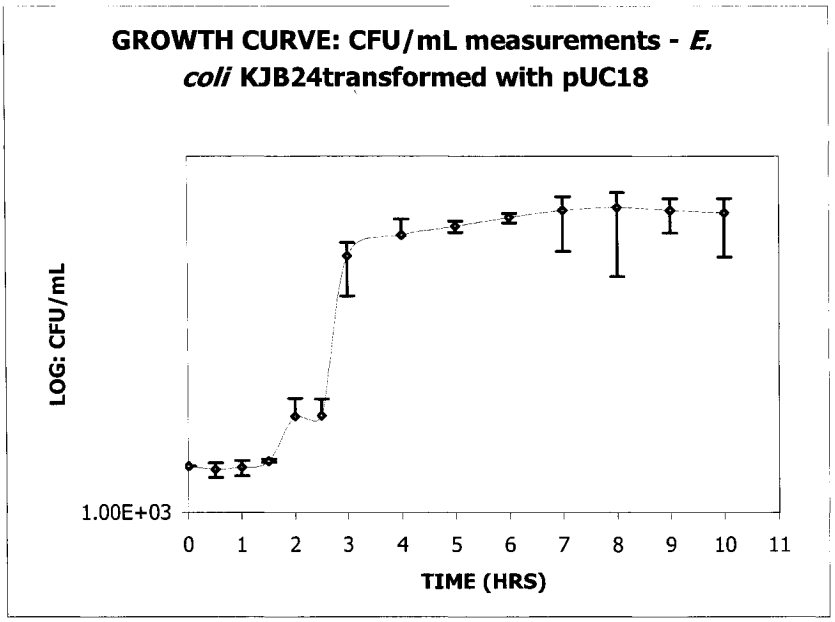
GROWTH CURVE: CFU/mL measurements - E. coli KJB24transformed with pUC18
LOG: CFU/mL
1.00E+03
0 1 2 3 4 5 6 7 8 9 10 11
TIME (HRS)

B.

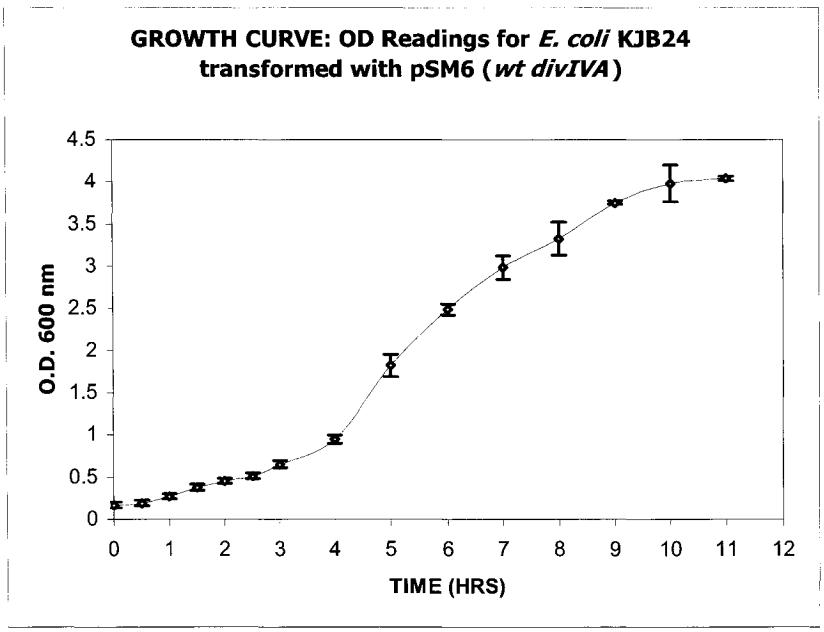
GROWTH CURVE: OD Readings for E. coli KJB24 transformed with pSM6 (wt divIVA)
O.D. 600 nm
4.5
4
3.5
3
2.5
2
1.5
1
0.5
0
0 1 2 3 4 5 6 7 8 9 10 11 12
TIME (HRS)

growth curve was produced and indicates various stages of growth beginning with the addition of cells to sterile media and ending with the death of all of the cells present (includes: lag phase, exponential phase, stationary phase and death phase).

E. coli KJB24 cells transformed with pSM6 (wt $divIVA_{Ef}$ - positive control) and grown in liquid LB_{Amp100}. Samples were taken at specified time points and plated on LB_{Amp100}. Cell growth could only be determined by turbidity measurements using optical density at 600 nm (OD_{600}) (Figure 4B) because cells carrying pSM6 failed to produce any culturable cells for counting following plating. Turbidity measurements determine the amount of light scattered by a suspension of cells and is directly to cell mass or cell number. A shallower curve relative to *E. coli* KJB24 transformants with pUC18 was observed, suggesting a lengthened exponential phase characterized by less growth.

The results of the growth curves demonstrate that mid-exponential phase of *E. coli* KJB24 transformants carrying pUC18 or pSM6 is 3- to 4-hours incubation of the diluted culture initiated from an original subculture incubated at 37^0C O/N with agitation.

E. faecalis JH2-2 cell growth was assessed to determine if increased $DivIVA_{Ef}$ concentration would alter cell phenotype causing the production of filamentous cells suggestive of cell division arrest reminiscent of $DivIVA_{Bs}$ overexpression in *B. subtilis* or if such overexpression would prove lethal in *E. faecalis* JH2-2 (Cha and Stewart, 1997).

Parental plasmid-free *E. faecalis* JH2-2 were transformed by electroporation with one of: pMSP3545 (negative control), the nisin-inducible pMSPSRDiv-1 (P_{nisA}::$divIVA_{Ef}$), or the non-inducible pMSPSRDiv-2 (P_{nisA}::$P_{divIVAEf}$::$divIVA_{Ef}$). *E. faecalis* JH2-2 transformants exhibited some similarity in growth pattern, duration and cell numbers as measured by colony-forming unit CFU/ml (Figure 5A). *E. faecalis* JH2-2 carrying

pMSPSRDiv-2 ($P_{nisA}::P_{divIVAEf}::divIVA_{Ef}$) demonstrated a surge of growth dramatically greater than transformants carrying either pMSP3545 or pMSPSRDiv-1 ($P_{nisA}::divIVA_{Ef}$) during the exponential phase. The onset of the stationary phase for transformants with pMSPSRDiv-2 is initiated earlier than those transformants with either pMSP3545 or pMSPSRDiv-1.

A nisin concentration titration experiment was performed using plasmid-free *E. faecalis* JH2-2 to determine DivIVA$_{Ef}$ overexpression induction. *E. faecalis* JH2-2 cells were permitted to grow to an OD_{600nm} ~ 0.5. The effects of nisin at concentrations: 0.0, 0.2, 0.5, 1.0, 1.5 and 2.0 µg/ml were permitted to exert their affects on cells for 7-Hrs. Figure 5B depicts the growth curve of the various nisin-induced cultures over time. The inhibitory concentration of nisin *E. faecalis* growth was determined to be 2.0 µg/ml. While cells grew better and maintained their inherent cell phenotype with low levels of nisin, cells did not overexpress DivIVA$_{Ef}$ as demonstrated by Western blot (Results not shown). Conversely, 1.5 µg/ml of nisin not only induced DivIVA$_{Ef}$ overexpression of *E. faecalis* JH2-2, but also is sub-inhibitory to growth.

E. faecalis JH2-2 transformed with pMSP3545, pMSPSRDiv-1, or pMSPSRDiv-2 each demonstrated an exponential phase at 2- to 4-Hrs following incubation of the diluted culture initiated from an original subculture incubated at 37^0C O/N without agitation.

In summary, mid-exponential phase for *E. coli* KJB24 transformants carrying pUC18 or pSM6 and for *E. faecalis* JH2-2 transformed with either pMSP3545, pMSPSRDiv-1,

Figure 5: Cell growth of *E. faecalis* JH2-2 transformed with pMSP3545 (negative control), pMSPSRDiv-1 (positive control: inducible system) or pMSPSRDiv-2 (positive control: natural promoter system). **A-** Growth curve measured by log CFU/mL using *E. faecalis* JH2-2 in **ORANGE** depicts transformants carrying pMSMPSRDiv-2 (P_{divIVA}); **PURPLE** depicts transformed with pMSP3545 (negative control) and **GREEN** depicts transformants carrying pMSPSRDiv-1 (P_{nisA}); **B-** Effect of nisin on cell growth of parental plasmid-free *E. faecalis* JH2-2. Logarithmic growth curve as measured at OD_{600}. Error bars represent ±1 standard deviation (SD) based on samples done in triplicate.

Figure 5

A.

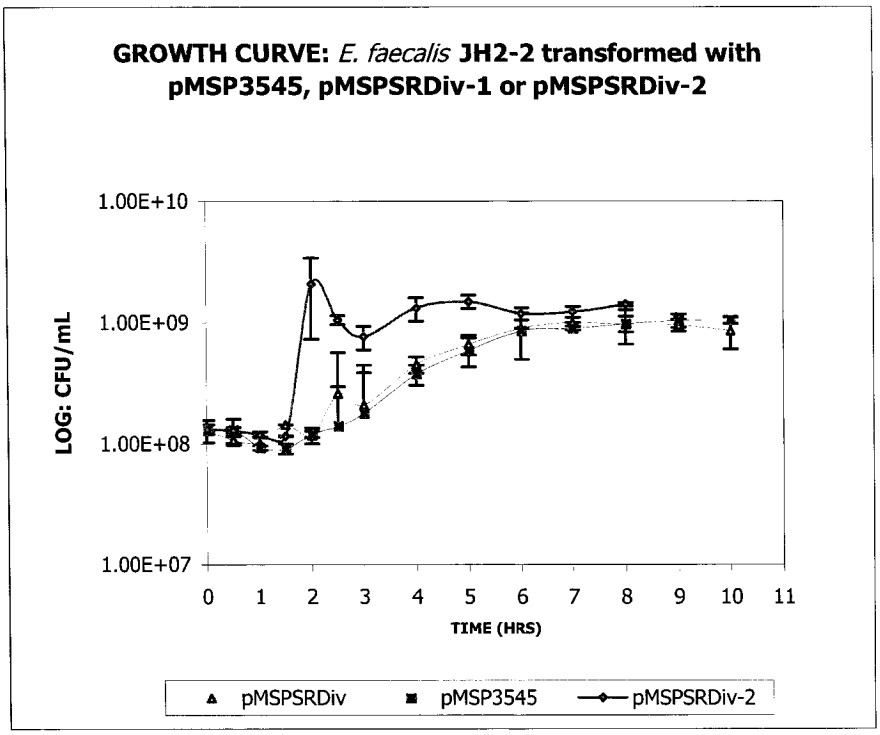
GROWTH CURVE: E. faecalis JH2-2 transformed with pMSP3545, pMSPSRDiv-1 or pMSPSRDiv-2
LOG: CFU/mL
1.00E+10
1.00E+09
1.00E+08
1.00E+07
0 1 2 3 4 5 6 7 8 9 10 11
TIME (HRS)
pMSPSRDiv
pMSP3545
pMSPSRDiv-2

B.

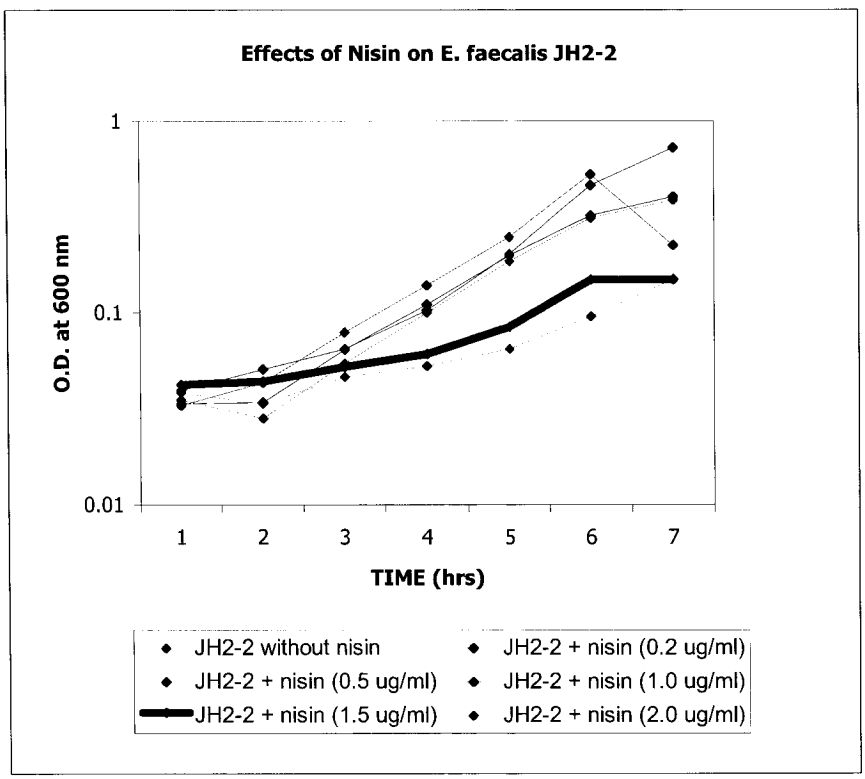
Effects of Nisin on E. faecalis JH2-2
O.D. at 600 nm
1
0.1
0.01
1 2 3 4 5 6 7
TIME (hrs)
JH2-2 without nisin
JH2-2 + nisin (0.2 ug/ml)
JH2-2 + nisin (0.5 ug/ml)
JH2-2 + nisin (1.0 ug/ml)
JH2-2 + nisin (1.5 ug/ml)
JH2-2 + nisin (2.0 ug/ml)

or pMSPSRDiv-2 is 3- to 4-hours incubation of the diluted culture initiated from an original subculture incubated at 37^0C O/N with (*E. coli*) or without (*E. faecalis*) agitation. The optimal concentration of nisin is 1.5 μg/ml for the induction *E. faecalis* JH2-2 transformants with pMSPSRDiv-1. Finally, *E. coli* KJB24 transformants carrying pSM6 seem to enter the VBNC state due to the presence of $DivIVA_{Ef}$ since transformants with pUC18 demonstrated a characteristic growth curve.

3.2 $DivIVA_{Ef}$ Overexpression using bacillary *E. coli*

This novel approach has been implemented to examine the effects of $DivIVA_{Ef}$ overexpression using the rod-shaped parental *E. coli* PB103 (*minB*) and the isogenic derivative PB114 (Δ*minB*). Most of the current research on DivIVA has been achieved using the rod-shaped *B. subtilis*, which has shown that $DivIVA_{Bs}$ acts in concert with the site-selection for cell division proteins MinC and MinD; however, *E. faecalis* possess no Min proteins and this strategy might highlight differences in species-specific functions of DivIVA. Moreover, this line of investigation permits the direct comparison of the effects of $DivIVA_{Ef}$ overexpression in the presence or absence of Min proteins in bacillary *E. coli*.

E. coli PB103 (*minB*) is characterized by regular rod-shaped cells while *E. coli* PB114 (Δ*minB*) is characterized by an irregular minicell phenotype. Would the presence of pUC18 alter the inherent cell phenotype of these strains? *E. coli* PB103 and *E. coli* PB114 were transformed with pUC18 (negative control) and compared to plasmid-free cells of the identical strain and no difference in cell morphology was ascertained by phase contrast microscopy, establishing pUC18 as a suitable negative control (data not shown).

The *divIVA$_{Ef}$* amplicons were subcloned in pUC18 within the MCS region, following the *lacZ* promoter to induce DivIVA$_{Ef}$ overexpression using IPTG. An IPTG optimization experiment was implemented using incubation time points 0-Hrs (defined as the addition of IPTG), 2-, 4- and 6-Hrs. Figure 6A depicts the DivIVA$_{Ef}$ overexpression results using *E. coli* PB103 (*minB*) transformants with pDiv.His (wt *divIVA$_{Ef}$::6XHis*) and similar DivIVA$_{Ef}$ overexpression levels were demonstrated by Western blot between 2-, 4- and 6-Hrs samples while no DivIVA$_{Ef}$ overexpression was observed at 0-Hrs. Conversely, *E. coli* PB114 transformants with pDiv.His demonstrated DivIVA$_{Ef}$ overexpression starting at 0-Hrs with increasing levels of DivIVA$_{Ef}$ overexpression with increased incubation by Western blot (Figure 6B). Samples containing pDiv.His (wt *divIVA$_{Ef}$::6XHis*) exhibited bands with a molecular weight of ~19kDa while purified DivIVA$_{Ef}$ exhibited a band corresponding to ~27 kDa as visualized by Western blot.

Bioinformatic analysis and biochemical studies (including native gel, gel filtration and DNA electrophoresis) employed by others have confirmed the sizes of wt and mutated *divIVA$_{Ef}$*. The coiled-coil domains of DivIVA$_{Ef}$ were confirmed by size exclusion chromatography indicating a DivIVA$_{Ef}$ oligomer of 10 - 12 subunits with a molecular weight of ~27 kDa (Rigden, 2005). These results have been used to assist in the interpretation of DivIVA$_{Ef}$ overexpression visualized by Western blot (Table 4).

The smaller molecular weight of DivIVA$_{Ef}$ observed by Western blot was thought to be the result of protein synthesis initiated at a downstream methionine (Met) instead of the initial Met. The monoclonal anti-His antibody detected the C-terminal 6X His tag fused to DivIVA$_{Ef}$ and should have eliminated any cross-reactivity. As anticipated,

Figure 6: Determination of the optimal incubation for $DivIVA_{Ef}$ overexpression post-IPTG (0.8mM) induction in bacillary *E. coli* strains as demonstrated by Western blot. **A-** *E. coli* PB103 transformants carrying either pUC18 (negative control) or pDiv.His (wt $divIVA_{Ef}$ positive control) at 0-, 2-, 4- and 6-Hrs incubation. Lanes: 1- pUC18 (2-Hrs); 2- pDiv.His (2-Hrs); 3- pUC18 (4-Hrs); 4- pDiv.His (4-Hrs); 5- pUC18 (6-Hrs); 6- pDiv.His (6-Hrs) and 7- Purified $DivIVA_{Ef}$; **B-** *E. coli* PB114 transformants carrying either pUC18 (negative control) or pDiv.His (wt $divIVA_{Ef}$ positive control) at 0-, 2-, 4- and 6-Hrs incubation. Lanes: 1- pUC18 (0-Hrs); 2- pDiv.His (0-Hrs); 3- pUC18 (2-Hrs); 4- pDiv.His (2-Hrs); 5- pUC18 (4-Hrs); 6- pDiv.His (4-Hrs); 7- pUC18 (6-Hrs); 8- pDiv.His (6-Hrs) and 9- Purified $DivIVA_{Ef}$. Densitometric analysis of duplicate samples was performed to ensure $DivIVA_{Ef}$ concentration equalized. Blots were probed with 1:1000 monoclonal anti-His antibody and 1:3000 goat anti-mouse IgG conjugated to alkaline phosphatase.

Figure 6

A. *E. coli* PB103 (*minB*)

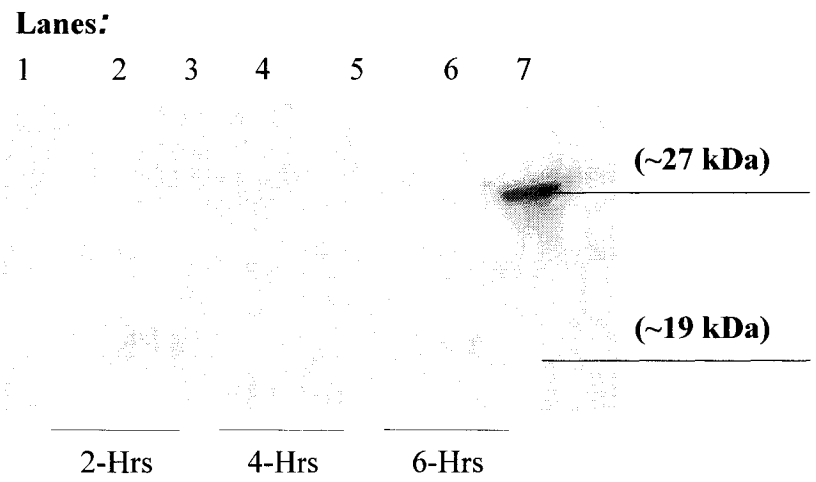

B. *E. coli* PB114 (Δ*minB*)

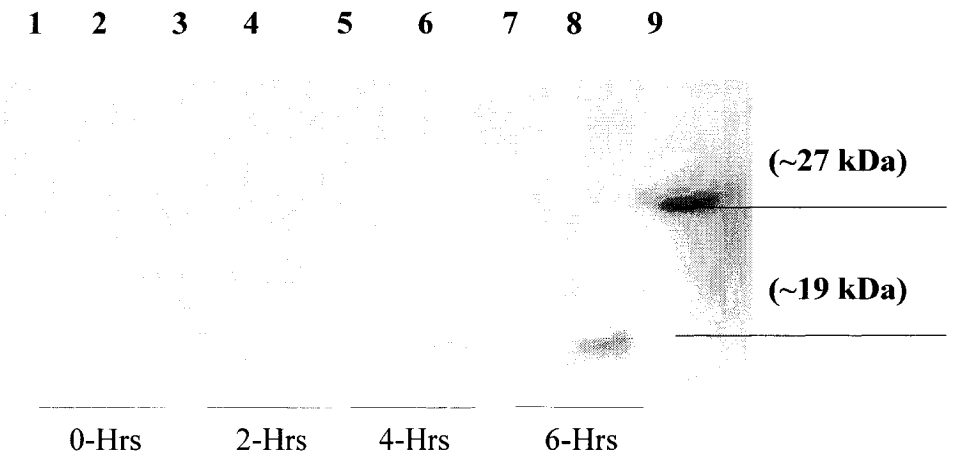

Table 4: Results for central coiled-coil domain mutations and deletions[a]

Name	Gel Filtration				Native Gel Electrophoresis	
	Superdex-200 A[b]	Monomer (kDa)	Superose-6 A[b]	Monomer (kDa)	A[b]	Monomer (kDa)
None	550/20	27.5	1011.83/37.47	27.0	288/10	28.8
pMR1	532/20	26.6	1028.94/38.10	27.0	299/11	27.2
pMR2	550/20	27.5	1046.33	27.0	332/12	27.7
pMR3	470/18	26.1	962.19/35.63	27.0	344/12	28.7
pMR4	526/20	26.3	1003.38/37.16	27.0	332/12	27.7
pMR5	550/25	22.0	834.4/38.4	21.7	332/12	27.7
pMR6	170/9	18.9	260/13	20	182/8	22.8
pMR7	ND[d]	ND[d]	ND[d]	ND[d]	52/3	17.3
pMR9	ND[d]	ND[d]	ND[d]	ND[d]	52/3	17.3
pMR10	ND[d]	ND[d]	841.1/31	27.1	125/4.6 and 78/2.8	27.2 and 27.8
pMR11	ND[d]	ND[d]	66.9/2.4	27.9	64.2/2.4	26.8
pMR12	ND[d]	ND[d]	29.9/1.1	27.2	64.2/2.4	26.8

NB:

Deletions[a] = Modified from: Marc Rigden. 2005. Determining the role of coiled-coil domain interactions in the oligomerization of DivIVA from *Enterococcus faecalis*. M. Sc. Thesis. Department of Biochemistry, Microbiology, and Immunology, Faculty of Medicine, University of Ottawa.

A[b] = complex Mass [kDa]/ Number of monomers[c]

monomers[c] = number of monomers based on molecular mass predicted by bioinformatics

ND[d] denotes the specific experiment was "Not Done".

NB: No accurate results for the monomeric or complex Mass were obtainable.

pUC18 transformants did not overexpress DivIVA$_{Ef}$ since no *divIVA$_{Ef}$* amplicon is present in the negative control.

Visualization of overexpressed proteins by Western blot demonstrates DivIVA$_{Ef}$ is produced in experimental samples for the investigation on the effects of DivIVA$_{Ef}$ overexpression on cell morphologies. The cell phenotype of wild type *E. coli* PB103 (*minB*) and *E. coli* PB114 (Δ*minB*) were compared against transformants carrying pUC18 (negative control) or pDiv.His (wt *divIVA$_{Ef}$::6XHis* – positive control). According to Nanninga (1998), the typical *E. coli* rod-shaped cell is 1.5 to 5.5 μm in length and has a diameter or cell depth of 0.5 to 1.0 μm. This appeared to be true only for samples of wt *E. coli* (*minB*) or transformants carrying pUC18 indicating that the positive control (pDiv.His) exhibited DivIVA$_{Ef}$ overexpression and the negative control (pUC18) did not, as anticipated.

Figure 7 demonstrates the cell lengths by class ranges of pUC18 transformants in either *E. coli* PB103 (*minB*) or *E. coli* PB114 (Δ*minB*). *E. coli* PB103 transformants displayed a short range of cell length classes (3), with the majority of the total cell population (77.9%) falling into the cell length class of 1 – 3 μm. *E. coli* PB114 transformants with pUC18 displayed a longer range of cell length classes (5), with the majority of the cell population (50.1%) falling into the class length class of 7 – 10 μm (Table 5).

The wt *E. coli* PB103 (*minB*) or negative control samples maintained a consistent morphology characterized by regular rod-shaped cells across time and exhibited a cell length of 0.5 to 5 μm (Table 5). *E. coli* PB103 transformants carrying pDiv.His (wt *divIVA$_{Ef}$::6XHis*) - the positive control - at 6-Hrs post-IPTG (0.8 mM) induction

Figure 7: Cell length classes for *E. coli* PB103 (*minB*) and *E. coli* PB114 (Δ*minB*) transformants carrying pUC18 at 6-Hrs post-IPTG (0.8mM) induction exhibit unique populations of cell lengths. **BLUE** depicts *E. coli* PB103 transformants carrying pUC18 and **RED** depicts *E. coli* PB114 transformants carrying pUC18.

Figure 7

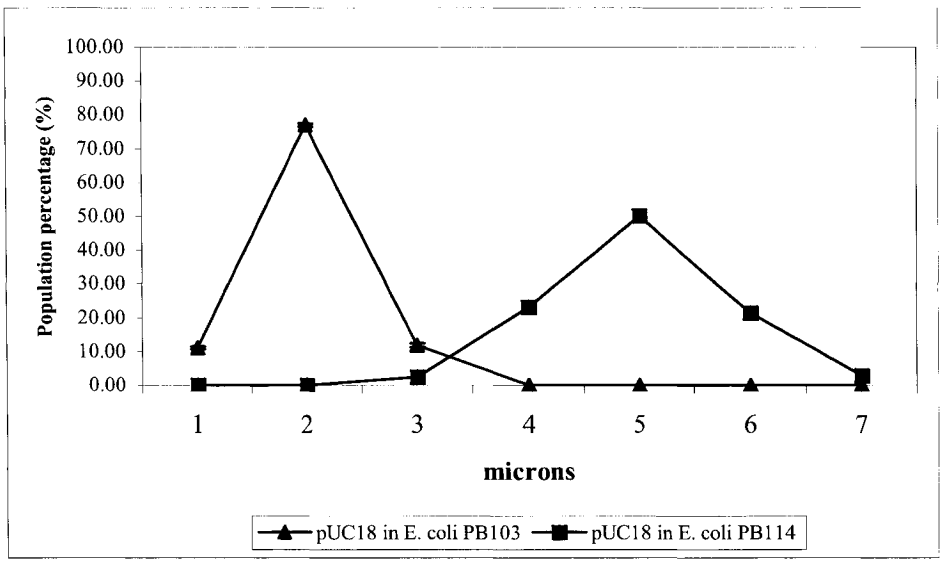
100.00
90.00
80.00
70.00
60.00
50.00
40.00
30.00
20.00
10.00
0.00
Population percentage (%)
1
2
3
4
5
6
7
microns
pUC18 in E. coli PB103
pUC18 in E. coli PB114

Table 5: Phase contrast microscopy assessment of fixed cells using *E. coli* heterologous overexpression systems demonstrates differences in cell length/area, due to the presence of wild-type or mutated *divIVA*$_{Ef}$ construct and dependent on bacterial strain used

	E. coli Bacilli (μm)		*E. coli* Cocci (μm^2)			
	PB103 (*minB*)	PB114 (Δ*minB*)	KJB24 (*minB, rodA*$^-$)		WM1250 (Δ*minB, rodA*-)	
Name	**(0.8 mM)[a]**	**(0.8 mM)**	**(0.4 mM)**	**(0.8 mM)**	**(0.4 mM)**	**(0.8 mM)**
pUC18	0.5 – 5	3 – 20	0.5 – 3[d]	0.5 – 3[e]	0.5 – 5	0.5 – 5
pDiv.His	0.5 – 40$^{12.5\%b}$	125 – 200$^{100\%}$	0.5 – 7$^{11.8\%}$	0.5 – 5$^{24.1\%}$	0.5 – 15$^{69.3\%}$	0.5 – 12$^{21.9\%}$
pSM1.His	ND[C]	ND[C]	0.5 – 7$^{33\%}$	ND[C]	ND[C]	ND[C]
pSM2.His	ND[C]	ND[C]	0.5 – 15$^{28.5\%}$	ND[C]	ND[C]	ND[C]
pSM3.His	0.5 – 5	0.5 – 40$^{35.1\%}$	0.5 – 10$^{32.7\%}$	0.5 – 5$^{1.8\%}$	ND[C]	0.5 – 12$^{13.1\%}$
pSM4.His	0.5 – 3	0.5 – 50$^{0.8\%}$	0.5 – 7$^{11.7\%}$	0.5 – 3	ND[C]	0.5 – 7$^{8.9\%}$
pSM5.His	ND[C]	ND[C]	0.5 – 10$^{50\%}$	ND[C]	ND[C]	ND[C]
pSM6.His	0.5 – 3	0.5 – 20	0.5 – 3	0.5 – 3	ND[C]	0.5 – 7$^{3.7\%}$
pSM7.His	0.5 – 10$^{3.9\%}$	0.5 – 20	ND[C]	0.5 – 3	ND[C]	0.5 – 7$^{8.9\%}$
pSM8.His	0.5 – 3	0.5 – 20	0.5 – 7$^{6.4\%}$	0.5 – 3	ND[C]	0.5 – 7$^{1.8\%}$
pSM9.His	0.5 – 3	0.5 – 12	ND[C]	ND[C]	ND[C]	0.5 – 7$^{2\%}$
pSM12.His	0.5 – 10$^{9.8\%}$	0.5 – 20	ND[C]	ND[C]	ND[C]	0.5 – 7$^{11.5\%}$

Nanninga (1998): *E. coli* rod-shaped cell is 1.5 - 5.5 μm. Corbin *et al.* (2002): *E. coli* KJB24 cells is 0.75 - 2.52 μm^2.

a) denotes IPTG concentration
b) denotes the cell population percentage exceeding the maximum cell size of transformants carrying pUC18.
c) denotes Not Done.
d) denotes *E. coli* KJB24 mutants using pSM series. For simplicity sake only the pSM.His series is shown. The identical constructs using the pSM series are: pDiv.His = pSM6; pSM1.His = pSM1; pSM2.His = pSM4; pSM3.His =pSM5; pSM4.His = pSM2; pSM5.His = pSM3; pSM6.His = pSM9; pSM7.His = pSM11, pSM8.His = pSM10; pSM9.His = pSM12; and pSM12.His does not exist in the pSM series.
e) denotes *E. coli* KJB24 mutants using the pSM.His series as found in column headed **Name**.

demonstrated a larger cell length range of 0.5 – 40 μm. This 8-fold increase in cell length was observed in ~13% of the population. The presence of filamentation demonstrates that $DivIVA_{Ef}$ overexpression in *E. coli* PB103 (*minB*) seems to cause cell division arrest as observed by cell filamentation indicating that the full-length protein is functional in this strain regardless of the presence of Min proteins not found in *E. faecalis* JH2-2.

E. coli PB114 transformants carrying the negative control (pUC18) exhibit an altered cell phenotype relative to the parental PB103 (*minB*) strain. The sole difference between the strains is the elimination of the *minB* operon that encodes for the proteins MinC, MinD and MinE (MinCDE). In *B. subtilis*, the inactivation of either MinC or MinD results in the formation of minicells with the notable presence of anucleated cells since cells divide at both poles and mid-cell (Cha and Stewart, 1997; Harry and Lewis, 2003; Thomaides *et al.*, 2001).

The absence of MinCDE resulted in a cell population possessing a greater cell length range of 3 – 20 μm (Table 5) and comprising a heterologous morphology characterized by minicells, rod-shaped and filamentous cells that conforms to findings by other researchers (Szeto *et al.*, 2001). This is an approximate 4-fold increase in cell length relative to those of *E. coli* PB103 transformants carrying the identical construct. Incredibly, *E. coli* PB114 (Δ*minB*) transformants carrying the positive control (pDiv.His) revealed extreme filamentation or a "spaghetti-like" phenotype with a cell length range between 125 – 200 μm (Table 5). This 10-fold increase in cell length was observed in virtually 100% of the population. The increased cell length between the positive control (pDiv.His) in *E. coli* PB114 is greater than that observed with *E. coli* PB103 possibly suggesting a greater degree of cell division arrest demonstrated by the presence of

filamentation indicating that the full-length protein is functional in this strain in the absence of Min proteins. The absence of Min proteins in *E. coli* PB114 may resemble more closely the native *E. faecalis* JH2-2 environment, which also does not possess Min proteins. This may well support a truer impression of DivIVA$_{Ef}$ functioning in its native system.

Figure 8A depicts the cell phenotype of *E. coli* PB103 (*minB*) with pUC18 (A1) or pDiv.His (A2) at 6-Hrs incubation post-IPTG (0.8 mM) induction and Figure 8B depicts the cell phenotype of *E. coli* PB114 (Δ*minB*) with pUC18 (B1) or pDiv.His (B2) at 6-Hrs incubation post-IPTG (0.8 mM) induction. *E. coli* PB103 transformants carrying full-length *divIVA$_{Ef}$* clearly demonstrated filamentation, but 100% of the cell population using *E. coli* PB114 transformants carrying the positive control (pDiv.His) were not only filamentous, they were 10-fold longer than the negative control in the same strain.

Having shown that wt *divIVA$_{Ef}$* is produced and overexpressed causing changes to the cell phenotype with the heterologous bacillary *E. coli* overexpression systems whether the Min proteins are present or absent, the mutated *divIVA$_{Ef}$* constructs that abrogate individual coiled-coil domains must be assessed in a similar manner. The mutated *divIVA$_{Ef}$* constructs examined in conjunction with the bacillary *E. coli* strains are: pSM3.His (E37P, N43P, L46D); pSM4.His (E37P, N43P, L46D, L50D, L50F); pSM6.His (1 - 190); pSM7.His (Δ130 – 190); pSM8.His (Δ60 – 190); pSM9.His (Δ60 – 130); or pSM12.His (L104P, L143P).

To ensure that mutated DivIVA$_{Ef}$ was being overexpressed, SDS-PAGE and Western blot protocols were carried out (Figure 9). DivIVA$_{Ef}$ overexpression in *E. coli* PB103 (*minB*) with the mutated *divIVA$_{Ef}$* constructs was weak for pSM6.His, pSM9.His and

Figure 8: Morphological phenotype of bacillary *E. coli* transformants carrying pUC18 (negative control) or pDiv.His (wt $divIVA_{Ef.}$ positive control) at 6-Hrs post-IPTG (0.8mM) induction using phase contrast microscopy (100X oil immersion). All images measured using single scale bar applicable to all image panels. **A-** *E. coli* PB103 (*minB*) with pUC18 (A1) or pDiv.His (A2) at 6-Hrs post-IPTG induction (0.8 mM); **B-** *E. coli* PB103 (Δ*minB*) with pUC18 (B1) or pDiv.His (B2) at 6-Hrs post-IPTG induction (0.8 mM); pUC18 at 6-Hrs post-IPTG induction (0.8 mM).

Figure 8

A. *E. coli* PB103 (*minB*) 6-Hrs post-IPTG

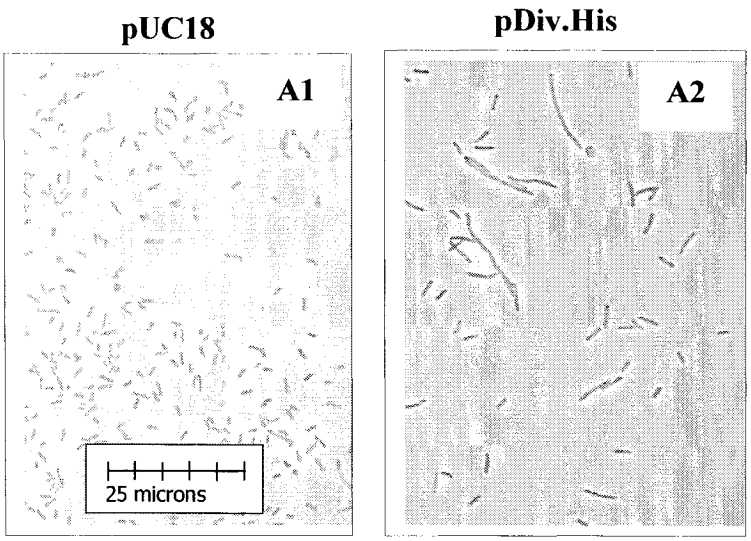

B. *E. coli* PB114 (Δ*minB*) 6-Hrs post-IPTG

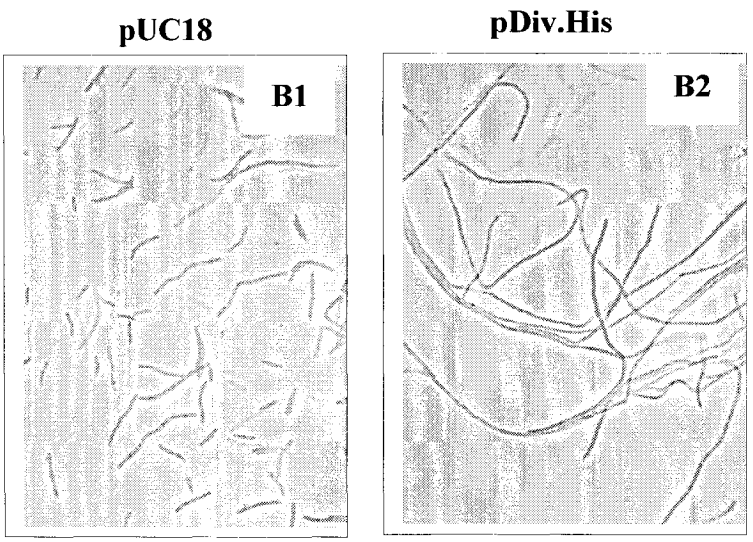

Figure 9: *E. coli* transformants carrying wt or mutated *divIVA*$_{Ef}$ demonstrate DivIVA$_{Ef}$ overexpression as demonstrated by Western blot. **A-** *E. coli* PB103 (*minB*) transformants in the presence of Min proteins - Lanes: 1- pUC18; 2- pDiv.His; 3- pSM6.His (1 - 190); 4- pSM3.His (E37P, N43P, L46D); 5- pSM4.His (E37P, N43P, L46D, L50D, L50F); 6- pSM9.His (Δ60 – 130); 7- pSM12.His (L104P, L143P); and 8- Purified DivIVA$_{Ef}$; **B-** *E. coli* PB114 (Δ*minB*) transformants in the absence of Min proteins - Lanes: 1- pUC18; 2- pDiv.His; 3- pSM3.His (E37P, N43P, L46D); 4- pSM4.His (E37P, N43P, L46D, L50D, L50F); 5- pSM6.His (1 - 190); 6- pSM9.His (Δ60 – 130); 7- pSM12.His (L104P, L143P); and 8- Purified DivIVA$_{Ef}$. Densitometric analysis of duplicate samples was performed to ensure DivIVA$_{Ef}$ concentration equalized. Blots were probed with 1:1000 monoclonal anti-His antibody and 1:3000 goat anti-mouse IgG conjugated to alkaline phosphatase.

Figure 9

A. *E. coli* PB103 (*minB*)

Lanes:
1 2 3 4 5 6 7 8

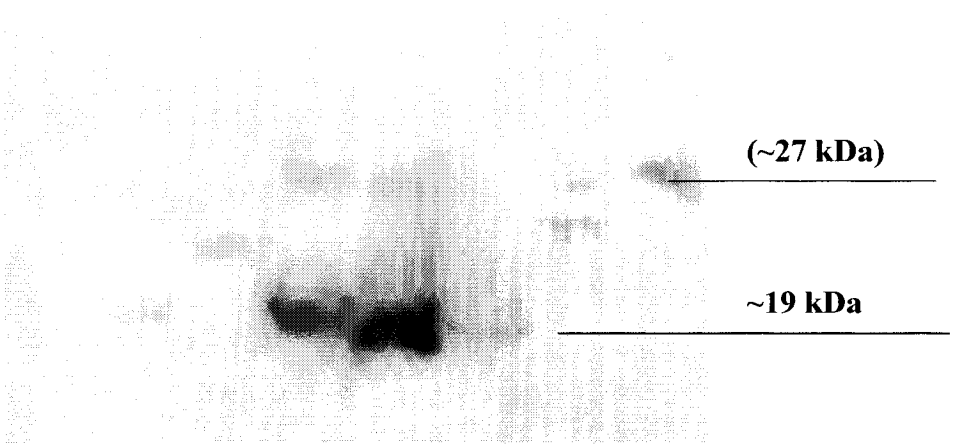

B. *E. coli* PB114 (Δ*minB*)

Lanes:
1 2 3 4 5 6 7 8

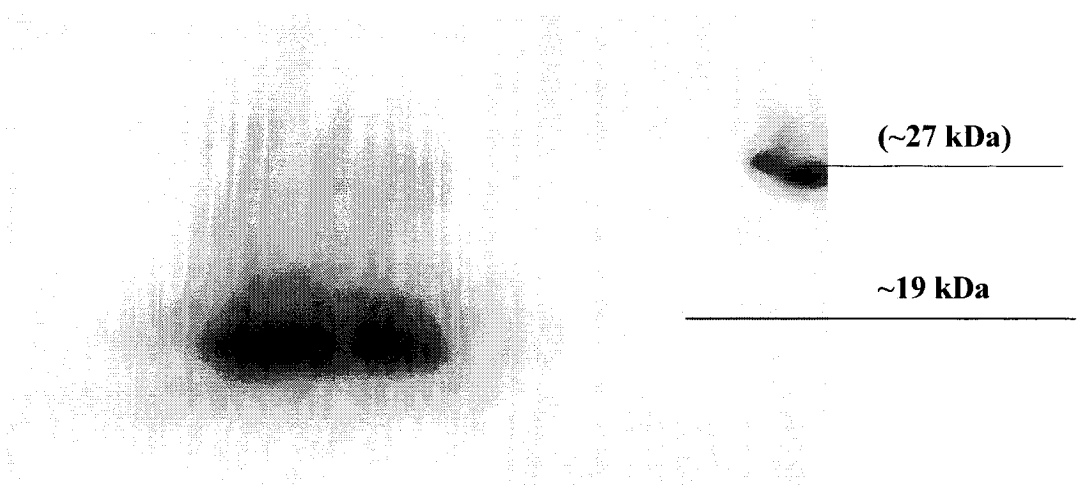

pSM12.His; very strong for pSM3.His and pSM4.His; and no DivIVA$_{Ef}$ overexpression was detected in samples with pSM7.His and pSM8.His. A faint band detected by Western blot denotes weak overexpression while a heavy, dark band characterizes strong overexpression. DivIVA$_{Ef}$ overexpression in *E. coli* PB114 (Δ*minB*) with the mutated *divIVA$_{Ef}$* constructs was weak for pSM9.His; very strong for pSM3.His and pSM4.His; and no DivIVA$_{Ef}$ overexpression was detected in samples with pSM6.His, pSM7.His, pSM8.His and pSM12.His (Table 6).

The mutated *divIVA$_{Ef}$* constructs transformed into rod-shaped *E. coli* strains with abrogated central coiled-coil domains (pSM7.His, pSM8.His) do not demonstrate any DivIVA$_{Ef}$ overexpression.

Multiple point mutations of *divIVA$_{Ef}$* should not have altered the molecular weight significantly since DivIVA$_{Ef}$ would be full-length and should include the constructs pSM3.His (E37P, N43P, L46D), pSM4.His (E37P, N43P, L46D, L50D, L57F) and pSM12.His (L104P, L143P). The C-terminal truncation of *divIVA$_{Ef}$* found in pSM6.His (1 – 190) should produce a mutated DivIVA$_{Ef}$ with a predicted molecular weight of ~23 kDa. The *divIVA$_{Ef}$* amplicons abrogating the central coiled-coil domains by large deletion should yield a protein product with a predicted molecular weight of ~17 kDa and include pSM7.His (Δ130 - 190), pSM8.His (Δ60 - 130) and pSM9.His (Δ60 - 190) (Table 4).

Western blot samples containing pDiv.His (wt *divIVA$_{Ef}$::6XHis*) exhibited bands with a molecular weight of ~27 kDa, corresponding to purified DivIVA$_{Ef}$, and ~19kDa as visualized by Western blot (Figures 6 and 9). *E. coli* rod transformants with wt *divIVA$_{Ef}$* constructs seemed to have a functional protein product with transformants exhibited by the filamentous cell morphology. Similar Western blot results were obtained for samples

Table 6: "No" DivIVA$_{Ef}$ over expression detected by Western blot using *E. coli* transformants carrying *divIVA$_{Ef}$* possessing abrogated central coiled-coil domain.

	***E. coli* (IPTG induction concentration)**			
	Bacilli		**Cocci**	
Name	**PB103 (*minB*) (0.8 mM)**	**PB114 (Δ*minB*) (0.8 mM)**	**KJB24[a] (*minB*, *rodA*$^-$) (0.4 mM/0.8 mM)**	**WM1250 (Δ*minB*, *rodA*$^-$) (0.4 mM/0.8 mM)**
pUC18	No	No	No/No[b]	No/No
pDiv.His	Yes	Yes	No/No[b]	Yes/Yes[d]
pSM3.His	Yes	Yes	No/No[b]	Yes
pSM4.His	Yes	Yes	No/ No[b]	Yes
pSM6.His	Yes	No	No/ No[b]	Yes
pSM7.His	No	No	No/ No[b]	No
pSM8.His	No	No	No/ No[b]	No
pSM9.His	Yes	Yes	**ND**[c]	Yes
pSM12.His	Yes	No	**ND**[c]	No

NB: **No** denotes no DivIVA$_{Ef}$ overexpression.
Yes denotes DivIVA$_{Ef}$ overexpression.

a) denotes *E. coli* KJB24 mutants with (0.8 mM) using pSM.His series and without (0.4 mM) His tag using the pSM series. For simplicity sake only the pSM.His series is shown. The identical constructs using the pSM series are: pDiv.His = pSM6; pSM3.His =pSM5; pSM4.His = pSM2; pSM6.His = pSM9; pSM7.His = pSM11, pSM8.His = pSM10; pSM9.His = pSM12; and pSM12.His does not exist in the pSM series.

b) denotes no DivIVA$_{Ef}$ overexpression with 0.4 mM IPTG induction and no DivIVA$_{Ef}$ overexpression with 0.8 mM IPTG induction.

c) denotes Not Done.

d) denotes DivIVA$_{Ef}$ overexpression with 0.4 mM IPTG induction and DivIVA$_{Ef}$ overexpression with 0.8 mM IPTG induction.

containing N-terminal mutations of *divIVA$_{Ef}$* including pSM3.His and pSM4.His. Oddly, *E. coli* PB103 (*minB*) transformants with pSM12.His, which abrogates both central coiled-coil domain by a double point mutation demonstrated two bands with a predicted molecular weight of ~24 kDa and ~27 kDa (Figure 9, Table 4).

Why would Western blot samples with pDiv.His (*divIVA$_{Ef}$::6XHis*), pSM3.His, pSM4.His and pSM12.His produce an identical double-banded pattern? Since the anti-His antibody was monoclonal and *divIVA$_{Ef}$* would only have been overexpressed with the C-terminal 6XHis-tag fusion sensitive to the anti-His antibody, the ~19 kDa could not have been attributable to cross-reactivity. The DivIVA$_{Ef}$ overexpression of this smaller band could have resulted from the initiation of a downstream methionine (Met) as opposed to the initial Met (Figure 10A). This may well have occurred in the creation of mutants developed for cloning in pUC18 resulting in a frame shift at the pUC18-DivIVA$_{Ef}$ juncture (Figure 10B) accounting for the demonstrated molecular weight of ~19 kDa as well as the production of full-length DivIVA$_{Ef}$ with a weight of ~27 kDa.

A major component of my hypothesis involves the effects of abrogating specific coiled-coil regions on the biological function of DivIVA$_{Ef}$, in the heterologous *E. coli* system. With the visualization of DivIVA$_{Ef}$ overexpression, the importance of abrogating specific coiled-coil domains begins to be observable. Samples carrying pSM9.His, which abrogates the first central coiled-coil domain of *divIVA$_{Ef}$* demonstrated DivIVA$_{Ef}$ overexpression, regardless of the *E. coli* rod strain employed. Conversely, samples carrying pSM7.His, which abrogates the second central coiled-coil domain of *divIVA$_{Ef}$*

Figure 10: Translation of DivIVA$_{Ef}$ and cloning vector pUC18. Sequences critical to the construct of the wt and mutant *divIVA$_{Ef}$* constructs. **A-** Translation of *divIVA$_{Ef}$* sequence (http://www.expasy.org/tools/dna.html) depicting the various **Met** positions; **B-** cloning vector pUC18 DNA sequence and translation with start codon GTA highlighted in **Red**.

Figure 10

A DivIVA$_{Ef}$ sequence depicting methionines (Met)

5'3' Frame 1
Met A L T P L D I Q N K D F S T K **Met** R G Y N Q D D V D D F L D Q V T
R D Y E D A L Q K N R E L E K S L K H A E E K L Q Y F N E L K D A L N
Q S I I V A Q D T A D K V K S S A N K E S E **Met** I I T S A D N Q A K E T
L V E A E R K S N A **Met** I A D A E A K S T Q I L A E A I E R A R Q L A G
E T E D L K K K T R V F H Q R L S L **Met** L E T Q L E Q V K S E E W E E I
L K P F S S Y V G D K H T A V K E I L D E Q D L D N E N E T V V N S E E
N T D A V V E K K P V I E V T E E T I E E E S K **Stop**

B DNA and protein sequence of pUC18 depicting initial Met

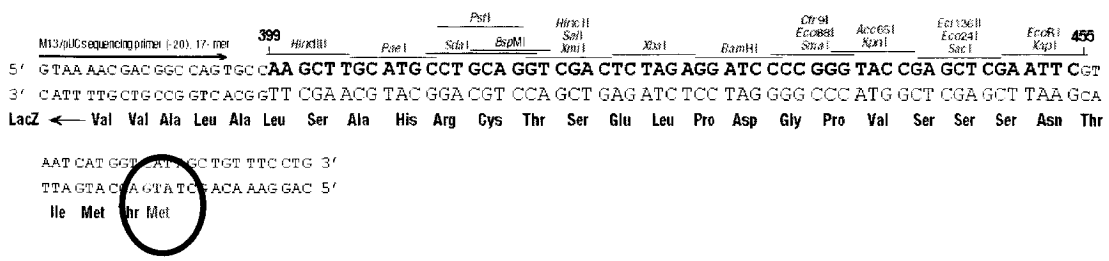

and pSM8.His, which abrogates both central coiled-coil domains of *divIVA$_{Ef}$* demonstrated no DivIVA$_{Ef}$ overexpression.

These results suggest that the abrogation of the first half (pSM3.His) or the complete (pSM4.His) N-terminal coiled-coil domain of *divIVA$_{Ef}$* does not alter the expression or presence of DivIVA$_{Ef}$. Moreover, the second central coiled-coil domain of *divIVA$_{Ef}$* appears to be a critical domain since its abrogation results in a loss of DivIVA$_{Ef}$ overexpression while abrogation of the first central coiled-coil domain of *divIVA$_{Ef}$* does not prevent DivIVA$_{Ef}$ overexpression.

The remaining two mutated *divIVA$_{Ef}$* constructs demonstrated DivIVA$_{Ef}$ overexpression differently depending on the *E. coli* strain employed. Samples carrying pSM6.His, which eliminates the C-terminal coiled-coil domain or pSM12.His which abrogates both central coiled-coil regions by a double point mutation; demonstrated DivIVA$_{Ef}$ overexpression in *E. coli* PB103 (*minB*), but not in *E. coli* PB114 (Δ*minB*). It is possible that in spite of manufacturer's specifications, a stronger concentration of the anti-His antibody was required to probe the blots or the antigen concentration was too low for the antibody to detect. The lack of DivIVA$_{Ef}$ overexpression suggests that no altered cell phenotype should occur due to the lack of DivIVA$_{Ef}$ produced in the cell. DivIVA$_{Ef}$ should exert changes in cell phenotype; illustrating the biological functioning of this protein.

Table 5 depicts all cell lengths following microscopic assessment of fixed cells by phase contrast microscopy. *E. coli* transformants carrying mutated *divIVA$_{Ef}$* constructs abrogating the N-terminal coiled-coil domain demonstrated DivIVA$_{Ef}$ overexpression and it was therefore anticipated that cells would result in altered cell morphology. Curiously,

this was not the case using *E. coli* PB103 (*minB*) but the supposition did hold true using *E. coli* PB114 (Δ*minB*) since filamentation was observed. Transformants carrying pSM3.His demonstrated a cell length range of 0.5 to 40 μm in cell length with 35.1% of the population exceeding the wild type cell length of 20 μm (Table 5).

E. coli PB103 (*minB*) transformants with pSM7.His (Δ130 – 190) and pSM12.His (L104P, L143P) exhibited cells larger than the wild type cell length of 5 μm comprising 4% and 9.8% of the cell populations, respectively (Table 5). Oddly, both constructs carry mutations of the central coiled-coil domain of $divIVA_{Ef}$ and were unable to overexpress $DivIVA_{Ef}$ by Western blot.

Overall, bacillary *E. coli* demonstrated dramatic changes in cell morphology reproducibly when transformed with the full-length $divIVA_{Ef}$ constructs. Although samples carrying $divIVA_{Ef}$ constructs did overexpress $DivIVA_{Ef}$ in both the presence or absence of Min proteins, these bacillary *E. coli* transformants did not reliably demonstrate altered cell morphology in a manner that would elucidate the biological functioning of $DivIVA_{Ef}$.

3.3 $DivIVA_{Ef}$ overexpression using coccal-shaped *E. coli*

This novel approach has been implemented to examine the effects of $DivIVA_{Ef}$ overexpression using the coccal-shaped parental *E. coli* KJB24 (*rodA*$^-$, *minB*) and the isogenic derivative WM1250 (*rodA*$^-$, Δ*minB*). The preponderance of DivIVA research has been achieved using the rod-shaped *B. subtilis*, however, *E. faecalis* is coccal-shaped and this strategy might highlight differences in species-specific functions of DivIVA. Moreover, this line of investigation permits the direct comparison of the effects of

DivIVA$_{Ef}$ overexpression in the presence or absence of Min proteins in coccal-shaped *E. coli* in an environment approximating *E. faecalis* JH2-2.

E. coli KJB24 (*rodA*$^-$, *minB*) is characterized by regular coccal-shaped cells while WM1250 (*rodA*$^-$, Δ*minB*) is characterized by cocci of a more variable size. Would the presence of pUC18 alter the inherent cell phenotype of these strains? *E. coli* PB103 and *E. coli* PB114 were transformed with pUC18 (negative control) and compared to plasmid-free cells of the identical strain and no difference in cell morphology was ascertained by phase contrast microscopy, establishing pUC18 as a suitable negative control (data not shown).

Wild type *divIVA*$_{Ef}$ and mutant *divIVA*$_{Ef}$ amplicons used to create the construct series pSM1 to pSM10 known as the "**pSM_**" series included: pUC18 (negative control), pSM6 (wt *divIVA*$_{Ef}$ - positive control) pSM1 (L29D from pMR1), pSM2 (E37P, N43P, L46D, L50D, L57F from pMR4), pSM3 (E37P, N43P, L46D, L50E, L57F from pMR5), pSM4 (E37P from pMR2), pSM5 (E37P, N43P, L46D from pMR3), pSM9 (1 – 190 from pMR6), pSM10 (Δ60 – 190 from pMR8), pSM11 (Δ130 – 190 from pMR7), pSM12 (Δ60 – 130 from pMR9) and pSM13 (L104P, L143P from pMR12). The constructs pSM1 to pSM5 afftect the N-terminal coiled-coil domain, pSM10 to pSM13 abrogate the central coiled-coil domains and pSM9 affects the C-terminal coiled-coil domain of *divIVA*$_{Ef}$.

The *divIVA*$_{Ef}$ amplicon was subcloned in pUC18 downstream of the *lacZ* promoter and to induce DivIVA$_{Ef}$ overexpression both 0.4 mM and 0.8 mM IPTG concentrations were employed for a 3-Hrs incubation post-IPTG. Western blots performed using a polyclonal anti-DivIA$_{Ef}$ antibody of proven reliability (Ramirez-Arcos *et al.*, 2001) demonstrated no discernible DivIVA$_{Ef}$ overexpression in *E. coli* KJB24 (*rodA*$^-$, *minB*)

due to extensive multiple bands along the length and breadth of the Western blot (data not shown). Interestingly, pUC18 transformants revealed identical banding patterns, although *divIVA$_{Ef}$* is absent in this negative control. These results were not anticipated since our laboratory had previously used this bacterial strain to advantage in gonococcal MinD overexpression and morphological studies (Ramirez-Arcos S *et al.*, 2004b; Ramirez-Arcos S *et al.*, 2002; Ramirez-Arcos S *et al.*, 2001; Szeto J *et al.*, 2001; Szeto, 2004). These results were reproducible with both 0.4 mM and 0.8 mM IPTG induction in overexpression studies.

The cell phenotype of wild type *E. coli* KJB24 (*rodA*$^-$, *minB*) was compared against transformants carrying pUC18 (negative control) or pDiv.His (wt *divIVA$_{Ef}$::6XHis* – positive control). According to Corbin *et al.* (2002), the typical *E. coli* KJB24 (*rodA*$^-$, *minB*) ranges in cell area from 0.75 to 2.52 μm^2 confirming the results obtained in this research (Table 5). Wild type *E. coli* KJB24 or transformants carrying pUC18 induced with 0.4 mM or 0.8 mM IPTG were characterized by a regular spherical morphological phenotype an area of 0.5 – 3 μm^2. In contrast, pSM6 transformants (wt *divIVA$_{Ef}$*) are characterized by an engorged spherical phenotype with an area of 0.5 – 7 μm^2 (0.4 mM IPTG) or of 0.5 – 5 μm^2 (0.8 mM IPTG) (Figure 11).

Having observed that full-length *divIVA$_{Ef}$* appeared to cause changes in cell morphology using *E. coli* KJB24 (*rodA*$^-$, *minB*), microscopic assessment of overexpression (0.4 mM IPTG) samples with *divIVA$_{Ef}$* constructs abrogating the N- or C-terminal coiled-coil domain transformed in the coccal-shaped strain was undertaken since biochemical techniques had previously demonstrated that these domains were not critical in the oligomerization processes in DivIVA$_{Ef}$ (Table 4) (Rigden, 2005).

Figure 11: *E. coli* KJB24 (*minB, rodA*$^-$) transformants carrying wt $divIVA_{Ef}$ reveal engorged cells at 3-Hrs post-IPTG (0.4 mM) induction as depicted by phase contrast microscopy (100X oil immersion). All images measured using single scale bar applicable to all image panels. **A-** pUC18 (negative control); **B-** pSM6 (wt $divIVA_{Ef}$, positive control).

Figure 11

E. coli KJB24 (*rodA*$^-$, *minB*) 6-Hrs post-IPTG

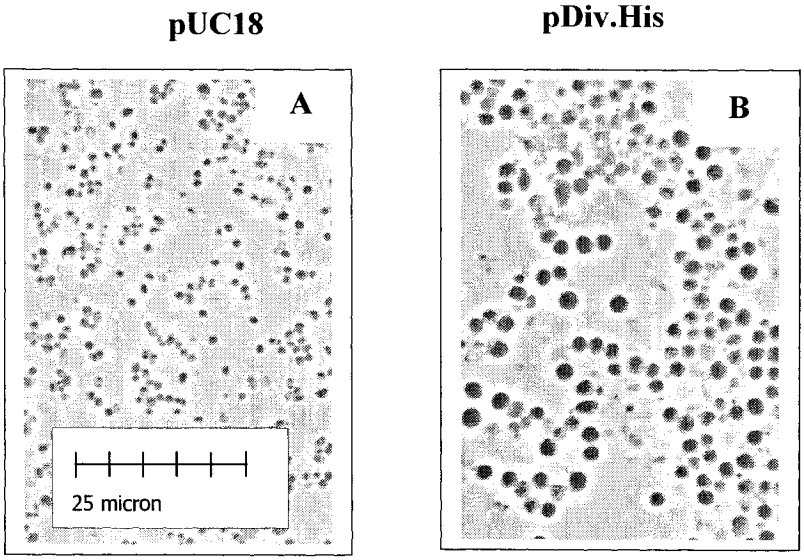

The mutated *divIVA$_{Ef}$* constructs abrogating the N-terminal coiled-coil domains were investigated in-depth and included: pSM1 (L29D), which pushes start of N-terminal coiled-coil domain back; pSM2 (E37P, N43P, L46D, L50D, L57F) and pSM3 (E37P, N43P, L46D, L50E, L57F) which completely abrogate the N-terminal coiled-coil domain; pSM4 (E37P) which abrogates beginning of N-terminal coiled-coil domain; and pSM5 (E37P, N43P, L46D) which abrogates the first half of the N-terminal coiled-coil domain. The mutated *divIVA$_{Ef}$* construct eliminating the C-terminal coiled-coil domain included pSM9 (1 - 190). Finally, the mutated *divIVA$_{Ef}$* construct abrogating both central coiled-coil domains, pSM10 (Δ60 - 190), was examined.

Although no concrete evidence demonstrating the production and presence of DivIVA$_{Ef}$ could be produced by Western blot due to extensive multiple bands along the length and breadth of the Western blots (data not shown), *E. coli* KJB24 (*rodA$^-$*, *minB*) transformants carrying one of pSM1, pSM2, pSM3, pSM4, pSM5 or pSM6 produced engorged, coccal-shaped cells (Figure 12). These constructs abrogate specific areas of the N-terminal coiled-coil domain of DivIVA$_{Ef}$ (Figure 3) and seem to cause cell division arrest indicating that the full-length mutated protein is functional as demonstrated by the engorged cell morphologies ranging in cell area from 7 to 15 μm^2. Table 5 provides the cell length ranges for each construct with the cell population percentage exceeding the maximum cell length of the pUC18 transformant in the same strain, in superscript. *E. coli* KJB24 transformants carrying the negative control (pUC18) maintained the wt cell phenotype with a maximum cell area of 3 μm^2.

E. coli KJB24 (*rodA$^-$*, *minB*) overexpression samples with pSM9 (1 - 190), which eliminate the C-terminal coiled-coil domain of DivIVA$_{Ef}$, retained the wild type cell

Figure 12: Aberrant morphological phenotype of *E. coli* KJB24 (*minB, rodA*$^-$) transformants carrying mutated $divIVA_{Ef}$ at 3-Hrs post-IPTG (0.4mM) induction as depicted by phase contrast microscopy (100X oil immersion). All images measured using single scale bar applicable to all image panels. **A**- pSM1 (L29D); **B**- pSM2 (E37P, N43P, L46D, L50D, L57F); **C**- pSM3 (E37P, N43P, L46D, L50E, L57F); **D**- pSM4 (E37P); and **E**- pSM5 (E37P, N43P, L46D).

Figure 12

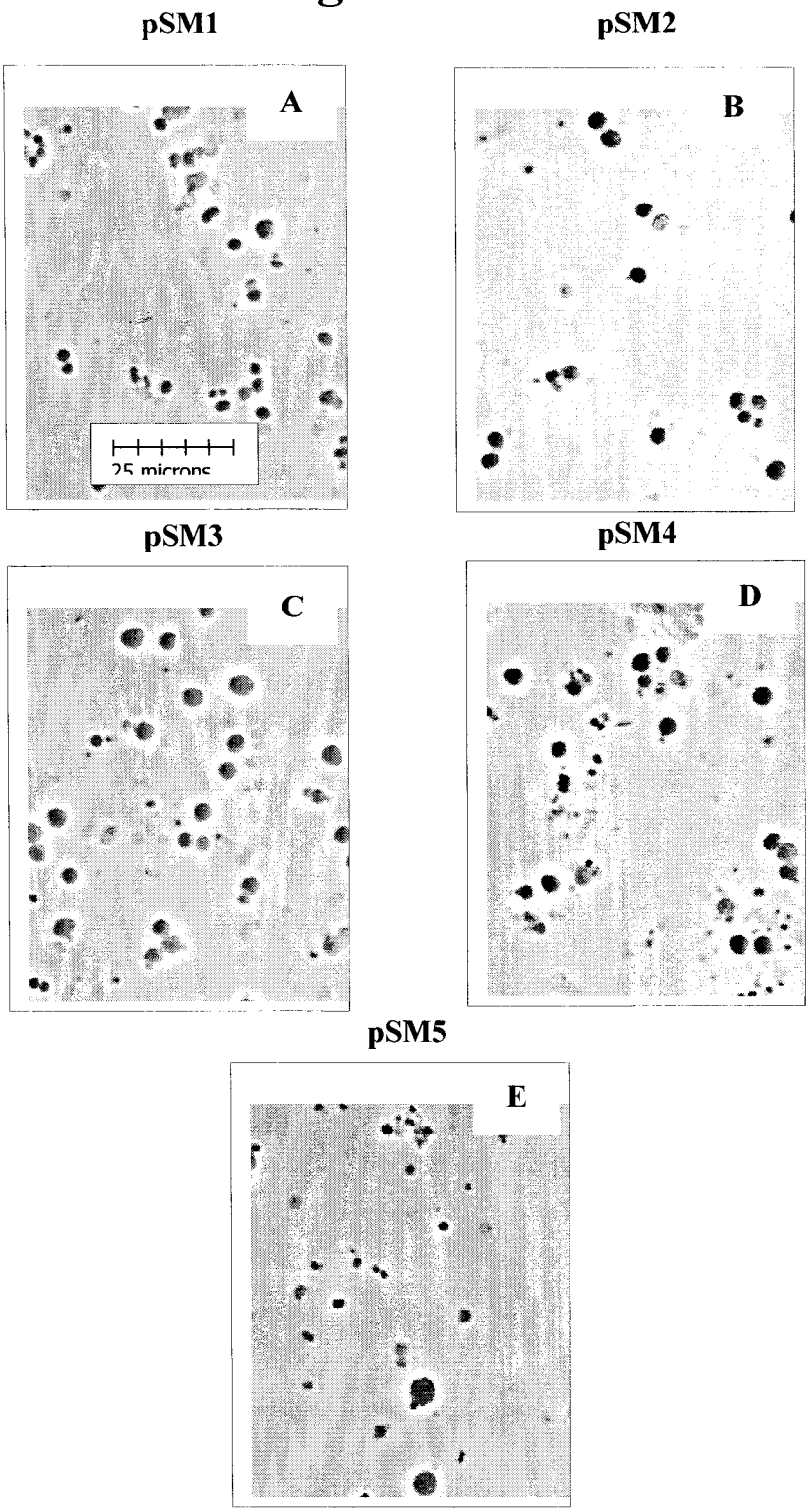

morphology. Moreover, both bacillary *E. coli* overexpression systems [PB103 (*minB*) and PB114 (*ΔminB*)] carrying the identical construct with a C-terminal 6X His tag known as pSM6.His also retained the inherent cell phenotype, although these results cannot be explained.

E. coli KJB24 (*rodA⁻, minB*) overexpression samples with pSM10 (Δ60 - 190), which affects both central coiled-coil domains of $DivIVA_{Ef}$, demonstrated a wild-type phenotype. The bacillary *E. coli* overexpression systems [PB103 (*minB*) and PB114 (*ΔminB*)] carrying the identical construct with a C-terminal 6X His tag known as pSM8.His also retained the inherent cell phenotype. This result was anticipated since biochemical analyses involving $divIVA_{Ef}$ constructs with abrogated central coiled-coil domains demonstrated altered $DivIVA_{Ef}$ self-interactions (Table 4). Elimination of either central domain resulted in a reduced protein complex from 10 to 4 subunits suggesting $DivIVA_{Ef}$ self-interaction has been abrogated (Rigden, 2005).

The $DivIVA_{Ef}$ overexpression studies were repeated using the identical constructs in *E. coli* KJB24 (*rodA⁻, minB*) with cells induced with 0.8 mM IPTG. Microscopic assessment demonstrated that cells exhibited a wild type cell areas of 3 μm^2, with the exception of pSM5, which demonstrated a maximum cell area of 5 μm^2 (Table 5). Western blot results produced the same multiple banding pattern previously demonstrated with samples induced with 0.8 mM IPTG.

The data obtained in the morphological studies using the *E. coli* KJB24 (*rodA⁻, minB*) heterologous overexpression system supports findings of the biological functioning of $DivIVA_{Ef}$. However, $DivIVA_{Ef}$ overexpression should be detectable by Western blot to confirm the presence of the protein of interest. Thus, another essential protein of *E.*

faecalis JH2-2 would be subcloned in pUC18 to act as a control that would require a different anti-body to probe Western blots.

$PrgX_{Ef}$ overexpression using *E. coli* KJB24 (*rodA*⁻, *minB*) transformed with pSR-X was achieved with 0.2mM IPTG induction at 37^0C, incubated for 2-, 3- and 4-Hrs as demonstrated by Western blot (Figure 13A). The levels of $PrgX_{Ef}$ overexpression are 17% higher at both 3- and 4-Hrs (lane 5 and 7, respectively) relative to the 2- Hrs (lane 3) post-IPTG induction. Moreover the IPTG-induced $PrgX_{Ef}$ samples exhibit greater $PrgX_{Ef}$ concentration following densitometric analysis than uninduced $PrgX_{Ef}$ samples.

Figure 13B depicts the cell morphology of *E. coli* KJB24 transformants carrying pSR-X. Uninduced or IPTG-induced (0.2 mM) $PrgX_{Ef}$ samples exhibited identical cell phenotypes. These results indicate that the presence of foreign non-cell division plasmid DNA and its protein product do not seem to affect normal functioning or cell morphology of transformants. Moreover, since a clear signal of $PrgX_{Ef}$ overexpression was obtain when Western blots were probed with polyclonal anti-PrgX antibody, it is possible that the polyclonal anti-Div antibody did cross-react with native *E. coli* KJB24 proteins.

In order to rule out any cross-reactivity between native *E. coli* KJB24 (*rodA*⁻, *minB*) proteins and the anti-$DivIVA_{Ef}$ antibody, a new construct approach was undertaken. All $divIVA_{Ef}$ mutant constructs were amplified to incorporate a C-terminal (6X) His - tag fusion and were re-introduced to pUC18, creating the construct series known as "**pSM_.His**" (Table 3).

$DivIVA_{Ef}$ overexpression studies using *E. coli* KJB24 (*rodA*⁻, *minB*) were transformed with pUC18 (negative control) or the new positive control pDiv.His

Figure 13: *E. coli* KJB24 (*minB, rodA*$^-$) transformants carrying pSR-X demonstrate $PrgX_{Ef}$ overexpression by Western blot without affecting cell phenotype. **A-** $PrgX_{Ef}$ overexpression demonstrated by Western blot. Lanes: 1- 1 Kb+ ladder; 2- uninduced $PrgX_{Ef}$ at 2-Hrs; 3- induced PrgX at 2-Hrs post-IPTG (0.2 mM); 4- uninduced $PrgX_{Ef}$ at 3-Hrs; 5- induced $PrgX_{Ef}$ at 3-Hrs post-IPTG (0.2 mM); 6- uninduced $PrgX_{Ef}$ at 4-Hrs; and 7- induced $PrgX_{Ef}$ at 4-Hrs post-IPTG (0.2 mM). Densitometric analysis of duplicate samples was performed to ensure $DivIVA_{Ef}$ concentration equalized. Blots were probed with 1:1000 anti- $PrgX_{Ef}$ (Dr. G Dunny, U of Minnesota) and 1:3000 goat anti-mouse IgG conjugated to alkaline phosphatase; **B-** *E. coli* KJB24 (*minB, rodA*$^-$) transformants carrying pSR-X do not affect cell phenotype. Uninduced $PrgX_{Ef}$ at 4-hrs incubation (B1), induced $PrgX_{Ef}$ at 4-hrs post-IPTG (0.2mM) (B2).

Figure 13

A. *E. coli* KJB24 (*rodA*$^-$, *minB*), 4-Hrs post-IPTG

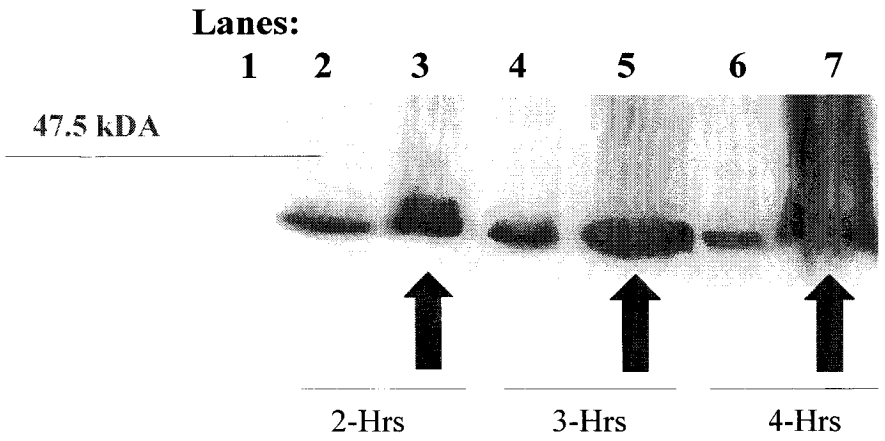

NB: Black arrow denotes IPTG-induced samples

B. *E. coli* KJB24 (*rodA*$^-$, *minB*), 4-Hrs post-IPTG

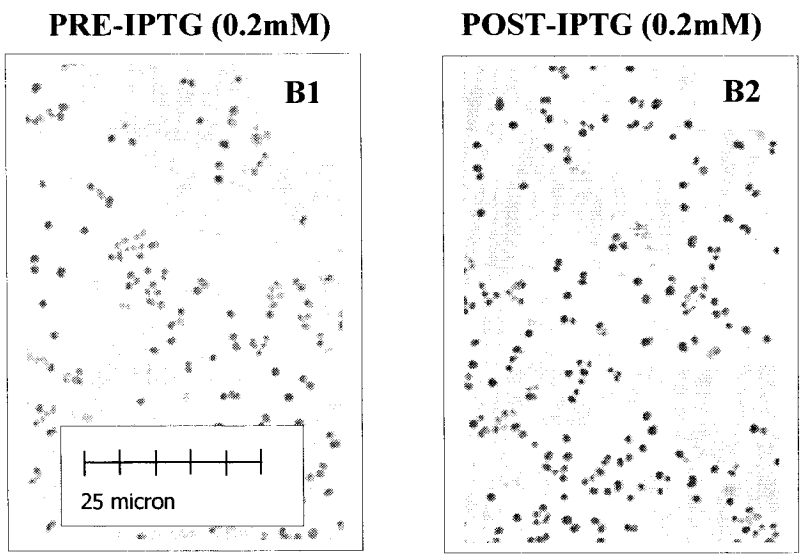

(*divIVA$_{Ef}$::6XHis*). Cells were induced with 0.8mM IPTG since this concentration proved successful in overexpression studies using the bacillary *E. coli* overexpression systems. Surprisingly, these Western blot results produced multiple bands and were identical to those achieved using *E. coli* KJB24 transformants from the construct series "**pSM_**" induced with 0.8 mM IPTG and probed with the polyclonal anti-DivIVA$_{Ef}$ antibody (data not shown).

E. coli KJB24 (*rodA*$^-$, *minB*) was transformed with pX-18, which is identical to pSR-X except for the incorporation of a C-terminal (6X) His - tag fusion to *prgX$_{Ef}$*. Similar PrgX$_{Ef}$ overexpression and morphological results were achieved (Figure 14).

E. coli KJB24 (*rodA*$^-$, *minB*) transformants carrying wt *divIVA$_{Ef}$* or *divIVA$_{Ef}$* with abrogated N-terminal coiled-coil domains exhibited an engorged cell morphology while the *divIVA$_{Ef}$* constructs with both central coiled-coil domains abrogated or the N-terminal coiled-coil domain truncated retained the wild-type cell phenotype. The presence of the foreign non-cell division plasmid DNA from *prgX$_{Ef}$* and its protein product (PrgX$_{Ef}$) do not seem to affect normal functioning or cell morphology of transformants as demonstrated by overexpression and morphological studies.

The fact that DivIVA$_{Ef}$ morphological studies seemed to indicate that DivIVA$_{Ef}$ interfered with the normal cell morphology but overexpression could not be verified by Western blot leads to another set of questions: Are the Min proteins competing with DivIVA$_{Ef}$? Are the activities of the Min proteins resulting in a sequestration, non-functionality or fragmentation of DivIVA$_{Ef}$? Is the round mutant cell shape responsible in part or completely for the observed augmented cell morphology? This none of these hold true, then why is the morphology of cells with *wt divIVA$_{Ef}$* construct altered?

Figure 14: *E. coli* KJB24 (*minB, rodA*$^-$) transformants carrying either pSR-X, pX-18, or pUC18 exhibit similar morphologies at 3-Hrs post-IPTG (0.2 mM) induction using phase contrast microscopy (100X oil immersion). All images measured using single scale bar applicable to all image panels. **A-** *E. coli* KJB24 transformed with pUC18; **B-** *E. coli* KJB24 carrying pSR-X; and **C-** *E. coli* KJB24 transformed with pX-18.

Figure 14

pUC18

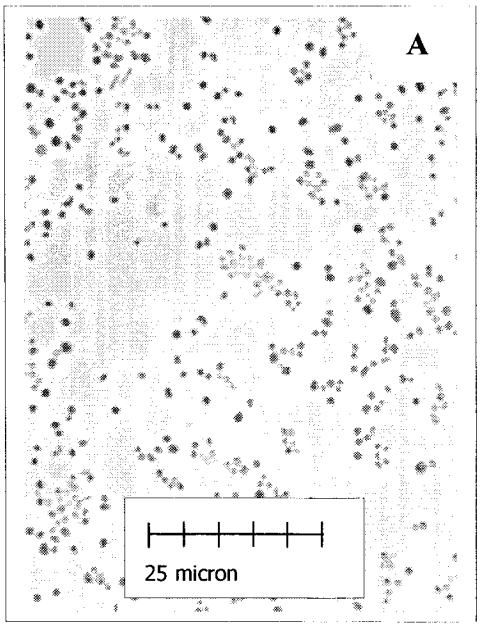

pSR-X

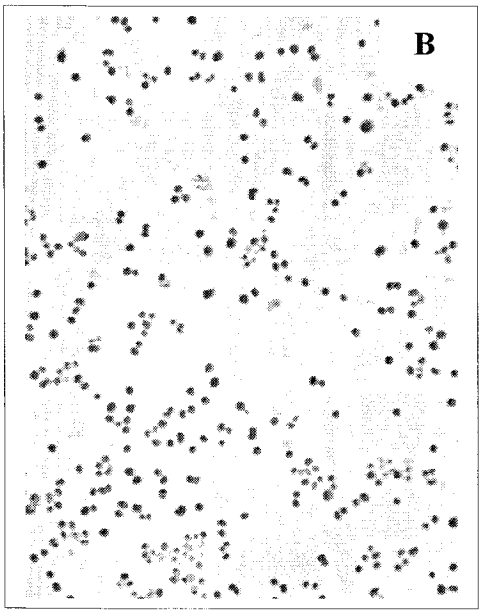

pX-18

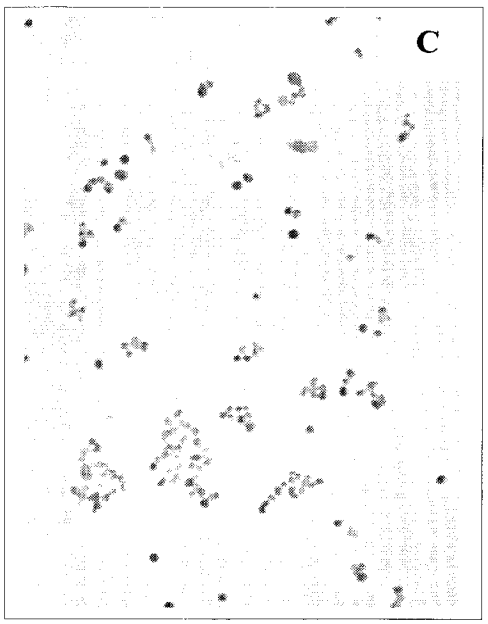

To address these questions, the isogenic derivative of *E. coli* KJB24 (*rodA*$^-$, *minB*) known as *E. coli* WM1250 (*rodA*$^-$, Δ*minB*), characterized by heterogeneous cocci, was used to examine the effects of DivIVA$_{Ef}$ overexpression.

E. coli WM1250 (*rodA*$^-$, Δ*minB*) were transformed with pUC18 (negative control) and compared to plasmid-free cells of the identical strain and no difference in cell morphology was ascertained by phase contrast microscopy, establishing pUC18 as a suitable negative control (data not shown).

The *divIVA$_{Ef}$* amplicons were subcloned in pUC18 following the *lacZ* promoter and to induce DivIVA$_{Ef}$ overexpression detectable by Western blot, an IPTG optimization experiment was implemented using a 3-Hrs incubation (Figure 15A). The **pSM_.His** construct series were employed in overexpression and morphological studies using *E. coli* WM1250. All *divIVA$_{Ef}$* constructs possess the C-terminal His-tag fusion to *divIVA$_{Ef}$* in this series. The Western blots demonstrated DivIVA$_{Ef}$ overexpression from pDiv.His (wt *divIVA$_{Ef}$::6XHis*) samples induced with 0.8mM IPTG. This result is comparable to those obtained using *E. coli* PB103 (*minB*) or *E. coli* PB114 (Δ*minB*) samples.

E. coli WM1250 transformed with pUC18 (the negative control) compared to plasmid-free cells of the identical strain and no difference in cell morphology was ascertained by phase contrast microscopy, establishing pUC18 as a suitable negative control (data not shown).

The cell phenotype of wild type *E. coli* KJB24 (*minB, rodA*$^-$) was compared against transformants carrying pUC18 (negative control) or pDiv.His (wt *divIVA$_{Ef}$::6XHis* – positive control). According to Corbin *et al.* (2002), *E. coli* WM1250 (Δ*minB, rodA*$^-$)

Figure 15: Determination of the optimal IPTG concentration *E. coli* WM1250 (Δ*minB, rodA*$^-$) transformants carrying pDiv.His (wt *divIVA*$_{Ef,}$ positive control) for DivIVA$_{Ef}$ overexpression in the absence of Min proteins at 3-Hrs post-IPTG induction as demonstrated by Western blot and microscopic assessment. **A-** *E. coli* WM1250 (Δ*minB, rodA*$^-$) transformants in the presence of Min proteins - Lanes: 1- Prestained marker; 2- pDiv.His - 0 mM IPTG; 3- pDiv.His - 0.05 mM IPTG; 4- pDiv.His - 0.1 mM IPTG; 5- pDiv.His - 0.2 mM IPTG; 6- pDiv.His - 0.4 mM IPTG; 7- pDiv.His - 0.8 mM IPTG; and 8- purified DivIVA$_{Ef}$. Densitometric analysis of duplicate samples was performed to ensure DivIVA$_{Ef}$ concentration equalized. Blots were probed with 1:1000 monoclonal anti-His antibody and 1:3000 goat anti-mouse IgG conjugated to alkaline phosphatase; **B-** Morphological phenotypes of *E. coli* WM1250 (Δ*minB, rodA*$^-$) transformants carrying wt *divIVA*$_{Ef}$ reveal engorged cells at 3-Hrs post-IPTG (0.8 mM) induction as depicted by phase contrast microscopy (100X oil immersion). All images measured using single scale bar applicable to all image panels. **B1-** pUC18 (negative control); **B2-** pDiv.His (wt *divIVA*$_{Ef,}$ positive control).

Figure 15

A. *E. coli* WM1250 (*rodA*$^-$, *ΔminB*) 3-Hrs post-IPTG

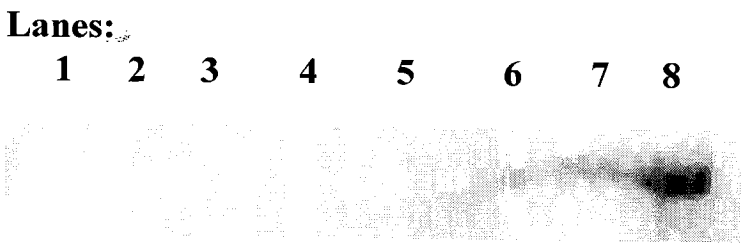

B.

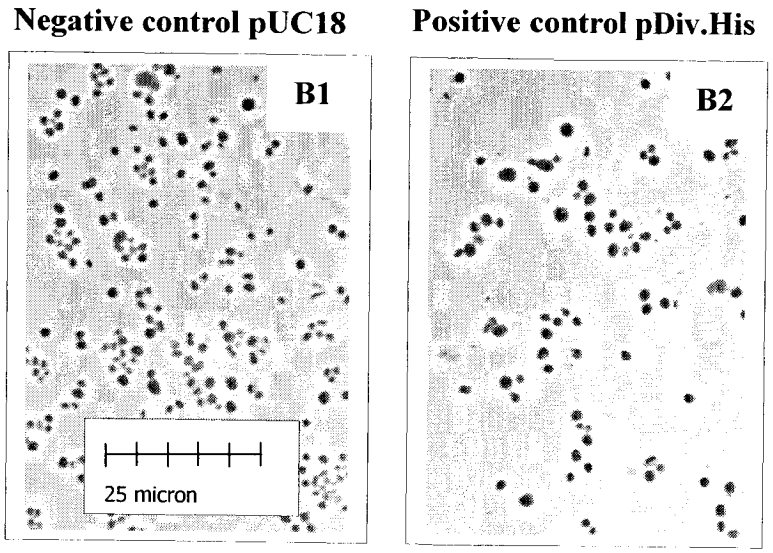

produced small and large cells with highly variable morphologies ranging in cell area from 2.2 to 9.3 μm^2. This appeared to be true only for samples of wt *E. coli* (*minB*) or transformants carrying pUC18, which were observed as small coccal-shaped cells with a cell area of 0.5 to 5 μm^2. Transformants carrying pDiv.His (wt $divIVA_{Ef}$*::His*) displayed an engorged cell phenotype with 21.9% of the cell population exceeding 5 μm^2 to a maximum area of 12 μm^2 (Table 5, Figure 15 B).

Full-length $divIVA_{Ef}$ transformed into all four *E. coli* [KJB24 (*rodA*$^-$, *minB*), WM1250 (*rodA*$^-$, *ΔminB*), PB103 (*minB*) and PB114 (*ΔminB*)] overexpression systems have consistently demonstrated significantly altered cell morphology suggestive of cell division arrest.

Having shown that the *E. coli* overexpression systems are suitable overexpression indicator systems for full-length $divIVA_{Ef}$ whether the Min proteins are present or absent, the mutated $divIVA_{Ef}$ constructs that abrogate individual coiled-coil domains were assessed in a similar manner. The mutated $divIVA_{Ef}$ constructs examined in conjunction with *E. coli* WM1250 (*rodA*$^-$, *ΔminB*) are: pSM3.His (E37P, N43P, L46D); pSM4.His (E37P, N43P, L46D, L50D, L50F); pSM6.His (1 - 190); pSM7.His (Δ130 – 190); pSM8.His (Δ60 – 190); pSM9.His (Δ60 – 130); or pSM12.His (L104P, L143P).

To ensure that mutated $DivIVA_{Ef}$ was being overexpressed, SDS-PAGE and Western blot protocols were carried out (Figure 16). $DivIVA_{Ef}$ overexpression in *E. coli* WM1250 (*rodA*$^-$, *ΔminB*) with the mutated $divIVA_{Ef}$ constructs was weak for pSM9.His; very strong for pSM3.His, pSM4.His and pSM6.His; and no $DivIVA_{Ef}$ overexpression was detected in samples with pSM7.His, pSM8.His and pSM12.His (Table 6). The lack of $DivIVA_{Ef}$

Figure 16: *E. coli* WM1250 (Δ*minB, rodA*$^-$) transformants carrying wt or mutated *divIVA*$_{Ef}$ demonstrate DivIVA$_{Ef}$ overexpression in the absence of Min proteins as demonstrated by Western blot. **Lanes: 1-** pUC18; **2-** pDiv.His; **3-** pSM3.His (E37P, N43P, L46D); **4-** pSM4.His (E37P, N43P, L46D, L50D, L50F); **5-** pSM6.His (1 - 190); **6-** pSM7.His (Δ130 – 190); **7-** pSM8.His (Δ60 – 190); **8-** pSM9.His (Δ60 – 130); **9-** pSM12.His (L104P, L143P) and **10-** purified DivIVA$_{Ef}$. Densitometric analysis of duplicate samples was performed to ensure DivIVA$_{Ef}$ concentration equalized. Blots were probed with 1:1000 monoclonal anti-His antibody and 1:3000 goat anti-mouse IgG conjugated to alkaline phosphatase

Figure 16

***E. coli* WM1250 (*rodA*$^-$, *ΔminB*) 3-Hrs post-IPTG**

Lanes:

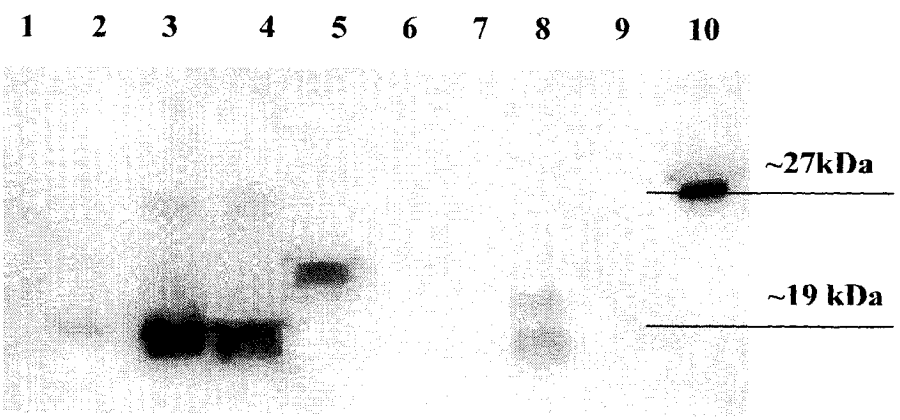

overexpression is consistent with results using the bacillary *E. coli* PB103 (*minB*) and *E. coli* PB114 (*ΔminB*). Like *E. coli* WM1250 transformants carrying pSM12.His, no DivIVA$_{Ef}$ overexpression was found using *E. coli* PB114. Oddly, DivIVA$_{Ef}$ overexpression was also found with *E. coli* transformants carrying pSM6.His using *E. coli* PB103 (*minB*) and *E. coli* WM1250 (Δ*minB*, rodA$^-$).

The western blot results using *E. coli* WM1250 samples containing *divIVA$_{Ef}$* constructs show similar results to those observed using the bacillary *E. coli* strains. The presence of two bands with molecular weights of ~19 kDa and ~27 kDa are observed using samples containing pSM3.His and pSM4.His. Wild type DivIVA$_{Ef}$ was observed possessing bands with molecular weights of ~19 kDa (Figure 16) and ~27 kDa (Figure 15) while samples containing pSM9.His demonstrated DivIVA$_{Ef}$ overexpression with bands having molecular weights of ~19 kDa and ~22 kDa (Figure 16). These results can be explained in a similar manner to the Western blot results obtained using bacillary *E. coli* strains. The DivIVA$_{Ef}$ overexpression of the smaller bands could have resulted from the initiation of protein synthesis by a downstream methionine (Met) as opposed to the initial Met (Figure 10).

The lack of mutated DivIVA$_{Ef}$ overexpression suggests that a change in cell phenotype should not be expected since the protein of interest in not present within the cell. The presence of DivIVA$_{Ef}$ should exert an effect on cell morphology and illustrate the biological functioning of this protein.

Table 5 depicts all cell lengths following microscopic assessment of fixed cells by phase contrast microscopy. *E. coli* WM1250 (*rodA$^-$*, *ΔminB*) transformants carrying mutated *divIVA$_{Ef}$* constructs abrogating the N-terminal coiled-coil domain demonstrated

DivIVA$_{Ef}$ overexpression. Since *E. coli* KJB24 (*rodA*$^-$, *minB*) transformants carrying *divIVA$_{Ef}$* constructs abrogating the N-terminal coiled-coil domain were observed as engorged cells, it was anticipated that a similar cell phenotype would result using *E. coli* WM1250. Curiously, this was true only with transformants carrying a mutation that abrogated only the first half of N-terminal coiled-coil domain (pSM3.His) while leaving the completely abrogated N-terminal coiled-coil domain mutation (pSM4.His) unaffected. Samples containing pSM3.His exhibited cells equal in area to that observed with wt *divIVA$_{Ef}$::6XHis* at 12 μm^2 while all other *E. coli* WM1250 transformants carrying mutated *divIVA$_{Ef}$* constructs demonstrated a cell area not larger than 7 μm^2 which conforms to cell area measurements by Corbin *et al.* (2002). Although samples carrying mutated *divIVA$_{Ef}$* constructs did overexpress DivIVA$_{Ef}$ in absence of Min proteins, these mutant coccal-shaped *E. coli* transformants did not reliably demonstrate altered cell morphology in a manner that would elucidate the biological functioning of DivIVA$_{Ef}$.

E. coli WM1250 transformants carrying pX-18 did overexpress PrgX$_{Ef}$; however microscopic assessment revealed some unexpected findings relating to the cell phenotype. While cells exhibited a cell area of ~1 – 3 μm^2, many cells had lysed and cell aggregation was observed (Figure 17). These effects could possibly be attributable to the lack of Min proteins in *E. coli* WM1250 (Δ*minB, rodA*$^-$) since *E. coli* KJB24 (*minB, rodA*$^-$) transformants carrying the identical construct revealed no such aberrations.

In conclusion, the heterologous *E. coli* DivIVA$_{Ef}$ overexpression indicator systems all exhibited altered cell morphology as a result of the presence of full-length *divIVA$_{Ef}$* protein product in cells. In general, bacillary *E. coli* strains demonstrated reproducibly

Figure 17: *E. coli* WM1250 (Δ*minB, rodA*$^-$) transformants with pX-18 exhibit aberrant morphology at 3-Hrs post-IPTG (0.2 mM) induction as depicted by phase contrast microscopy (100X oil immersion). All images measured using single scale bar applicable to all image panels. **A1-** and **A2-** *E. coli* WM1250 transformed with pX-18; **B-** DNA electrophoresis gel demonstrating molecular size of pUC18 (2686 bp) (**lane 1**) and pX-18 (~3657bp) (**lane 2** and **3**).

Figure 17

A. *E. coli* WM1250 (*rodA*⁻, *ΔminB*) 3-Hrs post-IPTG

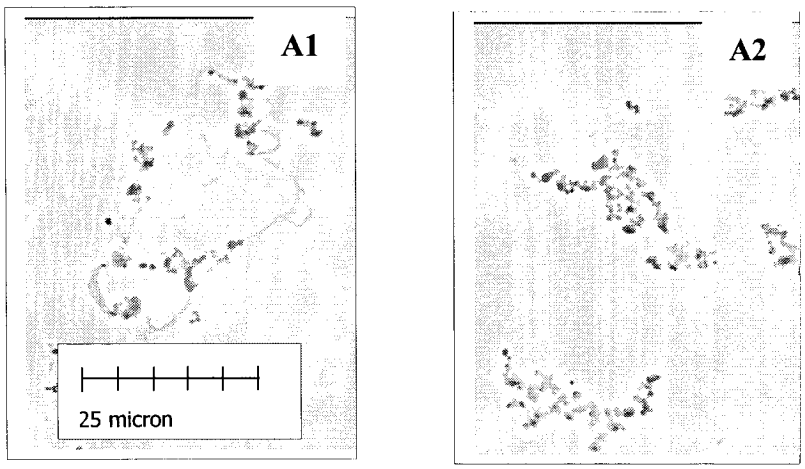

B. Lanes: 1 2 3

more dramatic changes in cell morphology relative to coccal-shaped *E. coli* strains when transformed with the full-length $divIVA_{Ef}$ constructs.

Bacillary *E. coli* PB103 (*minB*) and PB114 (Δ*minB*) transformants carrying mutated $divIVA_{Ef}$ constructs did overexpress $DivIVA_{Ef}$ in the presence or absence (respectively) of Min proteins. *E. coli* strains lacking Min proteins with pSM3.His, which abrogates the first half of the N-terminal coiled-coil domain of $divIVA_{Ef}$, resulted in cells of altered morphology. Thus, bacillary *E. coli* transformants did not reliably demonstrate altered cell morphology in a manner that would elucidate the biological functioning of $DivIVA_{Ef}$.

No $DivIVA_{Ef}$ overexpression could be conclusively determined by Western blot using *E. coli* KJB24 (*minB, rodA*$^-$) transformants because of the multiple binding patterns. The lack of Min proteins in *E. coli* WM1250 (Δ*minB, rodA*$^-$) is the only difference relative to *E. coli* KJB24 potentially explaining Western blot results. However, The rod-shaped *E. coli* PB103 transformants carrying mutated $divIVA_{Ef}$ constructs did overexpress $DivIVA_{Ef}$ in the presence of Min proteins. The elimination of *rodA*$^-$ is the only genetic change between *E. coli* PB103 (*minB*) and *E. coli* KJB24 (*minB*) that affects cell shape. Possibly this difference is sufficient to cause the different overexpression results. Finally, *E. coli* KJB24 (*rodA*$^-$) transformants with wt $divIVA_{Ef}$ appeared to grow in LB_{Amp100} broth, but following transfer onto LB_{Amp100} plates was unable to produce any colonies, suggestive of cell stress.

The cell phenotypes in coccal-shaped *E. coli* strains were not only more difficult to observe relative to bacillary *E. coli*, it was less consistently reproducible. Bacillary *E. coli* PB103 (*minB*) or *E. coli* PB114 (Δ*minB*) transformants demonstrated a cell length range readily observable using phase contrast microscopy. Thus, the heterologous bacillary *E.*

coli systems using PB103 (*minB*) or *E. coli* PB114 (Δ*minB*) proved to be overall the more experiment-friendly system.

Very little has been published about DivIVA$_{Ef}$ and the biological functions during cell division were uncharacterized. This is the first report demonstrating the ability of DivIVA$_{Ef}$ to overexpress in heterologous system; in the presence or absence of MinC, MinD and MinE; and in bacilli or cocci. This research has shown new information regarding the biological functioning of DivIVA$_{Ef}$.

3.3 DivIVA$_{Ef}$ Overexpression in coccal-shaped *E. faecalis* JH2-2

E. faecalis JH2-2 was selected since it is plasmid-free facilitating straightforward transformation, eliminating potential problems of plasmid recombination. The cloning vector for the homologous system made use of the *E. coli* - *E. faecalis* shuttle-vector pMSP3545 (Dr. G. Dunny, U of Minnesota). The plasmid pSMSP3545 is recognized as a suitable vector to investigate protein overexpression from enterococcal backgrounds (Bryan *et al.*, 2000).

The pMSP3545 plasmid contains a marker for selection using erythromycin (Ery) and provides the *nisRK* genes, critical to the nisin-control expression (NICE) system, which would permit the overexpression of DivIVA$_{Ef}$ in a controlled manner using *E. faecalis* JH2-2 as host (Bryan *et al;* 2000). The efficiency of genes under the control of the nisin promoter is reported to be greater than genes induced under the control of Gram-positive promoters like *PSpac, PxylA* and *PlacA* (Edwards *et al;* 2000).

To investigate nisin-inducible DivIVA$_{Ef}$ overexpression using *E. faecalis* JH2-2, I developed and optimized a NICE system specific to enterococci. A nisin concentration experiment was done using plasmid-free *E. faecalis* JH2-2. Cell growth was not

adversely affected using nisin between 0.2 to 1.5 μg/ml (Figure 5). While cells grew faster and longer using lower nisin concentrations of 0.2 to 1.0 μg/ml, no $DivIVA_{Ef}$ overexpression was demonstrated by Western blot using the polyclonal anti-Div antibody of proven reliability as reported by other researchers (Bryan *et al.*, 2000; Ramirez-Arcos *et al.*, 2001).

Nisin-induced (1.5 μg/ml) *E. faecalis* JH2-2 carrying the positive control pMSPSRDiv-1 (P_{nisA}::$divIVA_{Ef}$) demonstrated $DivIVA_{Ef}$ overexpression without altering the wild type cell phenotype (Table 7). $DivIVA_{Ef}$ overexpression was stronger using the nisin-induced *E. faecalis* JH2-2 carrying pMSPSRDiv-1 (P_{nisA}::$divIVA_{Ef}$) relative to the *E. faecalis* JH2-2 transformants carrying pMSP3545 (negative control) (Figure 18A). These results suggest that transformants carrying pMSP3545 demonstrated $DivIVA_{Ef}$ was expressed from the chromosomal DNA only while transformants carrying pMSPSRDiv-1 demonstrated $DivIVA_{Ef}$ was expressed from both chromosomal and plasmid DNA resulting in a stronger presence of protein (Figure 18A). Interestingly, $DivIVA_{Ef}$ overexpression was approximately equivalent in $DivIVA_{Ef}$ overexpression at point of nisin induction (t_0) and 3-Hrs post-Nisin (t_3), suggesting leaky expression. Moreover, $DivIVA_{Ef}$ overexpression did not alter the natural cell phenotype of *E. faecalis* JH2-2 demonstrating that the increased $DivIVA_{Ef}$ levels were not toxic to cells (Figure 18B).

Microscopic assessment of wt *E. faecalis* JH2-2 cells and transformants carrying either pMSP3545 (negative control) or pMSPSRDiv-1 (P_{nisA}::$divIVA_{Ef}$ - positive control) control demonstrated a similar cell phenotype characterized by small, regular coccal-shaped cells (data not shown).

Table 7: The transformants using *E. faecalis* JH2-2 homologous system carrying either the inducible *divIVA$_{Ef}$* (pMSPSRDiv-1) or non-inducible *divIVA$_{Ef}$* (pMSPSRDiv-1) demonstrate normal phenotypes and overexpress DivIVA$_{Ef}$.

Name	Induction	Phenotype	Overexpression (Western blot)
pMSP3545	Nisin (1.5 μg/ml)	Normal[a]	No
pMSPSRDiv-1	Nisin (1.5 μg/ml)	Normal	Yes
pMSPSRDiv-2	Non required	Normal	Yes

NB:

Normal[a] denotes the *E. faecalis* JH2-2 wild-type morphological phenotype.

Figure 18: *E. faecalis* JH2-2 transformants carrying *wt* $divIVA_{Ef}$ (pMSPSRDiv-1) demonstrate $DivIVA_{Ef}$ overexpression by Western blot without altering the cell phenotype. **A-** Western blot of *E. faecalis* JH2-2 transformants carrying the positive control pMSPSRDiv-1 (P_{nisA}*::*$divIVA_{Ef}$) or the negative control pMSP3545. "t_0" indicates introduction of nisin and "t_4" indicates 4-Hrs post-nisin (1.5 μg/ml) induction. Lanes: 1- pMSPSRDiv-1 (t_0); 2- pMSP3545 (t_0) (negative control); 3- pMSP3545 (t_4); and 4- pMSPSRDiv-1 (t_4). Densitometric analysis of duplicate samples was performed to ensure $DivIVA_{Ef}$ concentration equalized. Blots were probed with 1:2000 anti-Div_{Ef} (Ramirez-Arcos *et al.*, 2001) and 1:3000 goat anti-rabbit IgG conjugated to alkaline phosphatase; *E. faecalis* JH2-2 carrying either pMSP3545 or pMSPSRDiv-1 3-hrs post-nisin induction as depicted by phase contrast microscopy (100X oil immersion). All images measured using single scale bar applicable to all image panels. **B1-** *E. faecalis* JH2-2 carrying pMSP3545; **B2-** *E. faecalis* JH2-2 carrying pMSPSRDiv-1.

Figure 18

A. *E. faecalis* JH2-2, 3-Hrs post-IPTG

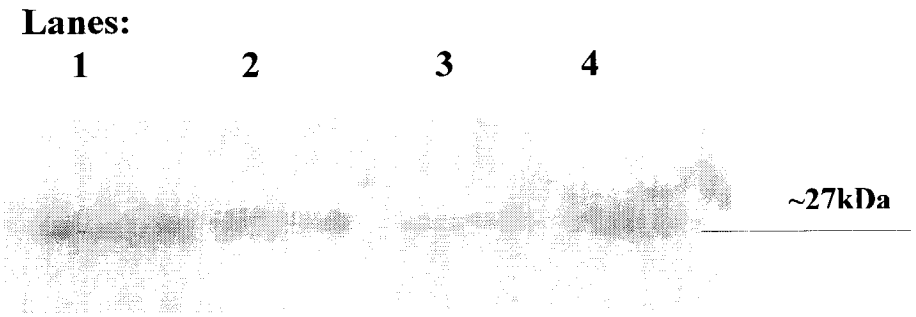

B. *E. faecalis* JH2-2, 3-Hrs post-IPTG

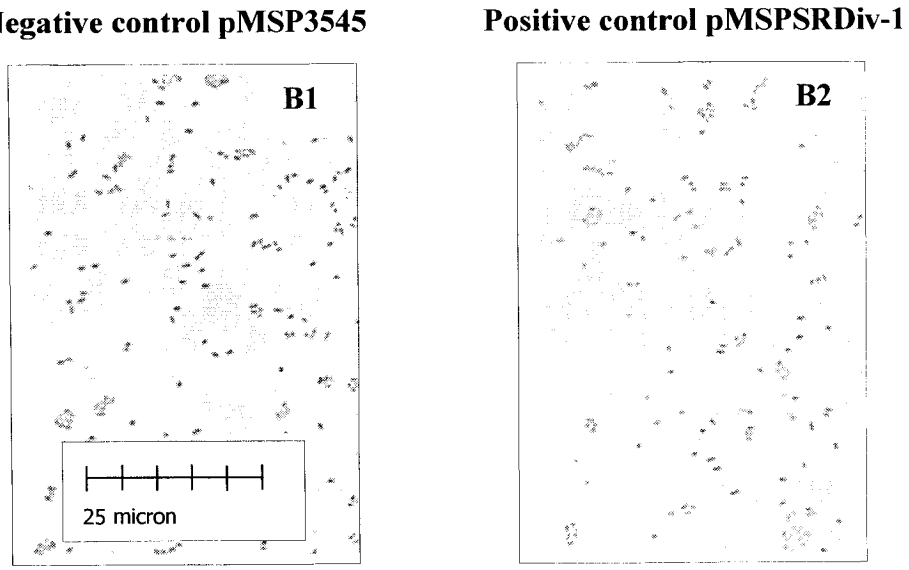

To investigate non-inducible $DivIVA_{Ef}$ overexpression, the plasmid known as pMSPSRDiv-2 ($P_{nisA}::P_{divIVAEf}::divIVA_{Ef}$) was transformed in *E. faecalis* JH2-2. The $divIVA_{Ef}$ gene, under the control of its own promoter ($PdivIVA_{Ef}$) should produce multiple transcription of the gene resulting in multiple translation of the protein product. This overexpression system would be compared against the nisin-inducible system to evaluate the concentration of $DivIVA_{Ef}$ overexpression, the changes in cell morphology attributable to the effects of increased $DivIVA_{Ef}$ overexpression and the simplicity of system. Eventually the mutated $divIVA_{Ef}$ constructs would be developed to investigate the effects of mutated $DivIVA_{Ef}$ overexpression in the native *E. faecalis* JH2-2.

The growth of *E. faecalis* JH2-2 transformants carrying pMSPSRDiv-2 ($P_{nisA}::P_{divIVAEf}::divIVA_{Ef}$) was also examined and compared to *E. faecalis* JH2-2 transformants carrying pMSPSRDiv-2 ($P_{nisA}::divIVA_{Ef}$) (Figure 5). The exponential phase of *E. faecalis* JH2-2 transformants carrying pMSPSRDiv-2 was initiated earlier, accelerated more quickly and had a shorter duration than *E. faecalis* cells carrying pMSP3545. This result contrasts sharply with results obtained using *E. coli* KJB24, where the presence of wt $divIVA_{Ef}$ (pSM6) produced slower growth (Figure 4).

Levels of $DivIVA_{Ef}$ overexpression in *E. faecalis* JH2-2 transformants with pMSPSRDiv-2 ($P_{nisA}::P_{divIVAEf}::divIVA_{Ef}$) were greater than background $DivIVA_{Ef}$ overexpression at 4-Hrs in transformants with pMSP3545 (negative control) without altering the inherent cell phenotype of *E. faecalis* JH2-2 (Figure 19).

Overexpression of $DivIVA_{Ef}$ was achieved in a nisin-inducible (1.5 μg/mL) manner using *E. faecalis* JH2-2 transformants with pMSPSRDiv-1 ($P_{nisA}::divIVA_{Ef}$) or in a non-inducible manner using *E. faecalis* JH2-2 transformants with pMSPSRDiv-2

Figure 19: *E. faecalis* JH2-2 transformants with pMSPSRDiv-2 (positive control) demonstrates increased $DivIVA_{Ef}$ overexpression relative to pMSP3545 (negative control) by Western blot. "t_4" indicates 4-Hrs post-nisin induction. **Lanes: 1**-Prestained marker at ~27 KDa; **2-** and **4-** *E. faecalis* JH2-2 transformed with pMSP3545 (t_4); **3-** and **5-** *E. faecalis* JH2-2 transformed with pMSPSRDiv-1 (t_4).

Figure 19

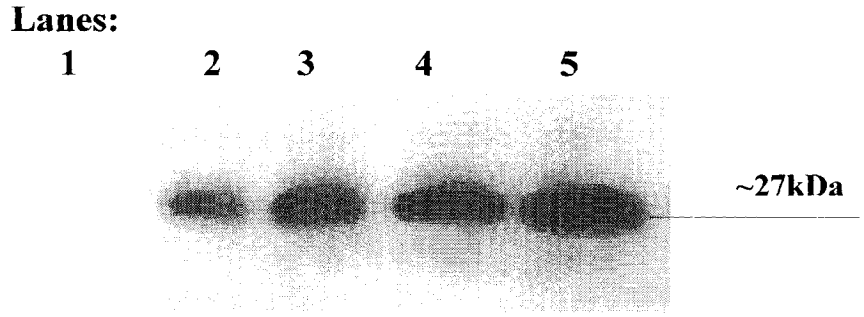

(P_{nisA}::$P_{divIVAEf}$::$divIVA_{Ef}$) without altering the cell phenotype. The non-inducible system proved to be easier to use and yielded stronger levels of DivIVA$_{Ef}$ overexpression. Finally, *E. faecalis* JH2-2 transformants carrying pMSP3545, pMSPSRDiv-1 (P_{nisA}::$divIVA_{Ef}$) or pMSPSRDiv-2 (P_{nisA}::$P_{divIVAEf}$::$divIVA_{Ef}$) were observed as small and regular cocci with a cell area of 0.5 – 1.0 μm^2 (Table 8).

3.5 *E. faecalis* JH2-2 cell development and localization of DivIVA$_{Ef}$

Cell morphology can provide information to assist in the elucidation of bacterial cell cycle. For example, immunogold labeling and transmission electron microscopy (TEM) were used in this research to determine the localization of DivIVA$_{Ef}$ in *E. faecalis* JH2-2 at the stationary phase of cell growth. The cells were depicted at different stages of the cell division processes from the initiation of the septal wall at the approximate mid-cell region to the fully formed septal wall support to Higgins *et al.* (1971, 1976) hypothesis on cell development in *E. faecalis*.

Wild type *E. faecalis* JH2-2 or *E. faecalis* JH2-2 transformed with pMSPSRDiv-1 (P_{nisA}::$divIVA_{Ef}$) or pMSPSRDiv-2 (P_{nisA}::$P_{divIVAEf}$::$divIVA_{Ef}$) were examined using TEM. *E. faecalis* JH2-2 transformed with pMSPSRDiv-1 (P_{nisA}::$divIVA_{Ef}$) or pMSPSRDiv-2 (P_{nisA}::$P_{divIVAEf}$::$divIVA_{Ef}$) fixed specifically for immunogold labeling and assessed by TEM.

The immunogold labelling determined DivIVA$_{Ef}$ localization and whether increased DivIVA$_{Ef}$ presence localized differently from normal DivIVA$_{Ef}$ concentrations.

Figure 20A depicts wt *E. faecalis* JH2-2 cells by TEM (5000X). Immature cells with a spherical shape seem to become ovoid with growth. New growth extended from the

Table 8: The cell area of transformants using *E. faecalis* JH2-2 homologous system carrying either the negative control (pMSP3545), inducible *divIVA$_{Ef}$* (pMSPSRDiv-1) or non-inducible *divIVA$_{Ef}$* (pMSPSRDiv-1) are near identical

Construct	Class Area (μm^2)	Population Total/in class (N/n)	Percentage (%)	Mean (μm) ± Standard Deviation (SD)
pMSP3545	0.5 – 1.0	568/479	84.3	0.67 ± 0.17
pMSPSRDiv-1	0.5 – 1.0	683/482	70.6	0.63 ± 0.20
pMSPSRDiv-2	0.5 – 1.0	508/429	84.5	0.63 ± 0.16

NB:

Normal[a] denotes the *E. faecalis* JH2-2 wild-type morphological phenotype.

Figure 20: Transmission electron microscopy reveals peripheral $DivIVA_{Ef}$ localization in wild-type *E. faecalis* JH2-2. **A-** wt *E. faecalis* JH2-2 as depicted by transmission electron microscopy (TEM) using direct magnification of 5400X; **B-** TEM, using direct magnification of 12040X. Immunogold labelling of $DivIVA_{Ef}$ observed as tiny black dots (**White** arrows) demonstrate $DivIVA_{Ef}$ localization. Immunogold labelling and TEM imaging done by Dr. Peter Rippstein.

Figure 20

Wild-type *E. faecalis* JH2-2

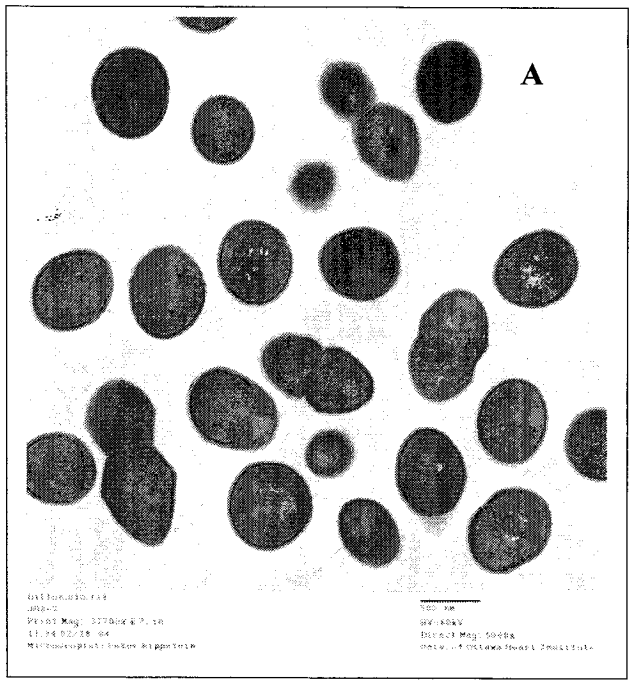

Wild-type *E. faecalis* JH2-2

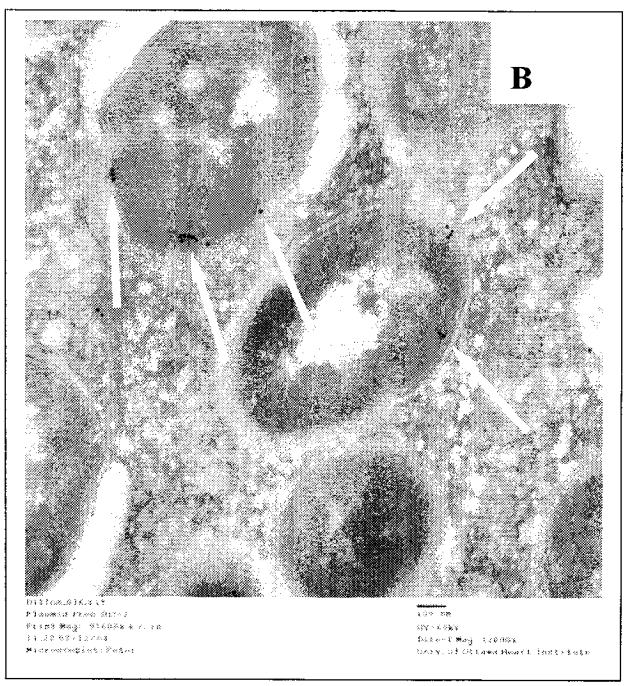

mid-cell region outward at an angle, extending the wall band distances such that cells resembled a double arrowhead of sorts. Figure 20B depicts DivIVA$_{Ef}$ localization at the cytoplasmic membrane periphery toward the cell poles. The development of cell poles is distinctive and may suggest a predetermined mid-cell region where cell division transpires and yet spherical cells are thought to have the potential for multiple division sites (Begg and Donachie, 1998; Corbin *et al.*, 2002; Daniel and Errington, 2003; Donachie *et al.*, 1995).

E. faecalis JH2-2 transformants carrying pMSPSRDiv-1 (P_{nisA}::$divIVA_{Ef}$) by TEM demonstrated a similar cell phenotype to wt *E. faecalis* JH2-2 cells. During cell division, cells developed discernible wall bands and growth caused the cell shape to change (Figure 21).

E. faecalis JH2-2 transformants carrying pMSPSRDiv-2 (P_{nisA}::$P_{divIVAEf}$::$divIVA_{Ef}$) by TEM exhibits cell morphology similar to wt *E. faecalis* JH2-2 and transformants with pMSPSRDiv-1 (Figure 22). DivIVA$_{Ef}$ localization exhibited to a broad range of locations detectable with immunogold labeling and included the cell membrane (1), newer peripheral cell walls (2), septal wall (3), nucleoid region (4), and external edges of the cell walls (5).

More DivIVA$_{Ef}$ localization seems present in *E. faecalis* JH2-2 carrying pMSPSRDiv-2 relative to wt *E. faecalis* JH2-2 (Figure 20 & Figure 22).

In conclusion, the defining of the mid-cell point by some unknown mechanism seems to signal the initiation of cell elongation necessary for division. At some undefined point, the septal wall commences its inward growth towards a mirror replica at the transverse side of the cell. The two wall halves meet at some internal cell mid-point. As the septal

Figure 21: Cell growth using *E. faecalis* JH2-2 transformants with pMSPSRDiv-1 (wt *divIVA*$_{Ef}$ positive control) using transmission electron microscopy. **A-** *E. faecalis* JH2-2 transformants carrying pMSPSRDiv-1 using direct magnification of 4404X; **B-** *faecalis* JH2-2 transformants carrying pMSPSRDiv-1 using direct magnification of 12040X. Immunogold labelling of DivIVA$_{Ef}$ observed as tiny black dots (**White** arrows) demonstrate DivIVA$_{Ef}$ localization. TEM imaging done by Dr. Peter Rippstein.

Figure 21

***E. faecalis* JH2-2 + pMSPSRDiv-1**

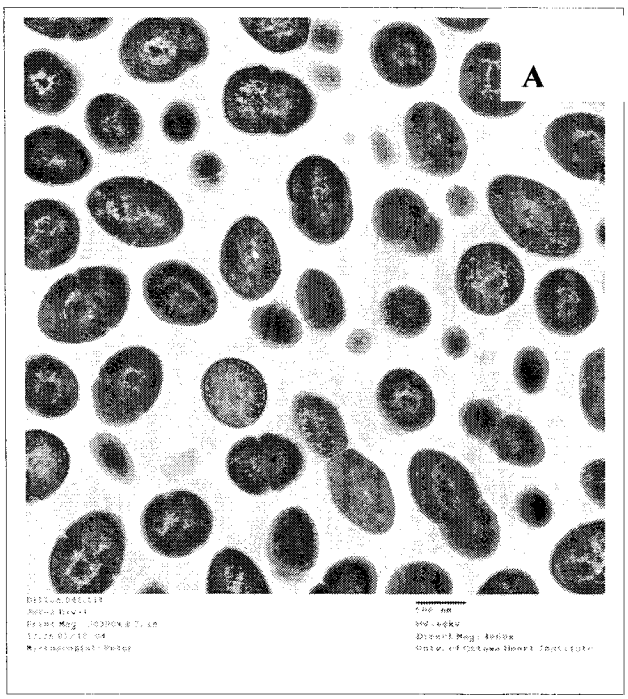

***E. faecalis* JH2-2 + pMSPSRDiv-1**

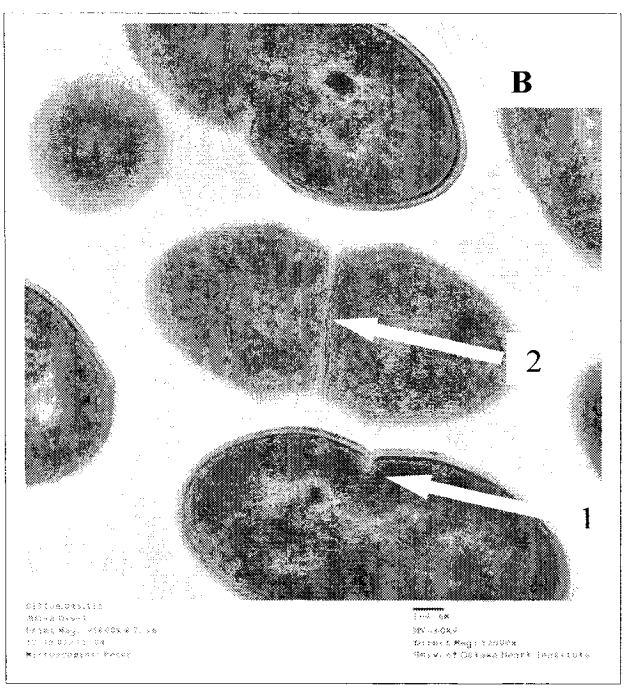

Figure 22: Transmission electron microscopy reveals $DivIVA_{Ef}$ localization in *E. faecalis* JH2-2 transformants carrying pMSPSRDiv-2 (wt $divIVA_{Ef}$ positive control). **A-** *E. faecalis* JH2-2 transformants carrying pMSPSRDiv-2 using direct magnification of 6000X; **B- -** *E. faecalis* JH2-2 transformants carrying pMSPSRDiv-2 using direct magnification of 15000X. Immunogold labeling seen as tiny black dots (**White** arrows) demonstrate the localization of $DivIVA_{Ef}$. Immunogold labelling and TEM imaging done by Dr. Peter Rippstein.

Figure 22

***E. faecalis* JH2-2 + pMSPSRDiv-2**

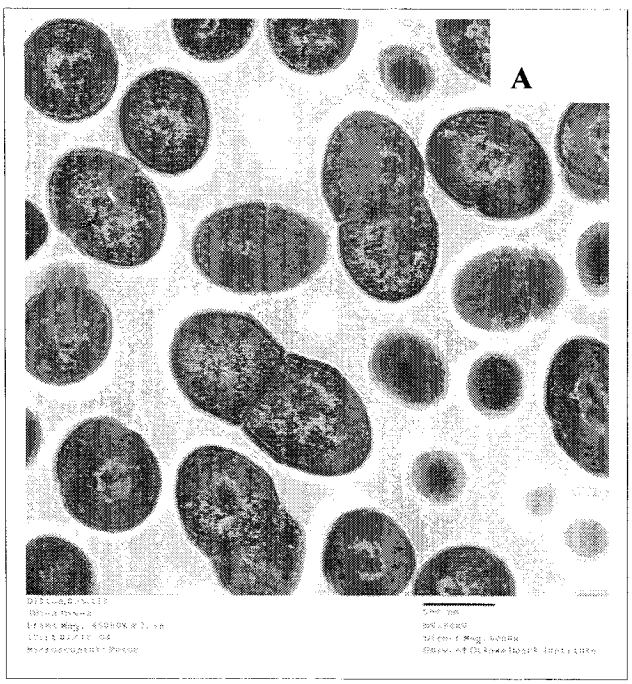

***E. faecalis* JH2-2 + pMSPSRDiv-2**

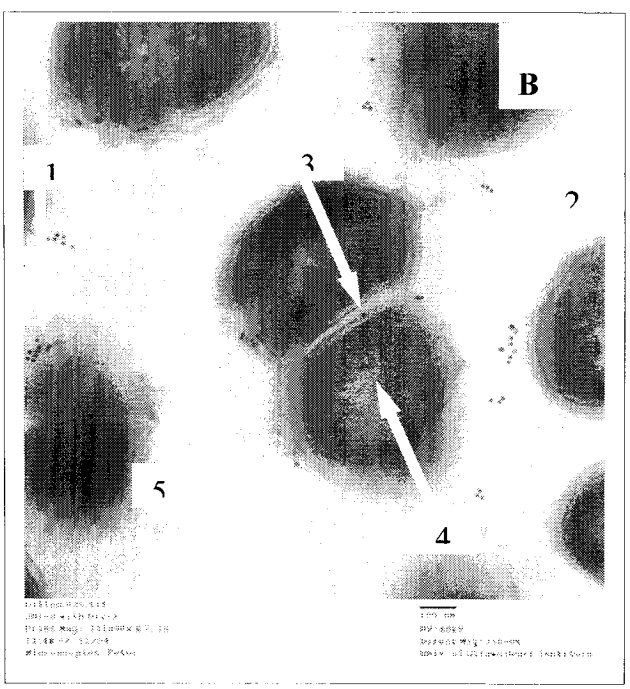

wall-halves approach each other, the outer cell wall appears to thicken over its entirety. Higgins *et al.* (1971) proposed a cell division model wherein peripheral surface enlargement is favored over cell wall thickening during chromosome replication, while chromosome termination is characterized by cell wall thickening, septation and by the last stages of cell separation. DivIVA$_{Ef}$ localization is the wt *E. faecalis* JH2-2 seems to be limited to the cell poles while *E. faecalis* JH2-2 transformants with pMSPSRDiv-2 ($P_{nisA}::P_{divIVAEf}::divIVA_{Ef}$ - the positive control) to exhibit a broad range of locations possibly attributable to the increased DivIVA$_{Ef}$ concentration.

DISCUSSION:

Overview

This research assessed a series of unique mutations created along the 699-nucleotide length of the *divIVA$_{Ef}$* gene with and without a C-terminal 6XHis tag fusion subcloned into pUC18. DivIVA$_{Ef}$ overexpression and morphological studies were conducted using *E. coli* PB103 (*minB*), *E. coli* PB114 (Δ*minB*), *E. coli* KJB24 (*minB, rodA*$^-$) and *E. coli* WM1250 (Δ*minB, rodA*$^-$) and *E. faecalis* JH2-2. Overexpression of wt and mutated *divIVA$_{Ef}$* constructs was performed to assess the biological role of DivIVA$_{Ef}$ and verify the morphological effects on bacteria using constructs which had previously been shown to lack of DivIVA$_{Ef}$ oligomerization. A specific goal was to elucidate the biological function of DivIVA$_{Ef}$ containing abrogated central coiled-coil domains where DivIVA$_{Ef}$ is thought to be involved in self-interaction (Rigden, 2005).

4.1 Molecular weights of wild type and mutated DivIVA$_{Ef}$

Bioinformatic analysis and biochemical approaches (including native gel and gel filtration) ultimately confirmed that wt DivIVA$_{Ef}$ has a molecular weight of ~27kDa with mutated DivIVA$_{Ef}$ having the following molecular weights (MW): pSM3 His, pSM4.His and pSM12.His at ~27 kDa since these mutations comprise multiple point mutations not significantly change the MW; pSM6.His at ~23 kDa due to the deletion of the C-terminal coiled-coil domain; pSM7.His, pSM8.His, and pSM9.His at ~17 kDa because these constructs contain *divIVA$_{Ef}$* amplicons with large deletions of the central coiled-coil domains (Table 4) (Rigden, 2005).

A discrepancy in size was observed in samples assessed by Western blot and could have been attributable to several factors such as proteolytic cleavage, satellite mutations,

or downstream initiation of translation. Proteolytic cleavage can be caused by the presence of proteolytic enzymes capable of breaking peptide bonds between specific amino acids in proteins (Griffiths *et al.*, 1996). My analysis indicated no obvious cleavage site in the $DivIVA_{Ef}$ sequence that would result in a C-terminal fragment. Moreover, nonspecific cleavage would be random and not produce such a consistent molecular weight.

The introduction of mutations occurring during the PCR procedure can result in satellite mutations and stutter patterns (Miller and Yuan, 1997; van Belkun *et al.*, 1998). The possibility of mutation introduced by PCR was ruled out because all constructs were DNA sequenced. Incorrect preparation of samples or protein aggregation as reported by investigator studying $DivIVA_{Bs}$ (Stahlberg *et al*, 2004) are all possible scenarios.

The initiation of translation at a downstream Met could have resulted. Figure 10 depicts the predicted translation of $DivIVA_{Ef}$ and the cloning vector pUC18. Five Met locations are found along the length of $DivIVA_{Ef}$. Primers used in PCR amplification of wt $divIVA_{Ef}$ resulted in a frame-shift at the pUC18 - $divIVA_{Ef}$ juncture. This may have prompted the translation machinery select any Met are located at aa 1, 17, 91 114 and 157 to initiate protein synthesis.

The construct pSM6.His was designed by eliminating the C-terminal coiled-coil domain of $divIVA_{Ef}$ amplicon resulting in a construct with a predicted molecular weight of ~23 kDa (Table 4). DivIVA homologues demonstrate high variability and inconsistent coiled-coil domain predictions along the C-terminal region of DivIVA, suggesting a potential role in species-specific interactions possibly involving unidentified binding proteins. In contrast, the high sequence conservation of the N-terminal domain of the

coiled-coil region of $DivIVA_{Ef}$ across bacteria may well be involved with the selection of cell division site and this would explain the high level of conservation with this domain across bacterial species possessing DivIVA homologues. Abrogation of the N-terminal coiled-coil domain was shown not to be involved in the oligomerization of $DivIVA_{Ef}$ and these mutated $DivIVA_{Ef}$ monomers are stable (Table 4) (Rigden, 2005).

Biochemical studies have determined that the central coiled-coil domain is most likely responsible for $DivIVA_{Ef}$ self-interactions (Table 8) (Rigden, 2005). My research supports this finding. The constructs pSM7.His (Δ130 - 190), pSM8.His (Δ60 - 190) never overexpressed $DivIVA_{Ef}$ in *E. coli* strains and therefore the cell phenotype of these transformants remained unaltered. The construct pSM12.His (L104P, L143P) only demonstrated DivIVA overexpression in *E. coli* PB103 without altering the natural cell phenotype of the *E. coli* strain employed.

4.2 The nature of shape

Exactly how shape is specified by imposition of the gene on wall assembly is very poorly understood (Daniel and Errington, 2003). Hydrostatic pressure and surface tension are the physical parameters involved in the formation of *E. coli* cell morphology, but this does not hold true for *B. subtilis* because of the differences in their cell division mechanisms (Koch, 1985; Nanninga, 1998). The formation of a septum in *B. subtilis* allows the cell to divide, whereas *E. coli* constricts prior to cell division causing a reduction in the cell diameter (Koch, 1985; Nanninga, 1998). Moreover, peptidoglycan synthesis in both *E. coli* and *B. subtilis* occurs relatively dispersed over the wall (Daniel and Errington, 2003).

Stable elongation will be successful in rod-shaped cells, if four criteria are fulfilled: the lateral walls should enlarge in a distributive way to permit the insertion of building blocks; rigid polar caps should be maintained; turgor pressure should be maintained; and the lateral walls require a certain fluidity dependent on the cells' synthetic and lytic activities relative to growth (Koch 1980). These criteria and specific constituents like cell shape determinants that result in the regular bacilli shape, characterize *E. coli* PB103 (*minB*) (Varley and Stewart, 1992).

According to Nanninga (1998), the typical *E. coli* rod-shaped cell is 1.5 to 5.5 μm in length and has a diameter or cell depth of 0.5 to 1.0 μm. The work achieved by Nanninga is confirmed by the morphological studies conducted by this research. I found that wt *E. coli* PB103 cells or *E. coli* transformants carrying pUC18 demonstrated small, regular bacilli no longer than 5 μm (Table 4). However, the presence of $DivIVA_{Ef}$ yielded a filamentous cell of 20 μm. The greatly increased cell length of transformants carrying pDiv.His (*$divIVA_{Ef}$::6XHis)* is suggestive of cell arrest.

E. coli PB103 transformants carrying one of: pSM3.His, pSM4.His, pSM6.His, pSM8.His, and pSM9.His also exhibited a cell length and depth within the range outlined by Nanninga (1998). *E. coli* PB103 transformants carrying one of: pDiv.His, pSM7.His, and pSM12.His demonstrated a small percentage of the entire cell population exceeding the 5.5 μm length at 12.9%, 3.9% and 9.8%, respectively with maximum cell lengths of 40 μm, 10 μm and 10 μm, respectively. The two-fold increase of cell length in pSM7.His and pSM12.His is harder to rationalize. $DivIVA_{Ef}$ overexpression was observed with samples containing pSM12.His, which is a double point mutation abrogating the central coiled-coil domains resulting in full-length $DivIVA_{Ef}$ while samples containing

pSM7.His which delete the second coiled-coil domain did not demonstrate any DivIVA$_{Ef}$ overexpression. The construct pSM8.His has the first coiled-coil domain deleted, but overexpression of the mutated *divIVA$_{Ef}$* construct did not result in any abnormal cells. Hence, the second coiled-coil domain of DivIVA$_{Ef}$ may not be as crucial to the biological functioning of this protein as the first central coiled-coil domain. Biochemical studies showed that first central coiled-coil domain is involved in protein oligomerization and thus, this may be an excellent example of structure affecting function.

The presence of the Min proteins in *E. coli* PB103 for the most part appears to render the expression of DivIVA$_{Ef}$ in any of its mutated forms unequal to usurping control of the cell division machinery and altering its inherent morphology. Moreover, since MinE or DivIVA$_{Bs}$ are both involved in topological specification in *E. coli* or *B. subtilis* and operate with the division inhibitor complex MinCD; it might well suggest that DivIVA$_{Ef}$ has a different biological role from DivIVA$_{Bs}$ (Marston *et al.*, 1999; Cha & Stewart, 1997; Edwards and Errington, 1997). For example, when DivIVA$_{Bs}$ is suppressed, *B. subtilis* can no longer divide properly and forms long rods (Cha and Stewart, 1997, Edwards and Errington, 1997).

Adler *et al.* (1969) documented the first known minicell-forming mutant of *E. coli* isolated from heterogeneous cell populations containing both wt and minicell phenotypes. Jaffé *et al.* (1990) and Åkerlund *et al.* (2002) assert that in *minB* mutants, the cell division site is not a mere random event and that the disturbed nucleoid segregation (relative to its wild-type counterpart) is attributable to the Min system directly. Typically, DNA-free cells or minicells arises from an abnormal cell division where division transpires at one-quarter and three-quarter length of the cells, but they are also known to occur in cells

where normal cell division is observed (Nanninga, 1998). In filamentous cells, division occurs at flanking regions of the cell away from the nucleoid (Wu and Errington, 2004).

The heterologous *E. coli* PB114 (Δ*minB*) system provided a more approximate environment representative to *E. faecalis* JH2-2, which does not support the Min proteins. *E. coli* PB114 transformants carrying pUC18 exhibited a cell length range between 3 to 20 μm while cells with wt $divIVA_{Ef}$ yielded massive multinucleated cells, well over 100 μm in length and suggestive of cell arrest. Similarly, Errington *et al.* found that the overexpression of $DivIVA_{Bs}$ produced a filamentous phenotype in *B. subtilis* cells (1997).

Approximately 35% of the *E. coli* PB114 carrying pSM3.His cell population exceeded the 20 μm cell length limit observed with pUC18 transformants. Potentially, full length $DivIVA_{Ef}$ had a strong enough concentration to exert an effect on cell growth since overexpression of wt $DivIVA_{Ef}$ and mutated $DivIVA_{Ef}$ was demonstrated on the Western blot (Figure 23).

E. coli PB114 carrying wt $divIVA_{Ef}$ produced cells that were a ~4-fold increase in cell length (filamentation) relative *E. coli* PB103 transformants. Incredibly, *E. coli* PB114 (Δ*minB*) transformants carrying the positive control (pDiv.His) revealed extreme filamentation or a "spaghetti-like" phenotype with a cell length range between 125 – 200 μm (Table 5). Moreover, this is a 10-fold increase in cell length of *E. coli* as cited by Nanninga (1998) was observed in virtually 100% of the population. The increased cell length between in *E. coli* PB114 relative to *E. coli* PB103 might well suggest a greater degree of cell division arrest permissible due to absence of Min proteins permitting a

truer representation of $DivIVA_{Ef}$ functioning in the native *E. faecalis* JH2-2 environment that also lacks Min proteins.

Bacillary *E. coli* strains demonstrated filamentation possibly attributable to $DivIVA_{Ef}$ overexpression and this suggests a fundamental difference from the biological function of $DivIVA_{Bs}$, which is known to sequester the MinCD complex at the poles to prevent division from occurring at these sites which would produce minicells (Cha and Stewart. 1997; Edwards, Thomaides, Errington. 2000). In the absence of MinC or MinD, *B. subtilis* results in the formation of minicells (Cha and Stewart. 1997; Thomaides *et al.*, 2001).

Many mutated genes result in altered cell phenotypes and affect the encoding of protein products involved in peptidoglycan formation. Exactly how shape is specified by imposition of the gene on wall assembly is very poorly understood (Daniel and Errington, 2003). The perceived importance of the cell envelope as a determinant of cell shape in bacteria is reflected by *E. coli* strains carrying mutations of *rodA* or *pbp2* (Jones *et al.*, 2001). While the enzymatic function of *rodA* is not full elucidated, it is speculated to support the rod shape during cell elongation and bears sequence similarity to the cell division protein FtsW and SpoVE of *B. subtilis* (Begg *et al.*, 1995; Nanninga, 1998). *E. coli* strains with mutations of the transmembranal *rodA* gene exhibit no significant difference in generation time relative to wild type cells under similar experimental conditions (Begg and Donachie, 1985).

A linked Tn5 and a *rodA* (Am) mutation into *E. coli* W3110 led to the construction of *E. coli* KJB24 (Begg and Donachie, 1998; Donachie *et al.*, 1995). Moreover, these mutations are segregated into pure clones (Begg and Donachie, 1998). Cell growth with

E. coli KJB24 carrying pUC18 produced a characteristic growth curve. *E. coli* KJB24 transformants with wt *divIVA$_{Ef}$* produced no viable cells following plating on LB$_{Amp100}$ agar. Corbin *et al.* also cited differences in cell morphology when using broth and solid media (2002).

When exposed to stress-provoking environmental conditions, many medically important bacteria set in motion a survival strategy known as the viable but non-culturable (VBNC) state. Although bacteria are no longer culturable on solid growth media in this state, they preserve their viability and pathogenicity genes/factors such that upon the restoration of favourable environmental conditions, cell begin to divide again, in a part of the cell population (Arana *et al.*, 2004; Boaretti *et al.*, 2004; Ohtomo and Saito, 2001; Signoretti *et al.*, 2002; Signoretti *et al.*, 2000).

The VBNC state is often accompanied with changes in the biochemical composition of the cell envelopes- most notably peptidoglycan as the main macromolecule involved - and have been linked to shape alterations, growth rate, and cell division inhibition during the stationary growth phase (Signoretti *et al.*, 2000). Analysis of peptidoglycan chemical composition, by separation in HPLC of muropeptides released by muramidase digestion of purified peptidoglycan, indicated a high degree of cross-linking, a threefold increase in unusual DAP-DAP cross-linking, an increase in muropeptides bearing covalently bound lipoprotein, and a shortening of the average length of glycan strands in comparison with dividing cells. Finally, VBNC cells displayed an autolytic capability that was far higher than that of exponentially growing cells (Signoretti *et al,.* 2002).

Little is known about the genetic mechanisms underlying the VBNC state. Boaretti *et al.* (2003) recently demonstrated the involvement of the rpoS gene in persistence of *E.*

coli in the VBNC state. The rpoS mutants could not activate the wild type survival strategy and died early, suggesting the rpoS gene in *E. coli* has an involvement of the rpoS gene in persistence in the VBNC state.

Another unexpected phenomenon was the inability of E. coli KJB24 (*minB, rodA*$^-$) transformants carrying wt or mutated *divIVA$_{Ef}$* constructs to overexpress DivIVA$_{Ef}$. If DivIVA$_{Ef}$ was present in the cytoplasm overexpression should occur. However, it was impossible to determine if DivIVA$_{Ef}$ did overexpress due to the multiple non-specific binding observed on Western blots.

Corbin *et al.* determined that *E. coli* KJB24 cells had a mean area of 1.50 ± 0.42 μm^2 and ranged in size from 0.75 to 2.52 μm^2 (2002). The wild type *E. coli* KJB24 cells or *E. coli* KJB24 cells pUC18 transformants ranged from 0.5 to 3 μm^2 confirming the findings of Corbin *et al.* However, transformants with wt or *divIVA$_{Ef}$* constructs bearing abrogated N-terminal coiled-coil domains incubated with 0.4 mM IPTG exhibited cell areas greater than 3 μm^2 indicating that DivIVA$_{Ef}$ was being overexpressed although Western blot results were inconclusive due to the presence of multiple bands. It is possible that either the antibody and/or antigen concentration were/was sufficiently potent to permit antigen-antibody binding. Moreover, the engorged cell morphology suggests that DivIVA$_{Ef}$ was functional and resulted in cell division arrest. The remaining constructs: pSM1 to pSM5 demonstrated engorged cell morphology above the wild type cell area of 3 μm^2 for 6.4% to 50% of the cell populations (Table 4). When wild type *divIVA$_{Ef}$* (pDiv.His) and pSM3.His with an N-terminal coiled-coil domain abrogation were incubated with 0.8 mM IPTG, *E. coli* KJB24 (*minB, rodA*$^-$) transformants demonstrated an engorged cell phenotype with 24.1% and 1.8% of the cell population exhibited cells larger than the wild

type area of 3 μm^2. Similarly, the identical constructs in *E. coli* WM1250 (*ΔminB, rodA*$^-$) produced engorged cells with 21.9% and 13.1% on the cell population exhibited cells larger than the wild type 3 μm^2. These results confirm biochemical studies employed to demonstrate that the N-terminal coiled- coil domains were not critical in the oligomerization processes in $DivIVA_{Ef}$ (Rigden, 2005).

In order to ascertain whether the presence of any foreign DNA in *E. coli* KJB24 cells would produce an altered cell phenotype and demonstrate multiple bands detectable by Western blots, another control was required. The non-cell division gene $prgX_{Ef}$ was an excellent choice as a control for several reasons. The protein product $PrgX_{Ef}$ is essential to *E. faecalis* JH2-2 and in the pheromone-responsive conjugative plasmid system ($pCF10_{Ef}$); the protein product $PrgX_{Ef}$ is able to repress the aggregation substance (Asc10) for pCF10; $PrgX_{Ef}$ is also slightly larger than $DivIVA_{Ef}$ at 317 aa; it possesses a larger molecular weight at ~ 50 kDa; and finally, $PrgX_{Ef}$ has been shown to oligomerize in *E. faecalis* as does $DivIVA_{Ef}$ (Bae and Dunny, 2001; Bae *et al.*, 2001). $PrgX_{Ef}$ overexpression was demonstrated by Western blot. Moreover, cells with $PrgX_{Ef}$ exhibited a cell phenotype identical to wt *E. coli* KJB24 cells. This result suggests that the presence of $DivIVA_{Ef}$ may well be sufficient to cause the engorged cell morphology and the results obtained by Western blot. Clearly, not just any foreign DNA is capable of altering cell morphology while not being visible by Western due to extensive banding, but there might be another explanation.

The two-competing-sites model for peptidoglycan assembly for bacterial cell shape regulation proposes that cell shape in bacilli hinges on the balance between two reactions (sites). Shape therefore is the balance manifested between these two forces (Daniel and

Errington, 2003). One site is responsible for lateral wall elongation and the other, for septum formation. The two reactions compete such that no lateral wall can be formed during septum formation. When the reaction leading to septum formation is hyperactive compared with the other, coccobacilli or cocci are formed (Lleo *et al.*, 1990). The elimination of the *rodA*$^-$ *gene* of *E. coli* to produce the strain KJB24 (*minB, rodA*$^-$) might well add to the tendency of septum formation. Such an internal strife would account for the inconclusive overexpression data and unstable morphology with different IPTG concentration observed in *E. coli* KJB24 transformants carrying wt or mutated *divIVA* constructs. Moreover, it might well explain the cell stress that seemed to cause the VBNC-like state in E. *coli* KJB24 transformants with wt *divIVA* during the experiments relating to cell growth.

According to Begg *et al.*, (1995) *E. coli* WM1250 (Δ*minB, rodA*$^-$) will divide exactly like *E. coli* KJB24. In *E. coli* KJB24 coccal-shaped cells, the single division furrow proceeds in an increasing arc and if free to move throughout this process, the furrow opens out the cell pair such that they rotate 90^0 until attached only at the point of the completed furrow (Begg and Donachie, 1998). Replication completion occurs 20 minutes before the completion of cell division and sister chromosomes separate from one another within 2 – 3 mins after replication is completed in *E. coli* strains (Begg *et al.*, 1995). Normal medial placement of Z-ring in most *E. coli* WM1250 cells (Sun et al., 1998; Yu and Margolin, 1999) and nucleoid occlusion may assist in the regulation of cell division (Corbin *et al.*, 2002).

Corbin *et al.* found that *E. coli* WM1250 (Δ*minB, rodA*$^-$) produced small and large cells with highly variable morphologies and a mean area of 5.3 ± 1.9 μm^2 and ranged in

size from 2.2 to 9.3 μm^2 (2002). This research confirms the morphological findings of Corbin *et al* (2002). While *E. coli* WM1250 transformants carrying either pDiv.His or pSM3.His did exhibit cells as large as 12 μm^2, transformants with other mutated $divIVA_{Ef}$ constructs fell within Corbin's cell area range of 2.2 to 9.3 μm^2.

Budding or kidney-shaped phenotypes were observed in some cells with both *E. coli* KJB24 and *E. coli* WM1250. According to Corbin *et al.*, budding is attributable to the presence of DNA (Corbin *et al.*, 2002). Kidney-shapes observed with *E. coli* KJB24 cells could be attributable to deep medial constriction of the mother cell (Begg and Donachie, 1998).

The western blot results of the overexpression studies using *E. coli* KJB24 (*minB, rodA*$^-$) and *E. coli* WM1250 (*ΔminB, rodA*$^-$) suggest that the two-competing-sites model is probably sufficient to explain the results obtained in experiments using *E. coli* KJB24. *E. coli* WM1250 lack all Min proteins while *E. coli* KJB24 possess all Min proteins. Because *RodA*$^-$ *E. coli* exhibit coccal-shaped cells more closely resembling the native *E. faecalis* JH2-2 environment, $DivIVA_{Ef}$ may exert it influence on cellular components more readily than in bacillary cells. However, the presence of Min proteins in cells with hyperactive septal formation may further burden already stressed cells.

E. coli KJB24 cells typically has a greater osmotic pressure than rod-shaped cell interior and the exterior, which is checked by the higher internal salt concentrations producing a swelling of the organism (Koch, 1985). This hydrostatic pressure is preserved during cell elongation in cell division and appears to be essential for the cell envelope enlargement (Morbach and Krämer, 2002). Autolysins activity continues through this process such that the wall is enlarging at a rate constant to the hydrostatic

pressure (Schwartz *et al.*, 1969; Koch, 1985). Moreover, in the coccal-shaped *E. coli*, the surface-to-volume ratio decreases during growth whereas bacilli maintain a constant surface-to-volume ratio (Tamames *et al.*, 2001). Higgins & Schockman (1971) and other researchers speculated that cocci expand their surfaces only through cross wall formation while bacilli must possess alternative or additional genetic information to produce lateral wall (Daneo-Moore and Schockman, 1977; Kraus *et al.*, 1985; Hartmann *et al.*, 1972). The complexity of cell stress in coccal-shaped *E. coli* rendered it the least satisfactory or experimental-friendly for this research. However, it proved useful in contrasting the effects on DivIVA overexpression in the presence or absence of Min proteins.

4.3 *E. faecalis* JH2-2:

In recent years, virtually no research has been published with regard to the cell division machinery in *E. faecalis*. To create a $DivIVA_{Ef}$ overexpression system for the elucidation of its biological functions, the research published by Bryan *et al.* (2000) was examined. Their study created a set of shuttle vectors capable of replication in *E. coli* and *E. faecalis*. The NICE system was originally developed using both a gene of interest under the control of the *nisA* promoter and the regulatory genes encoding the histidine protein kinase NisK and the response regulator NisR (Engelke *et al.*, 1994; Kuipers *et al.*, 1993; Kuipers *et al.*, 1995; Kuipers *et al.*, 1998; deRuyter *et al.*, 1996b; Kleerebezem *et al.*, 1997b). Nisin is an antimicrobial peptide of the lantibiotics family, a sub-group of bacteriocins, and is frequently used in the food industry as a natural preservative and it is responsible for inducing the transcription of genes under the control of both the *nisA* and *nisF* promoters, via a two-component regulatory system (Guder *et al.*, 2000; Stock *et al.*, 1995; Wanner, 1995; Klaenhammer, 1993; Delves-Broughton *et al.*, 1996).

In layman's terms, there are three elements needed to produce a functional NICE system and they include: a Gram-positive bacterium capable of expressing the *nisRK* genes, the inducer molecule itself – nisin, and a shuttle vector (like pMSP3545) containing the *nisA* promoter with a downstream multi-cloning polylinker site to insert the gene of interest (Kuipers *et al.*, 1998).

The cited advantages of this system include low cost; controllable expression levels determined by nisin concentration at the point of induction; recombinant protein synthesis should reach significant levels up to 60% of the total intracellular proteins; while not induced, no protein should be detectable and permits the production of lethal proteins; and finally, the NICE system has already been successfully transferred to other gram-positive bacteria (deRuyter *et al.*, 1996b; deRuyter *et al.*, 1997; Eichenbaum *et al.*, 1998; Kleerebezem *et al.*, 1997; Kuipers *et al.*, 1995; Kuipers *et al.*, 1997; Pavan *et al.*, 2000).

The NICE system was successfully transferred to *E. faecalis* JH2-2 and did overexpress $DivIVA_{Ef}$. However, $DivIVA_{Ef}$ overexpression levels were not significant and these levels detectable by western blot did not reach anywhere near 60% of the total intracellular protein. While nisin works in a concentration-dependent fashion, it was very poorly inducible in spite of cited research (Delves-Broughton *et al.*, 1996). Other researchers have also experienced difficulties (Pavan *et al.*, 2000). Guder *et al.* (2000) noted that amongst even closely related bacterial strains exhibited extreme differences in the nisin sensitivity, making optimization a more cumbersome procedure.

The use of this system did not, however, result in leaky expression. The optimization and implementation of the NICE system did demonstrate $DivIVA_{Ef}$ was overexpressed in its native *E. faecalis* JH2-2 carrying pMSPSRDiv-1 (P_{nisA}::*$divIVA_{Ef}$*) in an inducible

manner with 1.5 μg/ml nisin without disturbing the natural morphology (Ramirez *et al.*, 2004).

To circumvent this laboratory intensive protocol, a second homologous system was implemented utilizing the native promoter of *divIVA*$_{Ef}$ to transcript multiple copies of the gene for increased protein translation for overexpression studies. *E. faecalis* JH2-2 transformants carrying this non-inducible plasmid known as pMSPSRDiv-2 were tested in tandem with the negative control pMSP3545. The ability to overexpress $DivIVA_{Ef}$ using *E. faecalis* JH2-2 with pMSPSRDiv-2 proved to be a very simple and successful system. Moreover, without nisin induction, no damage could be incurred on the cytoplasmic membrane where nisin creates the formation of pores (Guder *et al.*, 2000). Using phase contrast microscopy, cell measurements demonstrated that wt *E. faecalis* JH2-2 morphology was maintained. Finally, the reproducibility of overexpression and morphological study results were exceedingly consistent as demonstrated by Western blot and phase contrast microscopy.

The implementation of the NICE system was a rational starting point to create an overexpression system in the homologous system using *E. faecalis* JH2-2. This step in turn, led to a more efficient, verifiable and consistent $DivIVA_{Ef}$ overexpression system, which should be used with the mutated *divIVA*$_{Ef}$ constructs at some later date.

Using both the heterologous and the homologous systems in this research revealed some valuable information furthering research into the cell division machinery of *E. faecalis*. The homologous system offers the advantage of functioning in the native system. Unfortunately due to time constraints, the mutated *divIVA*$_{Ef}$ genes could not be compared to the heterologous system.

Future Work:

Overview:

Future work should include the use of the heterologous system using rod-shaped *E. coli* PB103 and *E. coli* PB114 for several reasons. Overexpression results proved to be reliable and reproducible, while the morphological studies demonstrated obvious morphological phenotypes assessable by microscopy. Creating a bacterial environment closely approximating *B. subtilis* could further elucidate the unique function(s) of DivIVA$_{Ef}$ with respect to DivIVA$_{Bs}$. Moreover, Min proteins would be present in these transformants and the bacilli morphology would likely reflect this. Such experiments could illustrate not only what DivIVA$_{Ef}$ functionally does not do, but also what the DivIVA$_{Ef}$ functionally does do.

Future work should include the homologous coccal-shaped *E. faecalis* JH2-2 system. Expansion of the homologous system to incorporate the use of other parental plasmid-free strains such as *E. faecalis* OG1RF could prove invaluable. Such examination may highlight whether DivIVA$_{Ef}$ function(s) are subtly different at the strain level, whether DivIVA$_{Ef}$ is conserved at the genus and/or species level(s), and what evolutionary/phylogenetic implications may exist.

Finally, the Dillon laboratory has developed new mutated *divIVA$_{Ef}$* genes to identify which nucleotides are involved in diminished or eliminated self-interaction along the coiled-coil regions of DivIVA$_{Ef}$ (Marc Rigden, 2005). Analyses of the biochemical data using gel filtration and native gel electrophoresis suggest a reduction in the complex mass (kDa) and the number of monomers involved in self-interaction of DivIVA$_{Ef}$ of new *divIVA$_{Ef}$* mutations. Thus, these mutations warrant further exploration by overexpression

studies and microscopic analysis. These mutations include: L104P, I125P (MR13); L104P, I125P, L143P (MR14); L104P, I115P, I125P (MR15); and L104P, I115P, I125P, L143P (MR16) (Table 3) (Marc Rigden, 2005).

5.1 The heterologous systems:

Overexpression studies using the rod-shaped *E. coli* PB103 (*minB*) and its isogenic PB114 (Δ*minB*) should be continued for the newly developed mutated $divIVA_{Ef}$ construct mentioned above. Moreover, overexpression studies using bacillary *E. coli* DR105 (Min C3) and PB104 (*ΔminD*) should be implemented. Not only would this to establish any effect on $DivIVA_{Ef}$ overexpression in the absence of either MinC or MinD, but also this would elucidate any unique functioning of $DivIVA_{Ef}$ relative to $DivIVA_{Bs}$. Finally, such experimentation may substantiate the complementation experiments conducted by the Dillon laboratory.

In order to examine chromosomal segregation using DAPI staining, all mutations transformed into the heterologous systems including: PB103 (*minB*), PB114 (Δ*min*), DR103 (MinC3) and PB104 (*ΔminD*) should be undertaken. Direct assessment by fluorescence microscopy would demonstrate chromosomal segregation of transformants or suggest whether cell division is inhibited and where such inhibition may arise.

5.2 The homologous systems

Overexpression and microscopic studies must be established, for all mutated $divIVA_{Ef}$ constructs, similar to the protocol established for the pMSPSRDiv-2 transformed in *E. faecalis* JH2-2. The elimination of any inducer molecule facilitates easy of experimentation and produced superior results.

I have designed and synthesized all primers (Table 2) necessary to create the *divIVA*$_{Ef}$ constructs including pSM4.His (E37P, N43P, L46D, L50D, L57F), pSM6.His (1-190), pSM7.His (Δ130 - 190), pSM8.His (Δ60 - 190), pSM9.His (Δ60 - 130), and pSM12.His (L104P, L143P). The C-terminal His-tag in the primer design allows superior Western blot signal since the anti-His antibodies are monoclonal promoting noise reduction and non-specific binding.

Overexpression and microscopic studies for *divIVA*$_{Ef}$ mutations, including MR13, MR14, MR15 and MR16 (Table 3), should be done in duplicate, ensuring veracity of results.

DAPI staining of all *divIVA*$_{Ef}$ mutations transformed into the homologous system should include *E. faecalis* JH2-2 and OG1RF. Direct assessment by fluorescence microscopy would reveal chromosomal segregation of transformants and determine whether cell division is inhibited.

By dividing the overexpression studies and morphological studies into a heterologous system using *E. coli* and a homologous system using *E. faecalis*, I have created a comprehensive experimental investigation of assessing the biological function(s) $DivIVA_{Ef}$. The heterologous system permits direct comparison to *B. subtilis* DivIVA; important since the most detailed information available to date is on-going research on $DivIVA_{Bs}$. The homologous system permits exploration of $DivIVA_{Ef}$ in its native environment leading to the elucidation of cell division mechanism surrounding $DivIVA_{Ef}$. Through this dualistic approach a definitive cell division model for *E. faecalis* may be developed.

CONCLUSIONS:

The present research has attempted to characterize the biological functioning of DivIVA$_{Ef}$ using various overexpression and morphological studies. Constructs designed to abrogate specific coiled-coil regions located along the length of DivIVA$_{Ef}$ were used to elucidate the biological function of DivIVA$_{Ef}$ and to examine the biological effects on bacterial cells when the central coiled-coil domain of *divIVA$_{Ef}$*, responsible for the protein oligomerization, is abrogated. In conjunction with biochemical studies, this research has demonstrated that DivIVA$_{Ef}$ is unable to overexpress when the central coiled-coil domain in disrupted as demonstrated by overexpression and microscopic studies. The constructs used to demonstrate this included pSM7.His (Δ130 - 190), pSM8.His (Δ60 - 190) and pSM12.His (L104P, L143P).

The present study is significant, as it has elucidated a unique biological role for DivIVA$_{Ef}$ relative to DivIVA$_{Bs}$ by creating a Min paradigm to examine the effects on DivIVA$_{Ef}$ in the presence or absence of Min proteins. Moreover, this is the first report to establish that coccal-shaped *E. coli* transformants carrying *divIVA$_{Ef}$* cause differentiated cellular responses to those of bacillary *E. coli*.

Due to the conserved nature of the residues corresponding the protein product of coiled-coils in DivIVA across species, this information can be applied to studies of DivIVA from various Gram-positive prokaryotic organisms whether rod-shaped like *B. subtilis* or coccal-shaped such as *S. pneumoniae*. Through analysis of division-associated proteins such as DivIVA$_{Ef}$, it will eventually become possible to target antimicrobial agents to these proteins to impede cell division and control microbial growth.

APPENDIX 1- *E. coli* DR105 STUDIES

1.1 Methods & Materials:

In order to investigate whether a specific Min protein is directly involved in chromosomal segregation in transformants carrying the *divIVA$_{Ef}$* gene, *E. coli* DR105 carrying a mutation at MinC3 rendering the protein non-functional was employed. This would investigate the consequences on chromosomal segregation when the MinCD complex is unable to be established. The negative (pUC18) and positive control (pDiv.His) constructs were separately transformed in *E. coli* DR105 competent cells and plated on LB$_{amp100}$ and incubated O/N at 37^{0}C. Only fresh transformant were used in the overexpression studies.

DivIVA$_{Ef}$ overexpression and morphological studies using *E. coli* DR105 transformants carrying pDiv.His (positive control) and pUC18 (negative control) were performed. Cell fixation, SDS-PAGE and Western blot protocols conducted as found in section 2 (Methods & Materials).

1.2 Results:

Figure 23A illustrate the results by Western blot for *E. coli* DR105 transformants carrying either pUC18 (negative control) or the pDiv.His (positive control). Interestingly, the results show very similar levels of DivIVA$_{Ef}$ overexpression irrespective of incubation duration between 2- to 6-Hrs. This result is similar that obtained with the positive control transformed in *E. coli* PB103. No DivIVA$_{Ef}$ overexpression was observed prior to or at the point of IPTG induction when cells were incubated (37^{0}C) to an OD$_{600nm}$ ~0.5. Moreover, pUC18 transformants did not overexpress DivIVA$_{Ef}$ at any time point (0-, 2-, 4- and 6- Hrs).

Figure 23: *E. coli* DR105 (*minC5*) transformants carrying wt $divIVA_{Ef}$ demonstrated $DivIVA_{Ef}$ overexpression in the absence of MinC by Western blot while altering the cell morphology. **A-** $DivIVA_{Ef}$ overexpression in the absence of MinC by Western blot. Lanes: 1- 1 Kb+ ladder, 2- pUC18 (0-Hrs); 3- pUC18 (0-Hrs); 4- pUC18 (6-Hrs); 5- pUC18 (6-Hrs); 6- pDiv.His (6-Hrs); 7- pDiv.His (6-Hrs); 8- pDiv.His (0-Hrs); 9- pDiv.His (0-Hrs); 10- purified $DivIVA_{Ef}$. . Densitometric analysis of duplicate samples was performed to ensure $DivIVA_{Ef}$ concentration equalized. Blots were probed with 1:1000 monoclonal anti-His antibody and 1:3000 goat anti-mouse IgG conjugated to alkaline phosphatase; **B-** Aberrant morphological phenotype of *E. coli* DR105 (*minC5*) transformants carrying $divIVA_{Ef}$ at 3-Hrs post-IPTG (0.8 mM) induction as depicted by phase contrast microscopy (100X oil immersion). All images measured using single scale bar applicable to all image panels. *E. coli* DR105 transformants carrying pUC18 at 6-Hrs post-IPTG (0.8 mM) induction (B1); and *E. coli* DR105 transformants carrying pDiv.His at 6-Hrs post-IPTG (0.8 mM) induction (B2).

Figure 23

A. *E. coli* DR105 (*minC5*) 6-Hrs post-IPTG (0.8 mM)

Lanes:
1 2 3 4 5 6 7 8 9 10

B. *E. coli* DR105 (*minC5*) 6-Hrs post-IPTG (0.8 mM)

Negative control (pUC18)

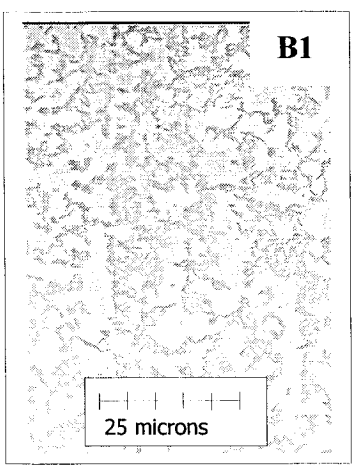

Positive control (pDiv.His)

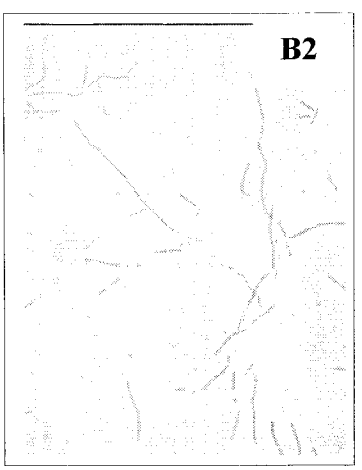

Figure 23B illustrates the results of the morphological studies using the controls transformed in *E. coli* DR105. Transformants carrying pUC18 exhibited a minicell phenotype with a cell length range from 0.5 to 5 μm. This morphological phenotype is similar to either E. coli PB103 or *E. coli* PB114 transformants carrying pUC18. *E. coli* DR105 transformants carrying pDiv.His also possessed a minicell phenotype with a cell length range from 0.5 to 40 μm.

1.3 Discussion:

E.coli DR105 lacks a functional MinC, the general inhibitor of division, thus cells produce the minicell phenotype (deBoer *et al.*, 1992). *E. coli* PB114 transformants with either pUC18 or pDiv.His behaved similarly. In fact, because of the complete absence of the *minB* system, the filamentous phenotype is increased as demonstrated by the large percentage of anucleated cells and longer cell lengths. The presence of the minicell phenotype is suggestive of a lack of chromosomal segregation while the presence of filaments indicates cell division arrest at a later point in the process of cell division.

The filamentous nature of *E. coli* PB103, *E. coli* PB114 or *E. coli* DR105 transformants with pDiv.His resulted in unique cell lengths in accordance to the strain employed in overexpression studies. *E. coli* PB114 or *E. coli* DR105 transformants with wt $divIVA_{Ef}$ produced cell lengths ranging from 0.5 – 40 μm while *E. coli* PB103 transformants ranged to over 200 μm. Unlike *B. subtilis*, the inactivation of MinC does not result in minicell formation; but rather results in cells that are filamentous and provides concrete evidence that $DivIVA_{Ef}$ does have a unique function from $DivIVA_{Bs}$.

APPENDIX 2 - BIOFINFORMATICS STUDIES

2.1 Methods & Materials:

A comparison of DivIVA$_{Ef}$ sequences from several bacterial species were obtained from the TIGR website (http://www.tigr.org/tdb/mdbinproress.html). BLAST searches for *divIVA$_{Ef}$* homologues in other organisms were carried out in their respective sequence databases, provided by the Institute for Genomic Research (http://www.tigr.org/tdb/mdb.mdb.html). Translation of *divIVA$_{Ef}$* gene sequences was done using PCgene Software (Intelligenetics, Inc.). Protein alignments were performed using ClustalW Version 1.8 software (http://dot.imgen.bcm.tmc.edu:933/multi-align/multi-align.html), and shading was achieved with BOXSHADE Version 3.21 (http://www.ch.embnet.org/software/BOX_form.html).

2.2 Results:

The *divIVA$_{Ef}$* gene (EF1002) used throughout this study was originally found using TIGR website for *E. faecalis* V583 (http://www.tigr.org/tdb/mdbinproress.html). A bioinformatics search was undertaken to ascertain if other *E. faecalis* V583 proteins had similarities to DivIVA$_{Ef}$ to assist in the elucidation of DivIVA$_{Ef}$.

Figure 24 depicts the alignment of EF1002 with a second but hypothetical DivIVA protein identified as EF1151. The "new" protein is approximately half the length of EF1002 (234 amino acids (aa)) with 136 aa. The percentage of identity between the two aligned sequences is 34.7% and the percentage of similarity is 53.5%. Figure 24 depicts the multi-alignment across organisms with completed genomes from the TIGR database. While some of the proteins with percentages of identity and/or similarity are designated as hypothetical proteins with an unknown function, some proteins have a known function

Figure 24: Bioinformatics reveal a second hypothetical $DivIVA_{Ef}$ in a multi-sequence alignment of DivIVA. **A-** Using the Tigr database, a second but hypothetical DivIVA, identified as EF1151 (136 aa), was located by comparing EF1002 (234 aa) to any similar proteins within *E. faecalis* V583. The percentage of identity = 34.7% and the percentage of similarity = 53.5%; **B-** Alignment of DivIVA proteins from various species. Abbreviations: lp_1754 (*Lactobacillus plantarum* WCFS1), lmol1888 (*Listeria monocytogenes EGD-e*), lin_2002 (*Listeria innocua* clip 11262), BC1562 (*Bacillus cereus* ATCC14579), BA1583 (*Bacillus anthracis Ames*), Sps0475 (*Streptococcus pyogenes SSI-1*), SpyM3-1387 (*Streptococcus pyogenes MGAS315*), spyM18_1658 (*Streptococcus pyogenes MGAS8232*), SPy1646 (*Streptococcus pyogenes SF370 serotype M1*), ypsB (*Bacillus subtilis Ames*), and CAC0766 (*Clostridium acetobutylicum ATCC824*).

Figure 24

A

```
EF1151       1 ----------ENSRLMAKLDQLSNAQPTP-----------------------RVAQEVPK
EF1002       1 LQYFNELKDALNQSIIVAQDTADKVKSSANKESEMIITSADNQAKETLVEAERKSNAMIA
consensus    1 lqyfnelkda N  lm   D   K    t nkesemiitsadnqaketlveaeR  q v

EF1151      28 SAAVTNFDILKRLSNLEREVFGKKLDETPSTPVTPSAPSMPASPANHDVDNAQTRQF---
EF1002      61 DAEAKSTQILAEAIERARQLAGETEDLKKKTRVFHQRLSLMLETQLEQVKSEEWEEILKP
consensus   61  A       IL        R v G   D    T V      Sm  E      V         lkp

EF1151          ------------------------------------------------------------
EF1002     121 FSSYVGDKHTAVKEILDEQDLDNENETVVNSEENTDAVVEKKPVIEVTEETIEEESK
consensus  121 fssyvgdkhtavkeildeqdldnenetvvnseentdavvekkpvievteetieeesk
```

B

```
EF1151         1 SRLMAKLDQLSKAQPTPRVAQ------EVPKSAAVTNFDILKR-LSNLEREVFGKKLDET
lp_1754        1 ERLRAKVDELTKQVAVGATSP------SSQPTSTVTNMDILKR-LSNLERHVFGAQLDNN
lmo1888        1 IRLVQELDNAPLRTSTQPAPT---FQAAAQPAG-TTNFDILKR-LSNLEKHVFGNKLDDN
lin2002        1 IRLVQELDNAPVRTTTQPAPT---FQAAAQPAG-TTNFDILKR-LSNLEKHVFGNKLDDN
BC1562         1 ARLKRELEEQKLAVTQVPQQP--VQTPVAQPVYNNTNTDILKR-LSNLEKAVFGSKLYE-
BA1583         1 ARLKRELEEQKLAATQVPQQPV-VQTPVAQPVYNNTNTDILKR-LSNLEKAVFGSKLYE-
Sps0475        1 EALKKAKFQARNTVSATVQQP---VPQPTRVAQSATNFDILKR-ISKLEKEVFGKQIIE-
SpyM3_1387     1 EALKKAKFQARNTVSATVQQP---VPQPTRVAQSATNFDILKR-ISKLEKEVFGKQIIE-
spyM18_1658    1 EALKKAKFQARNTVSATVQQP---VPQPTRVAQSATNFDILKR-ISKLEKEVFGKQIIE-
SPy1646        1 EALKKAKFQARNTVSATVQQP---VPQPTRVAQSATNFDILKR-ISKLEKEVFGKQIIE-
CAC0766        1 LSIEVLIEYVKMFQEGNSTIGTRKQLLIEQRSQLVKKIKVMQQTLERLDKKIDGYEKRIL
consensus      1  rlkr ldqak  vs   qqp         q a   tnfdilkr lsnLek vfG  l e

EF1151        54 PSTPVTPSAPSMPAEPANHDVDNAQTRQF
lp_1754       54 ---------------------QNESHRL-
lmo1888       56 E----------------------------
lin2002       56 E----------------------------
BC1562           ----------------------------
BA1583           ----------------------------
Sps0475          ----------------------------
SpyM3_1387       ----------------------------
spyM18_1658      ----------------------------
SPy1646          ----------------------------
CAC0766       61 LREKELKSQ--------------------
consensus     61
```

Black boxes indicate amino acid residues that are identical to the consensus at their respective positions. Gray boxes are similar to the consensus.

and include lp_1754 (*Lactobacillus plantarum* WCFS1) as a methylase and BC1562 (*Bacillus cereus* ATCC14579) as a DivIVA homologue. This is the first report that demonstrates a DivIVA homologue in *Bacillus cereus* ATCC14579 citing a known cell division function as DivIVA. No literature is available aside from published blasts.

Figure 25 depicts the predicted coiled-coil regions of both $DivIVA_{Ef}$ proteins identified as EF1002 and EF1151 (hypothetical protein). Both proteins demonstrate a large N-terminal coiled-coil region, a smaller central coiled-coil domain and a small C-terminal domain.

These preliminary bioinformatics results do suggest some similarities in properties and characteristics between the $DivIVA_{Ef}$ proteins both found in the organism *E. faecalis* V583 and may warrant further investigation.

2.3 Discussion:

Completed genomes offer the researcher new possibilities for resolving or elucidating biological questions. Unfortunately, many annotations of completed genomes fall short of categorizing anywhere from 40 to 60 percent of gene products. In the last five years over 30 bacterial genomes have been completed and it is anticipated that within the next few years upwards of 100 completed genomes will be available (Janulczyk and Rasmussen, 2001; Fraser *et al.*, 2000). As more information on the physiology and evolution of microbial species becomes readily available, any lapses in inaccurate classification of gene products will habilitate researchers in resolving biological issues.

Based on the information found on the Tigr database, the hypothetical *E. faecalis* DivIVA protein (EF1151) has an unknown function.

Figure 25: Structural analyses of two $DivIVA_{Ef}$ proteins determine probable regions involved in Self-Association. **A-** The structural analysis predicts the probable regions involved in self-association in the $DivIVA_{Ef}$ protein known as EF1002; **B-** The structural analysis predicts the probable regions involved in self-association in the $DivIVA_{Ef}$ protein known as EF1151.

Figure 25

Wild-type $DivIVA_{Ef}$ (EF1002)

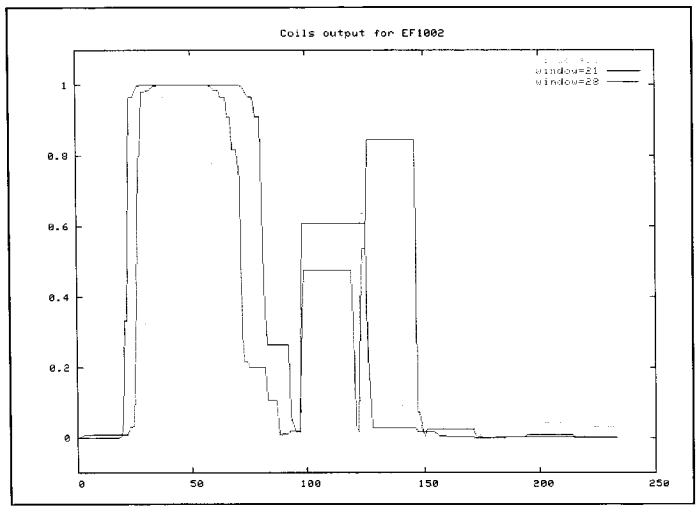

Wild-type $DivIVA_{Ef}$ (EF1151)

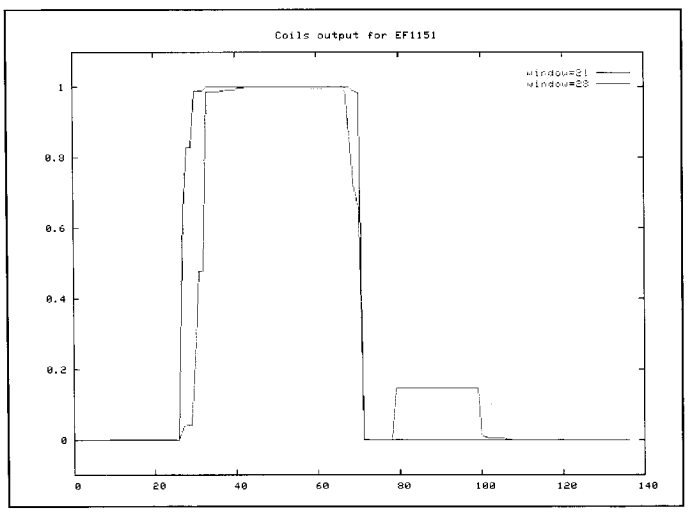

The primary structure alone should not be considered representative of the protein function or structure (Barák *et al.*, 2004). Prediction of secondary elements might aid in the elucidation of proteins without determine its three-dimensional structure. However, many believe the prediction of secondary structures leads to better prediction of three-dimensional protein structures. Typically structure prediction methods involve the propensities for amino acids to form beta-strands, helices or turns. A caveat should be added to state that most secondary structures predictions only predict three to four different secondary structures which may not be the inclusive structures comprised by any a protein (Jones *et al.*, 2000).

A comparison of the predicted coiled-coil regions using the Lupas Method was employed. By comparing the flanking sequences with sequences of known coiled-coil protein, the probability can be assessed of any residue in a typically globular protein forming part of a coiled-coil (Lupas *et al.*, 1991). On first glance the images of the coiled-coil outputs seems very different but at closer scrutiny, three coiled-coil domains including: N-terminal, central region and C-terminal can be ascertained (Figure 25).

Bioinformatics analyses have indicated that the two DivIVA proteins found in *E. faecalis* are both cytoplasmic, have similar a percentage of identity of 34.7% and a percentage of similarity of 53.5%; and possess three coiled-coil regions comprising alpha helices and random coils. Moreover, homologues in other organisms suggest unique functions possibly related to transcription and cell division. This preliminary data suggests that further investigation is warranted and might well assist in the further elucidation of DivIVA$_{Ef}$ (EF1002).

STATEMENT OF COLLABORATION

The author of this study extends gratitude to all members of the laboratory of Dr. Jo-Anne Dillon for their advice and guidance during the course of the present study. SJ Marthaler constructed all pSM_ and pSM_.His series plasmids; those so accredited in Table 2 constructed other plasmids used in this research.

All sequencing and primer synthesis would not have been possible without the assistance of D. Tessier and H. Wang at The University of Ottawa Core Facility for DNA Synthesis and Sequencing.

Gratitude must also be extended to Cathy Stafford for endless administrative tasks, which are often taken for granted.

REFERENCES:

Adler HI, Fisher IWD, Hardigree AA. 1969. Cell division in *Escherichia coli. Trans NY Acad Sci.* **31:** 1059 - 1070.

Åkerlund T, Gullbrand B, Nordstrom K. 2002. Effects of the Min system on nucleoid segregation in *Escherichia coli. Microbiol.* **148(Pt 10):** 3213 - 3222.

Akiyama T, Inouye S, Komano T. 2003. Novel developmental genes, *fruCD* of *Myxococcus xanthus*: Involvement of a cell division protein in multicellular development. *J Bacteriol.* **185(11):** 3317 - 3324.

Anderson DE, Gueiros-Filho FJ, Erickson HP. 2004. Assembly dynamics of FtsZ rings in *Bacillus subtilis* and *Escherichia coli* and effects of FtsZ-regulating proteins. *J Bacteriol.* **186(17):** 5775 - 5781.

Arana I, Seco C, Epelde K, Muela A, Fernandez-Astorga A, Barcina I. 2004. Relationships between Escherichia coli cells and the surrounding medium during survival processes. *Antonie Van Leeuwenhoek.* 86(2): 189 - 199.

Autret S, Errington J. 2003. A role for division-site-selection protein MinD in regulation of internucleoid jumping of Soj (ParA) protein in *Bacillus subtilis. Mol Microbiol.* **47(1):** 159 - 169.

Ayala JA, Garrido T, de Pedro MA, Vicente M. 1994. Molecular biology of bacterial septation. In: Ghuysen JM, Hakenbeck R (eds.), Bacterial Cell Wall. Elsevier, Amsterdam. Pages: 73 – 102.

Bae T, Dunny GM. 2001. Dominant-negative mutants of prgX: evidence for a role for PrgX dimerization in negative regulation of pheromone-inducible conjugation. *Mol Microbiol.* **39(5):** 1307 - 1320.

Barák I, Florek P, Muchová K, Pribišová, Chromilová Z. 2004. Bacterial cell division – structure and function of proteins involved. *Materials Structure.* **11(1):** 25 – 28.

Barrick D, Villanueba K, Childs J, Kalil R, Schneider T, Lawrence CE, Gold L, Stormo G. 1994. Quantitative analysis of ribosome binding sites in *E. coli. Nucl Acids Res.* **22(7):** 1287 – 1295.

Begg KJ, Donachie WD. 1998. Division planes alternate in spherical cells of *Escherichia coli. J Bacteriol.* **180:** 2564 - 2567.

Begg KJ, Donachie WD. 1995. Cell shape and division in Escherichia coli: experiments with shape and division mutants. *J Bacteriol.* **163(2):** 615 - 622.

Begg KJ, Dewar SJ, Donachie WD. 1995. A new *Escherichia coli* cell division gene, *ftsK*. *J Bacteriol.* **177:** 6211 – 6222.
Ben-Yehuda S, Losick R. 2002. Asymmetric cell division in *B. subtilis* involves a spiral-like intermediate of the cytokinetic protein FtsZ. *Cell.* **109(2):** 257 - 266.

Bernatchez S, Francis FM, Salimnia H, Beveridge TJ, Li H, Dillon JA. 2000. Genomic, transcriptional and phenotypic analysis of *ftsE* and *ftsX* of *Neisseria gonorrhoeae*. *DNA Res.* **7(2):** 75 - 81.

Bi E, Lutkenhaus J. 1991. FtsZ ring structure associated with division in *Escherichia coli*. *Nature*. **354:** 161 – 164.

Boaretti M, Lleo MM, Bonato B, Signoretto C, Canepari P. 2003. Involvement of rpoS in the survival of Escherichia coli in the viable but non-culturable state. *Environ Microbiol.* **5(10):** 986 - 996.

Bramhill D, Thompson CM. 1994. GTP-dependent polymerization of *Escherichia coli* FtsZ protein to form tubules. *PNAS.* **91:** 5813 - 5817.

Britton RA, Lin DCH, Grossman AD. 1998. Characterization of a prokaryotic SMC protein involved in chromosomal partitioning. *Gene Dev.* **12:** 1254 - 1259.

Bryan EM, Bae T, Kleerebezem M, GM Dunny. 2000. Improved vectors for nisin-controlled expression in gram-positive bacteria. *Plasmid.* **44:** 183 – 190.

Centers for Disease Control and Prevention. 1993. Nosocomial enterococci resistant to vancomycin - United States 1989-93. *Morbid Mortal Wkly Rep.* **42:** 597 - 599.

Cesareni G, Muesing MA, Polisky B. 1982. Control of ColE1 DNA replication: the *rop* gene product negatively affects transcription from the replication primer promoter. *Proc Natl Acad Sci USA.* **79(20):** 6313 - 6317.

Cha J-H, Stewart G. 1997. The *divIVA* minicell locus of *Bacillus subtilis*. *J Bacteriol.* **179(5):** 1671 - 1683.

Chenowth C, Schaberg D. 1990. The epidemiology of enterococci. *Eur J Clin Microbiol Infect Dis.* **9:** 80 - 89.

Corbin BD, Yu X-C, Margolin W. 2002. Exploring intracellular function of the Min system in round-shaped *Escherichia coli*. *EMBO J.* **21(8):** 1998 – 2008.

Coykendall AL. 1989. Classification and identification of the viridans streptococci. *Clin Microbiol Rev.* **2:** 315 – 328.

Dal K, Xu Y, Lutkenhaus, J. 1996. Topological characterization of the essential *Escherichia coli* cell division protein FtsN. *J Bacteriol.* **178:** 1328 - 1334.

Daneo-Moore L, Shockman GD. 1977. The bacterial cell surface ingrowth and division. Cell surface reviews. **4:** 597 – 715.Elsevier/North-Holland Biochemical Press. Amsterdam, Holland.

Daniel RA, Errington J. 2003. Control of cell morphogenesis in bacteria: two distinct ways to make a rod-shaped cell. *Cell.* **113:** 767 - 776.

de Boer PAJ, Crossley RE, Rothfield LI. 1992. Roles of MinC and MinD in the site-specific septation block mediated by the MinCDE system of *Escherichia coli. J Bacteriol.* **174:** 63 - 78.

de Boer PAJ, Crossley RE, Rothfield LI. 1989. A division inhibitor and a topological specificity factor coded for by the minicell locus determine proper placement of the division septum in *E. coli. Cell.* **56:** 641 - 649.

de Boer PAJ, Crossley RE. 1988. Isolation of properties of *minB,* a complex genetic locus involved in correct placement of the division site in *E. coli. J Bacteriol.* **170:** 2106 – 2112.

Delves-Broughton J, Blackburn P, Evans RJ, Hugenholtz J. 1996. Applications of the bacteriocin, nisin. *Antonie Van Leeuwenhoek.* **69:** 193 - 202.

de Ruyter PGGA, Kuipers OP, Meijer WC, de Vos WM. 1997. Food-grade controlled lysis of *Lactococcus lactis* for accelerated cheese ripening. *Nat Biotechnol.* **15:** 976 – 979.

de Ruyter, PGGA, Kuipers OP, de Vos WM. 1996. Controlled gene expression systems for *Lactococcus lactis* with the food-grade inducer nisin. *Appl. Environ. Microbiol.* **62:** 3662 – 3667.

de Ruyter PGGA, Kuipers OP, Beerthuyzen MM, van Alen-Boerrigter I, de Vos WM. 1996b. Functional analysis of promoters in the nisin gene cluster of *Lactococcus lactis. J Bacteriol.* **178:** 3434 - 3439.

Ding, Z., Z. Zhao, S. J. Jakubowski, A. Krishnamohan, W. Margolin, and P. J. Christie. 2002. A novel cytology-based, two-hybrid screen for bacteria applied to protein-protein interaction studies of a type IV secretion system. *J Bacteriol.* **184:** 5572 - 5582.

Donachie WD. 2001.Co-ordinate regulation of the *Escherichia coli* cell cycle or the cloud of unknowing. *Mol Microbiol.* **40:** 779 - 785.

Donachie WD, Begg KJ. 1970. Growth of the bacterial cell. *Nature.* **227:** 1220 – 1224.

Edelstein EM, Rosenzweig MS, Daneo-Moore L, Higgins ML. 1980. Unit cell hypothesis for *Streptococcus faecalis. J Bacteriol.* **143(1):** 499 – 505.

Edwards DH, Errington J. 1997. The *Bacillus subtilis* DivIVA protein targets to the division septum and controls the site specificity of cell division. *Mol Microbiol.* **24(5):** 905 - 915.

Edwards DH, Thomaides HB, J Errington. 2000. Promiscuous targeting of *Bacillus subtilis* cell division protein DivIVA to division sites in *Escherichia coli* and fission yeast. *EMBO J.* **19(11):** 2719 - 2727.

Eichenbaum Z, Federle MJ, Marra D, de Vos WM, Kuipers OP, Kleerebezem M, Scott JR. 1998. Use of the lactococcal *nisA* promoter to regulate gene expression in gram-positive bacteria: comparison of induction level and promoter strength. *Appl Environ Microbiol.* **64:** 2763 – 2769.

Engelke G, Gutowski-Eckel Z, Kiesau P, Siegers K, Hammelmann M, Entian KD. 1994. Regulation of nisin biosynthesis and immunity in *Lactococcus lactis* 6F3. *Appl Environ Microbiol.* **60:** 814 - 825.

Errington J, Daniel RA, Scheffers D-J. 2003. Cytokinesis in bacteria. *Microbiol Mol Biol Rev.* **67(1):** 52 – 65.

Errington J. 2003. Dynamic proteins and a cytoskeleton in bacteria. *Nat Cell Biol.* **5(3):** 175 - 178.

Fadda D, Pischedda C, Caldara F, Whalen MB, Anderluzzi D, Domenici E, Massidda O. 2003. Characterization of *divIVA* and other genes located in the chromosomal region downstream of the *dcw* cluster in *Streptococcus pneumoniae. J Bacteriol.* **185(20):** 6209 - 6214.

Feucht A, Lucet I, Yudkin MD, Errington J. 2001. Cytological and biochemical characterization of the FtsA cell division proteins of *Bacillus subtilis. Mol Microbiol.* **40(1):** 115 – 125.

Fitz-James P. 1964. Thin sections of dividing *Neisseria gonorrhoeae. J Bacteriol.* **87:** 1477 - 1482.

Flärdh K. 2003. Essential role of DivIVA in polar growth and morphogenesis in *Streptomyces coelicolor* A3 (2). *Mol Microbiol.* **49(6):** 1523 - 1536.

Fraser CM, Eisen JA, Salzberg SL. 2000. Microbial genome sequencing. *Nature.* **406(6797):** 799 – 803.

Frenkiel-Krispin D, Ben-Avraham I, Englader J, Shimoni E, Wolf SG, Minsky A. 2004. Nucleoid restructuring in stationary-state bacteria. *Mol Microbiol.* **51(2):** 395 – 405.

Gilmore MS, Coburn PS, Nallapareddy SR, Murray BE. 2002. The Enterococci; chapter 8. ASM Press. Pages 301 - 354.

Gitai Z, Shapiro L. 2003. Bacterial cell division spirals into control. *PNAS.* **100(13):** 7423 – 7424.

Gordon GS, Sitnikov D, Webb CD, Teleman A, Straight A, Losick R, Murray AW, Wright A. 1997. Chromosome and low copy plasmid segregation in *E. coli. Cell.* **90:** 1113 - 1121.

Graumann PL. 2000. *Bacillus subtilis* SMC is required for proper arrangement of the chromosome and for efficient segregation of replication termini but not for bipolar movement of newly duplicated origins. *J Bacteriol.* **182:** 6463 - 6471.

Greco VS. 2004. Functional analysis of the role of conserved glycine residues and N-terminus motifs in the cell division inhibitor MinC from Neisseria gonorrhoeae. M. Sc. Thesis. Department of Biochemistry, Microbiology, and Immunology, Faculty of Medicine, University of Ottawa.

Griffiths AJF, Miller JH, Suzuki DT, Lweontin RC, Gelbart WM. 1996. An Introduction to Genetic Analysis-6th Edition. WH Freeman and Co. New York, USA. Page 347.

Guder A, Wiedermann I, Stahl H-G. 2000. Posttranslationally modified bacteriocins – the lantibiotics. *Biopolymers.* **55:** 62 – 73.

Gueiros-Filho FJ, Losick R. 2002. A widely conserved bacterial cell division protein that promotes assembly of the tubulin-like protein FtsZ. *Genes Dev.* **16(19):** 2544 - 2556.

Gugolya, Z., A. Muskotal, A. Sebestyen, Z. Dioszeghy, and F. Vonderviszt. 2003. Interaction of the disordered terminal regions of flagellin upon flagellar filament formation. *FEBS Lett.* **535:** 66-70.

Hamoen LW, Errington J. 2003. Polar Targeting of DivIVA in *Bacillus subtilis* is not directly dependent on FtsZ or PBP 2B. *J Microbiol.* **185(2):** 693 - 697.

Harry EJ, Lewis PJ. 2003. Early targeting of Min proteins to the cell poles in germinated spores of Bacillus subtilis: evidence for division apparatus-independent recruitment of Min proteins to the division site. *Mol Microbiol.* **47(1):** 37 - 48.

Hebrard E, Drucker M, Leclerc D, Hohn T, Uzest M, Froissart R, Strub JM, Sanglier S, van Dorsselaer A, Padilla A, Labesse G, Blanc S. 2001. Biochemical characterization of the helper component of Cauliflower mosaic virus. *J Virol.* **75:** 8538-8546.

Higgins ML, Shockman GD. 1971. Prokaryotic cell division with respect to wall and membranes. *CRC Crit Rev Microbiol.* **1:** 29 - 72.

Higgins ML, Shockman GD. 1976. Study of a cycle of cell wall assembly in *Streptococcus faecalis* by three-dimensional reconstructions of thin sections of cells. *J Microbiol.* **127(3):** 1346 – 1358.

Hill TM. 1996. Features of the chromosomal terminus region in *Escherichia coli* and *Salmonella:* Cellular and molecular biology. Neidhardt *et al.* (eds.). ASM Press. Page: 1602 - 1614.

Holmes VF, Cozzarelli NR. 2000. Closing the ring: links between SMC proteins and chromosome partitioning, condensation and supercoiling. *PNAS USA.* **97(4):** 1322 – 1324.

Howard M. 2004. A mechanism for polar protein localization in bacteria. *J Mol Biol.* **335(2):** 655 - 663.

Hu Z, Mukherjee A, Pichoff S, Lutkenhaus J. 1999. The MinC component of the division site selection system in *E. coli* interacts with FtsZ to prevent polymerization. *PNAS USA.* **96:** 14819 - 14824.

Huang J, Cao C, Lutkenhaus J. 1996. Interaction between FtsZ and inhibitors of cell division. *J Bacteriol.* **178(17):** 5080 – 5085.

Ishino F, Jung HK, Ikeda M, Doi M, Wachi M, Matsuhashi M. 1989. New mutations *fts-36, lts-33* and *ftsW* clustered in the *mra* region of the *Escherichia coli* chromosome induce thermosensitive cell growth and division. *J Bacteriol.* **171:** 5523 - 5530.

Jacobs C, Shapiro L. 1999. Bacterial cell division: A moveable feast. *PNAS.* **96(11):** 5891 – 5893.

Jaffé A, Boye E, D'Ari R. 1990. Rule governing the division pattern in *Escherichia coli minB* and wild-type filaments. *J Bacteriol.* **172(6):** 3500 - 3502.

Janulczyk R, Rasmussen M. 2001. Improved pattern for genome-based screening identifies novel cell wall-attached proteins in Gram-positive bacteria. *Infect Immun.* **69(6):** 4019 – 4026.

Jones LJF, Carbillido-López R, Errington J. 2001. Control of cell shape in bacteria: helical, actin-like filaments in *B. subtilis. Cell.* **104:** 913 – 922.

Jones S, Marin A, Thornton JM. 2000. Protein domain interfaces: characterization and comparison with oligomeric protein interfaces. *Protein Eng.* **13(2):** 77 - 82.

Kahl BC, Belling G, Reichelt R, Herrmann M, Proctor RA, Peters G. 2003. Thymidine-dependent small-colony variants of *Staphylococcus aureus* exhibit gross morphological and ultrastructural changes consistent with impaired cell separation. *J Clin Microbiol.* **41(1):** 410 – 413.

Karkowsky JA, Zhenel GG, Hoban DJ. 1999. Vancomycin-resistant enterococci (VRE) colonization of high-risk patients in tertiary care Canadian hospitals. Canadian VRE Surveillance. *Diagn Microbiol Infect. Dis.* **35:** 1-7.

Katis VL, Wake RG, Harry EG. 2000. Septal localization of the membrane-bound division protein of *Bacillus subtilis* DivIVB and DivIVC is codependent only at high temperatures and requires FtsZ. *J Bacteriol.* **182:** 3607 - 3611.

Kek V, Chow JW. 2002. The Enterococci. Chapter 9 Gilmore MS (ed.). ASM Press. Pages 355 – 384.

Khattar MM, Begg KJ, Donachie WD. 1994. Identification of FtsW and characterization of a new *ftsW* division mutant of *Escherichia coli. J Bacteriol.* **176:** 7140 – 7147.

Khattar MM, Addinall SG, Stedul KH, Boyle DS, Lutkenhaus J, Donachie WD. 1997. Two polypeptide products of the *Escherichia coli* cell division gene *ftsW* and a possible role for FtsW in FtsZ function. *J Bacteriol.* **179:** 784 – 793.

Klaenhammer TD. 1993. Genetics of bacteriocins produced by lactic acid bacteria. *FEMS Microbiol Rev.* **12:** 39 - 86.

Kleerebezem M, Beerthuyzen MM, Vaughan EE, de Vos WM, Kuipers OP. 1997. Controlled gene expression systems for lactic acid bacteria: transferable nisin-inducible expression cassettes for *Lactococcus*, *Leuconostoc*, and *Lactobacillus* spp. *Appl Environ Microbiol.* **63(11):** 4581 – 4584.

Koch AL. 2003. Were Gram-positive rods the first bacteria? *Trends Microbiol.* **11(4):** 166 – 170.

Koch AL. 1985. Bacterial growth and form. Chapman & Hall, Inc. New York, USA.

Kuipers OP, de Ruyter PGGA, Kleerebezem M, de Vos WM. 1998. Quorum sensing-controlled gene expression in lactic acid bacteria. *J Biotechnol.* **64:** 15 – 21.

Kuipers OP, de Ruyter PGGA, Kleerbezem M, de Vos WM. 1997. Controlled overproduction of proteins by lactic acid bacteria. *Trends Biotechnol.* **15:** 135 - 140.

Kuipers OP, Beerthuyzen MM, de Ruyter PGGA, Luesink EJ, de Vos WM. 1995. Autoregulation of nisin biosynthesis in *Lactococcus lactis* by signal transduction. *J Bio. Chem.* **270:** 27299 - 27304.

Kuipers OP, M. M. Beerthuyzen MM, Siezen RJ, de Vos WM. 1993. Characterization of the nisin gene cluster *nisABTCIPR* of *Lactococcus lactis*, requirement of expression of the *nisA* and *nisI* genes for development of immunity. *Eur J Biochem.* **216:** 281 - 291.

Lemon KP, Grossman AD. 2001. The extrusion-capture model for chromosome partitioning in bacteria. *Gene Dev.* **15(16):** 2031 - 2041.

Lemon KP, Kurtser I, Grossman AD. 2001. Effects of replication termination mutants on chromosome partitioning in *Bacillus subtilis*. *PNAS.* **98:** 212 - 217.

Levin PA, Shim JJ, Grossman AD. 1998. Effect of *minCD* on FtsZ ring position and polar septation in *Bacillus subtilis*. *J Bacteriol.* **180:** 6048 – 6051.

Lleo MM, Canepari P, Satta G. 1990. Bacterial cell shape regulation: testing of additional predictions unique to the two-competing sites Model for peptidoglycan assembly and isolation of conditional rod-shaped mutants from some wild-type cocci. *J Bacteriol.* **192(7):** 3758 – 3771.

Lu C, Stricker J, Erickson HP. 1998. FtsZ from *Escherichia coli, Azotobacter vinelandii*, and *Thermotoga maritima*--quantitation, GTP hydrolysis, and assembly. *Cell Motil Cytoskeleton.* **40(1):** 71 - 86.

Lupas, A. 1996. Prediction and analysis of coiled-coil structures. *Methods Enzymol.* **266:** 513 - 525.

Lupas A, Van Dyke M, Stock J. 1991. Predicting coiled coils from protein sequences. *Science.* **252(5010):** 1162 - 1164.

Lutkenhaus J, Addinall SG. 1997. Bacterial cell division and the Z ring. *Annu Rev Biochem.* **66:** 93 – 116.

Margolin W. 2000. Themes and variations in prokaryotic cell division. *FEMS Microbiol Rev.* **24:** 531 - 548.

Margolin W. 2001. A moving MinE sweeper boggles the MinD. *Curr Biol.* **11:** R395 – R398.

Margolin W. 2001b. Spatial regulation of cytokinesis in bacteria. *Curr Opin Microbiol.* **4:** 647 – 652.

Marston AL, Errington J. 1999. Selection of the midcell division site in *Bacillus subtilis* through MinD-dependent polar localization and activation of MinC. *Mol Microbiol* **33(1):** 84 - 96.

Marston AL, Thomaides HB, Edwards DH, Sharpe ME, Errington J. 1998. Polar localization of the MinD protein of *Bacillus subtilis* and its role in selection of the mid-cell division site. *Genes Dev.* **12(21):** 3419 - 3430.

Massidda O, Anderluzzi D, Friedli L, Feger G. 1998. Unconventional organization of the division and cell wall gene cluster of *Streptococcus pneumoniae. Microbiol.* **144:** 3069 - 3078.

Migocki MD, Freeman MK, Wake RG, Harry EJ. Epub 2002. The Min system is not required for precise placement of the midcell Z ring in *Bacillus subtilis. EMBO Rep.* **3(12):** 1163 - 1167.

Miller MJ, Yuan BZ. 1997 Semiautomated resolution of overlapping stutter patterns in genomic microsatellite analysis. *Anal Biochem.* **251(1):** 50 - 66.

Mirelman D. 1978. Biosynthesis and assembly of cell wall peptidoglycan. Bacterial outer membranes. Inouye M (ed). John Wiley & Sons New York USA. Pages: 115 – 116.

Mitchell P, Moyle J. 1956. Osmotic function and structure of bacteria. *Symp Soc Gen Microbiol.* **6:** 150 – 180.

Moellering Jr, RC. 1992. The Enterococcus: a classic example of the impact of antimicrobial resistance on therapeutic options. *J Antimicrob Chemother.* **28:** 1 - 12.

Møller-Jensen J, Jensen RB, Gerdes K. 2000. Plasmid and chromosome segregation in prokaryotes. *Trends Microbiol.* **8(7):** 313 - 320.

Morbach S, Krämer R. 2002. Body shaping under water stress: Osmosensing and osmoregulation of solute transport in Bacteria. *Chem BioChem.* **3:** 384 – 397.

Muchová K, Kutejová E, Pribišová, Wilkinson AJ, Barák. *Bacillus subtilis* division protein DivIVA – screen for stable oligomer state conditions. *Acta Cryst.* D589: 1542-1243.

Muchová K, Kutejová E, Scott DjJ, Brannigan JA, Lewis RL, Wilkinson AJ, Barák I. 2002. Oligomerization of the *Bacillus subtilis* division protein DivIVA. *Microbiol.* **148:** 807 - 813.

Nanninga N. 1998. Morphogenesis of *Escherichia coli. Microbiol Mol Biol Rev.* **62(1):** 110 – 129.

Noirclerc-Savoye M, Morlot C, Gerard P, Vernet T, Zapun A. 2003. Expressio and purification of FtsW and RodA from *Streptococcus pneumoniae*, two membrane proteins involved in cell division and cell growth, respectively. *Protein Expr Purif.***30:** 18 – 25.

Norris V, Woldringh C, Mileykovskaya E. 2004. A hypothesis to explain division site selection in Escherichia coli by combining nucleoid occlusion and Min. *FEBS Lett.* **561(1-3):** 3 - 10.

Ohtomo R, Saito M. 2001. Increase in the Culturable Cell Number of Escherichia coli during Recovery from Saline Stress: Possible Implication for Resuscitation from the VBNC State. *Microb Ecol.* **42(2):** 208 - 214.

Park, Y. C., V. Burkitt, A. R. Villa, L. Tong, and H. Wu. 1999. Structural basis for self-association and receptor recognition of human TRAF2. *Nature.* **398:** 533 - 538.

Pavan S, Hols P, Delcour J, Geoffroy M-C, Grangette C, Kleerebezem M, Mercenier A. 2000. Adaptation of the Nisin-Controlled Expression System in *Lactobacillus plantarum*: a Tool To Study In Vivo Biological Effects. *App Environ Microbiol.* **66(10):** 4427 – 4432.

Pichoff S, Vollrath B, Bouche JP. 1997. MinCD-independent inhibition of cell division by a protein that fuses MalE to the topological specificity factor MinE. *J Bacteriol.* **179(14):** 4616 – 4619.

Pucci MJ, Thanassi JA, Discotto LF, Kessler RE, Dougherty TJ. 1997. Identification and characterization of cell wall-cell division gene clusters in pathogenic Gram-positive cocci. *J Bacteriol.* **179(17):** 5632 - 5635.

Ramirez-Arcos S, Lio M, Marthaler S, Rigden M and Dillon JR. 2004. *Enterococcus faecalis divIVA*: An essential gene involved in cell division, cell growth and chromosomal segregation. (Microbiology submission: 27718).

Ramirez-Arcos S, Greco V, Douglas H, Tessier D, Fan D, Szeto J, Wang J, Dillon JA, Margolin W. 2004b Conserved glycines in the C terminus of MinC proteins are implicated in their functionality as cell division inhibitors. *J Bacteriol.* **186(9):** 2841 - 2855.

Ramirez-Arcos S, Szeto J, Dillon JA, Margolin W. 2002. Conservation of dynamic localization among MinD and MinE orthologues: oscillation of *Neisseria gonorrhoeae* proteins in *Escherichia coli. Mol Microbiol.* **46(2):** 493 - 504.

Ramirez-Arcos S, Salimnia H, Bergevin I, Paradis M, Dillon JA. 2001. Expression of Neisseria gonorrhoeae cell division genes ftsZ, ftsE and minD is influenced by environmental conditions. *Res Microbiol.* **152(9):** 781 - 791.

Ramos, A, Honrubia MP, Valbuena N, Vaquera J, Mateos LM, Gil JA. 2003. Involvement of DivIVA in the morphology of the rod-shaped actinomycete *Brevibacterium lactofermentum.* Microbiology **149:** 3531 - 3542.

Reeve JN, Mendelson NH, Coyne SI, Hallock LL, Cole RM. 1973. Minicells of *Bacillus subtilis*. *J Bacteriol*, **114:** 860 – 873.

Rigden MD. 2005. Determining the role of coiled-coil domain interactions in the oligomerization of DivIVA from *Enterococcus faecalis.* M. Sc. Thesis. Department of Biochemistry, Microbiology, and Immunology, Faculty of Medicine, University of Ottawa.

Rothfield L, Justice S, García-Lara J. 1999. Bacterial cell division. *Annu Re. Gene.* **33:** 423 – 448.

Rothfield LI, Shih YL, King G. 2001. Polar explorers: membrane proteins that determine division site placement. *Cell.* **106(1):** 13 - 16.

Ryan KR, Shapiro L. 2003. Prokaryotic cell cycle progression and development. *Annu Rev Biochem.* **72:** 367 – 394.

Sambrooke J, Russell DW. 2001. Molecular cloning: A laboratory manual. Cold Spring Harbor Laboratory Press, Cold Spring Harbor, New York.

Scheffers DJ, Errington J. 2004. PBP1 is a component of the *Bacillus subtilis* cell division machinery. *J Bacteriol.* **186(15):** 5153 - 5156.

Schwartz U. Asmus A, Frank H. 1969. Autolytic enzyme and cell division of *Escherichia coli. J Mol Biol.* **98:** 749 – 759.

Shih YL, Le T, Rothfield L. 2003. Division site selection in *Escherichia coli* involves dynamic redistribution of Min proteins within coiled structures that extend between the two cell poles. *PNAS.* **100(13):** 7865 - 7870.

Shockman GD, Daneo-Moore L, Higgins ML. 1974. Problems of cell wall and membrane growth, enlargement and division. *Ann NY Acad Sci.* **235:** 161 – 197.

Signoretto C, Lleo MM, Canepari P. 2002. Modification of the peptidoglycan of Escherichia coli in the viable but nonculturable state. *Curr Microbiol.* **44(2):** 125 - 131.

Signoretto C, Lleo MM, Tafi MC, Canepari P. 2000. Cell Wall Chemical Composition of *Enterococcus faecalis* in the Viable but Nonculturable State. Applied and Envirol Microbiol. **66(5):** 1953-1959.

Stahlberg H, Kutejová, Muchová K, Gregorini M, Lustig A, Műller SA, Olivieri V, Engel A, Wilkinson AJ and Barák I. 2004. Oligomeric structure of the *Bacillus subtilis* cell division protein DivIVA determined by transmission electron microscopy. *Mol Microbiol.* **52(5):** 1281 - 1290.

Stock JB, Surette MG, Levit M, Park P. 1995. Two-component transduction systems: structure-function relationships and mechanisms of catalysis. *In* Hoch JA, Silhavy TJ (ed.), Two-component signal transduction. AMS Press. Pages 25 – 51.

Still K, Edward L, Friedman B, Fuhrman S, Newton T. 2001. Vancomycin-resistant organisms on a burn unit. *S Med J.* **94:** 810 - 812.

Swartz MN. 1994. Hospital-acquired infections: diseases with increasingly limited therapies. *PNAS USA.* **91:** 2420 - 2427.

Szeto J, Eng NF, Acharya S, Rigden MD, Dillon JA. 2005. A conserved polar region in the cell division site determinant MinD is required for responding to MinE-induced oscillation but not for localization within coiled arrays. *Res Microbiol.* **156(1):** 17 – 29.

Szeto J, Acharya S, Eng NF, Dillon JA. 2004. The N terminus of MinD contains determinants which affect its dynamic localization and enzymatic activity. *J Bacteriol.* **186(21):** 7175 – 7185.

Szeto J. 2004. Splitting heirs: A study of the cell division site determinant MinD from the coccus Neisseria gonorrhoeae. PhD Thesis. Department of Biochemistry, Microbiology, and Immunology, Faculty of Medicine, University of Ottawa.

Szeto J, Ramirez-Arcos S, Raymond C, Hicks LD, Kay CM, Dillon J. 2001. MinD affects cell division in *Neisseria gonorrhoeae* and *Escherichia coli* and exhibits a novel self-interaction. *J Bacteriol.* **183(21):** 6253 – 6264.

Tamames J, González-Moreno, Mingorance J, Valencia A, Vicente M. 2001. Bringing gene order into bacterial shape. *Trends genet.* **117(3):** 124 – 126.

Tamames J. 2001b. Evolution of gene order conservation in prokaryotes. *Genome Biol.* **2(6):** research0020.1-0020.11.

Tenover FC, Biddle JW, Lancaster MV. 2001. Increasing resistance to vancomycin and other glycopeptides in *Staphylococcus aureus. Emerg Infect Dis.* **7:** 327 - 332.

Thanedar S, Margolin W. 2004. FtsZ exhibits rapid movement and oscillation waves in helix-like patterns in *E. coli. Curr Biol.* **14(13):** 1167 – 1173.

Thomaides HB, Freeman M, Karoui ME, Errington J. 2001. Division site selection protein DivIVA of *Bacillus subtilis* has a second distinct function in chromosome segregation during sporulation. *Gene dev.* **15:** 1662 - 1673.

Touhami A, Jericho MH, Beveridge TJ. 2004. Atomic force microscopy of cell growth and division in *Staphylococcus aureus. J Bacteriol.* **186(11):** 3286 – 3295.

van Belkum A, Scherer S, van Aplhen L, Verbrugh H. 1998. Short-sequence DNA repeats in prokaryotic genomes. *Microbiol Mol biol Rev.* **62(2):** 275 – 293.

Vicente M, Gomez MJ, Ayala JA. 1998. Regulation of transcription of cell division genes in the Escherichia coli dcw cluster. *Cell Mol Life Sci.* **54(4):** 317 - 324.

Wang H, Gayda RC. 1992. Quantitative determination of FtsA at different growth rates in *Escherichia coli* using monoclonal antibodies. *Mol Microbiol.* **6:** 2517 – 2524.

Wanner BL. 1992. Is cross regulation by phosphorylation of two-component response regulator proteins important in bacteria? *J Bacteriol.* **174:** 2053 - 2058.
Weart RB, Levin PA. 2003. Growth rate-dependent regulation of medial FtsZ ring formation. *J Bacteriol.* **185(9):** 2826 - 2834.

Westling-Häggström B, Elmrs T, Normark T, Winblad B. 1977. Growth pattern and cell division in *Neisseria gonorrhoeae. J Bacteriol.* **129:** 1412 - 1423.

Williamson R, Le Bouguenec C, Gutmann L, Horaud T.1985. One or two low affinity penicillin-binding proteins may be responsible for the range of susceptibility of *Enterococcus faecium* to benzylpenicillin. *J Gen Microbiol.***131:** 1933 - 1940.

Woldringh CL, Mulder E, Huls PG and Vischer N. 1991. Toporegulation of bacterial division according to the nucleoid occlusion model. *Res Microbiol.* **142:** 309 – 320.

Wu L, Errington J. 2004. Co-ordination of cell division and chromosome segregation by a nucleoid occlusion protein in *B. subtilis. Cell.* **117:** 915 – 925.

Yu X-C, Margolin W. 1999. FtsZ ring clusters in *min* and partition mutants: role of both the Min system and the nucleoid in regulating FtsZ ring localization. *Mol Microbiol.* **32:** 315 – 326.

Yura T, Mori H, Nagai H, Nagata T, Ishihama A, Fujita N, Isono K, Mizobuchi K, Nakata A. 1992. Systematic sequencing of the *Escherichia coli* genome: analysis of the 0-2.4 min region. *Nuclc Acids Res.* **20(13):** 3305 - 3308.